3 Quantification of Early Diagenesis: Dissolved Constituents in Pore Water and Signals in the Solid Phase

Horst D. Schulz

A chapter on the pore water of sediments and the processes of early diagenesis, reflected by the concentration profiles therein, can certainly be structured in different ways. One possibility is, for example, to start with the sample-taking strategies, followed by the analytical treatment of the samples, then a model presentation to substantiate the processes, and finally a quantitative evaluation of the measured profiles with regard to material fluxes and reaction rates. The reader who would prefer this sequence is recommended to begin with the Sections 3.3, 3.4, 3.5 and to consult the Sections 3.1 and 3.2 later. However, in our opinion, marine geochemistry departed from its initial development stage of sample collection and anlysis some years ago. This book is therefore written with a different structure from earlier texts. The well understood theoretical knowledge on concentration profiles has to be introduced from the beginning. Only then do problems arise which necessitate the investigation of particular substances in pore water and the application of specific methods of sampling and analysis.

Particularly, two fundamental approaches are conceivable for investigating diagenesis processes, both having their advantages and disadvantages. The classical way leads to a sedimentological, mineralogical, and in the broadest sense geochemical examination of the solid phase. The advantage of this approach is that sample withdrawal and analytical procedures are generally easier to carry out and produce more reliable results. On the other hand, in most cases this approach will not provide us with any information on the timing at which specific diagenetical alterations in the sediment took place. Nothing will be learnt about reaction rates, reaction kinetics, and mostly we do not even know whether the processes, interpreted on account of certain measurements and/or observations, occur today or whether they were terminated some time before. Furthermore, the distinction between the primary signals from the water column and the results of diagenetic reactions, often remains unclear.

A section dealing with the concentrations of elements in the solid phase of the sediment should not be missing despite the mentioned disadvantages and problems that come along with a geochemical description of a sediment/pore water system. Section 3.7 therefore contains a brief presentation of the various sample-processing methods and analyses, next to some examples of measured element profiles. One of the greatest problems encountered in interpreting element concentrations in the sediment's solid phase will always be one's ability to distinguish between a primary signal from the water column, i.e. from the introduction into the sediment, and the diagenetic alteration of the material.

If the processes of diagenesis and their time-dependency are to be recorded directly, then a second approach appears to be more reasonable; one that includes the measurement of concentration profiles in pore water. Figure 3.1 shows various concentration profiles of substances dissolved in the pore water of sediments taken at a depth of approximately 4000 m, off the estuary of the River Congo. The differently shaped curves shown here directly reflect the reactions that are happening today. The investigation of pore water thus constitutes the only way to determine the reaction rates and the fluxes of material which they produce. Yet, this procedure is rather laborious and unfortunately contains numerous opportunities for errors. Most errors are caused as soon as the sediment sample is taken, others are caused upon preparing the pore water from the sediment, or in the course of

GeoB 1401

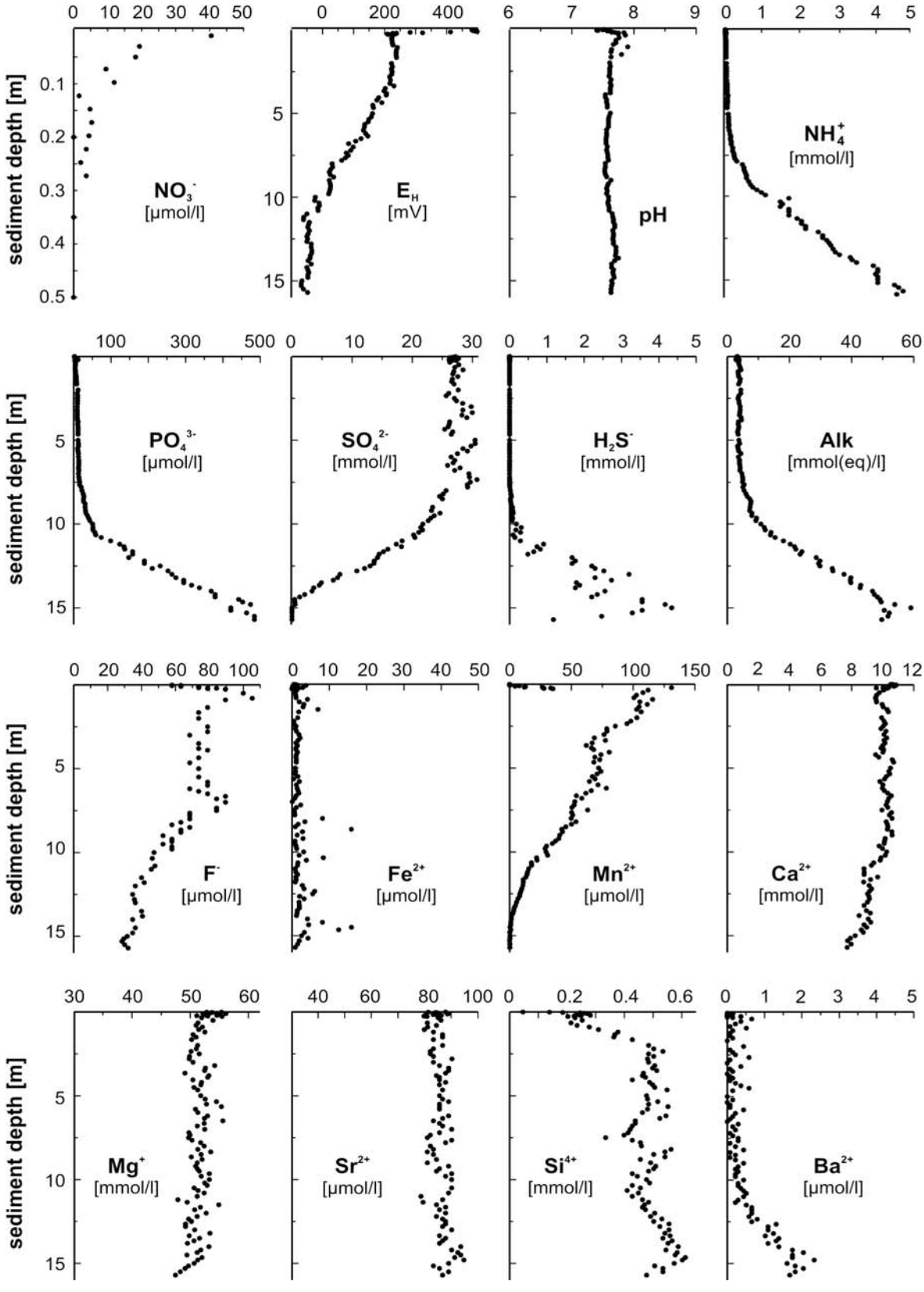
sediment depth [m]
NO3- [µmol/l]
EH [mV]
pH
NH4+ [mmol/l]
PO43- [µmol/l]
SO42- [mmol/l]
H2S- [mmol/l]
Alk [mmol(eq)/l]
F- [µmol/l]
Fe2+ [µmol/l]
Mn2+ [µmol/l]
Ca2+ [mmol/l]
Mg+ [mmol/l]
Sr2+ [µmol/l]
Si4+ [mmol/l]
Ba2+ [µmol/l]

Fig. 3.1 Concentration profiles in the pore water fractions of sediments obtained off the estuary of the River Congo, at a depth of approximately 4000 m. The sediments contain a relatively high amount of TOC. Values ranging from 1 to 3.5 wt. % indicate that this sediment is characterized by the high reaction rates of various early diagenesis processes. These processes are reflected by diffusion fluxes over gradients and by reaction rates determined by gradient changes (after Schulz et al. 1994).

analyzing low concentrations obtained from small sample amounts. Actually, one would prefer to gain all results by *in situ* measurements at the bottom of the ocean, which is feasible, however, only in very few exceptional cases.

3.1 Introduction: How to Read Pore Water Concentration Profiles

The processes of early diagenesis - irrespective of whether we are dealing with microbiological redox-reactions or predominantly abiotic reactions of dissolution and precipitation - are invariably reflected in the pore water of sediments. The aquatic phase of the sediments is the site where the reactions occur, and where they become visible as time-dependent or spatial distributions of concentrations. Thus, if the early diagenesis processes are to be examined and quantified in the young marine sediment, the foremost step will always consist of measuring the concentration profiles in the pore water fraction.

For reasons of simplification and enabling an easy understanding of the matter, only three fundamental processes will be considered in this section, along with their manifestation in the pore water concentration profiles:

- Consumption of a reactant in pore water (e.g. consumption of oxygen in the course of oxidizing organic material)
- Release of a substance from the solid phase into the pore water fraction (e.g. release of silica due to the dissolution of opal).
- Diffusion transport of dissolved substances in pore water and across the sediment/ bottom water boundary.

Figure 3.2 shows schematic diagrams of some possible concentration profiles occurring in marine pore water. Here, the profile shown in Figure 3.2a is quite easy to understand. In the event of a substance that is not subject to any early diagenetic process, the pore water as the formation water contains exactly the same concentration as the supernatant ocean water. If the concentration in the ocean floor water changes, this change will

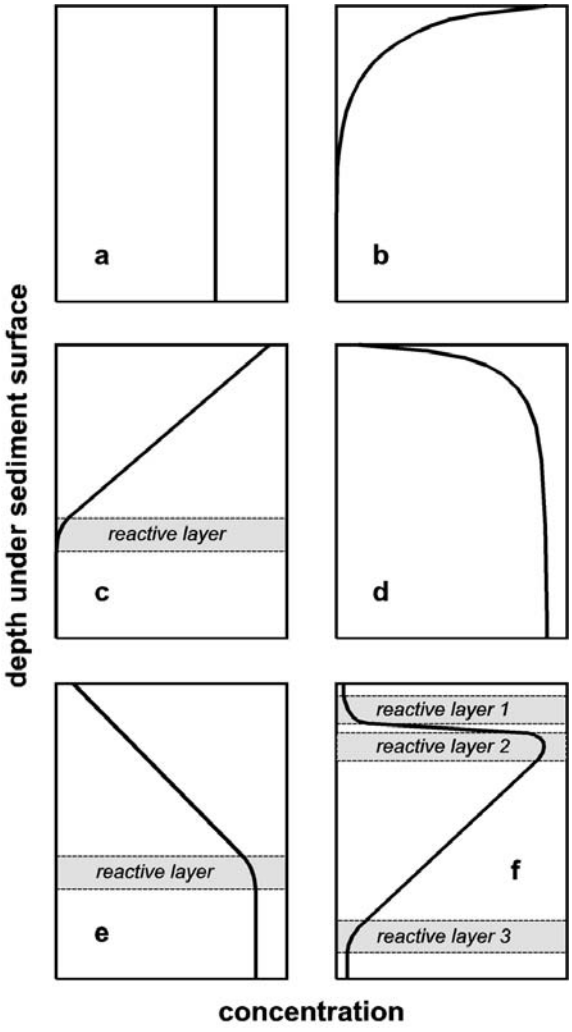

Fig. 3.2 Principal concentration profile shapes as in measured pore water:
a: Profile of a non-reacting substance (e.g. chloride); b: profile of a substance that is depleted in the upper layers of the sediment (e.g. oxygen); c: profile of a substance that is consumed in a particular reactive layer; d: profile of a substance that is released into pore water in the upper layers of the sediment (e.g. silica); e: profile of a substance that is released into the pore water in specific reactive layers; f: profile of a substance that is released into pore water in one discrete depth (reactive layer 2), and, in two other depths (reactive layers 1 and 3) is removed from the pore water by consumption (e.g. manganese).

be reproduced in the pore water fraction on account of diffusion processes. After a definite time of non-stationary conditions, which depends on the depth of the profile under study and the required accuracy of the measurement, the concentration of the ocean floor water prevails again, stationary and constant within the entire profile. The details and the problems concerning stationary and non-stationary conditions in pore water will be thoroughly discussed in Section 3.2.

Figure 3.2b shows the concentration profile of a substance which is consumed by early diagenetic reactions in the upper layers of the sediment. For example, the profiles of dissolved oxygen often look like this (cf. Chap. 6). Assuming steady-state conditions (cf. Sect. 3.2), the concentration gradient near the sediment surface will display its highest increases, because whatever is consumed in the deeper layers will arrive there by means of diffusion. With increasing depths the concentration gradient and the diffusive material transport will decline, until, at a particular depth, concentration, gradient, and diffusion simultaneously approach zero. This sediment depth, referred to as the penetration depth of a substance, often represents a steady-state condition composed of the diffusive reinforcement from above and the depletion of the substance in the sediment by the reactions of early diagenesis.

In principle, the situation depicted in Figure 3.2c is quite the same. Here, the process is just limited to one reactive layer. With an example of oxygen as the dissolved substance, this could be a layer containing easily degradable organic matter, or the sedimentary depth in which oxygen encounters and reacts with a reductive solute species coming from below (e.g. Mn^{2+} or Fe^{2+}). At any rate, the space above the reactive layer is characterized by a constant gradient in the concentration profile and thus by a diffusive transport which is everywhere the same. Within the reactive layer the dissolved substance is brought to zero concentration by depletion.

The reverse case, which is in principle quite similar, is demonstrated in Figure 3.2d and e. Here, a substance is released anywhere into the layers near the sediment surface (Fig. 3.2d), whereas it might be released into the pore water only in one particular layer (Fig. 3.2e). The solute could be, for example, silica that often displays such concentration profiles on account of the dissolution of sedimentary opal.

The concentration profile shown in Figure 3.2f is much more complex than the others in Figure 3.2 and only comprehensible if the interactions of several processes taking place at various depths below the sediment surface are regarded. Such a profile is characteristic, for example, of the concentrations of divalent manganese in marine pore water (see also Figure 3.1, Figure 3.8, and Chapter 11). Manganese oxide functions as an electron acceptor and reacts with organic matter in reactive layer 2, whereupon chemically reduced divalent manganese dissolves. A small percentage diffuses downwards (flat gradient) and precipitates as manganese carbonate or manganese sulfide in reactive layer 3. The major proportion diffuses upwards (much steeper gradient), encounters dissolved oxygen from the sediment surface once again in reactive layer 1, is reoxidized and precipitates back to manganese oxide.

The described relations can be summarized by stating a few rules for reading and understanding of pore water concentration profiles:

- Diffusive material fluxes always occur in the form of concentration gradients; concentration gradients always represent diffusive material fluxes.
- Reactions occurring in pore water in most cases constitute changes in the concentration gradient; changes in the concentration gradient always represent reactions occurring in pore water.
- A concave-shaped alteration in the concentration gradient profile (cf. Fig. 3.2b, c) signifies the depletion of a substance from pore water; conversely, a convex-shaped concentration gradient profile (cf. Fig. 3.2d, e) always depicts the release of a substance into the pore water.

However, the following also needs to be observed:

- If a substance is involved in two reactions taking place at the same depth, and is released into the pore water fraction by one reaction and then withdrawn again by the other, neither of the participating reactions will become evident in the pore-water concentration profile.

In the following Section 3.2, the laws of diffusion and the particularities of their application to sediment pore waters will be treated in more detail. In this context, the problem of steady state and non-steady state situations will have to be covered, since the simple examples described above have anticipated steady state situations. Moreover, as a further simplification, the examples of this section have by necessity neglected advection, bioirrigation, and bioturbation. These processes will be discussed in detail in Section 3.6. Section 3.7 will then cover the investigations of the sediment's solid phase and thereby disclose the result of one or the other process of early diagenesis.

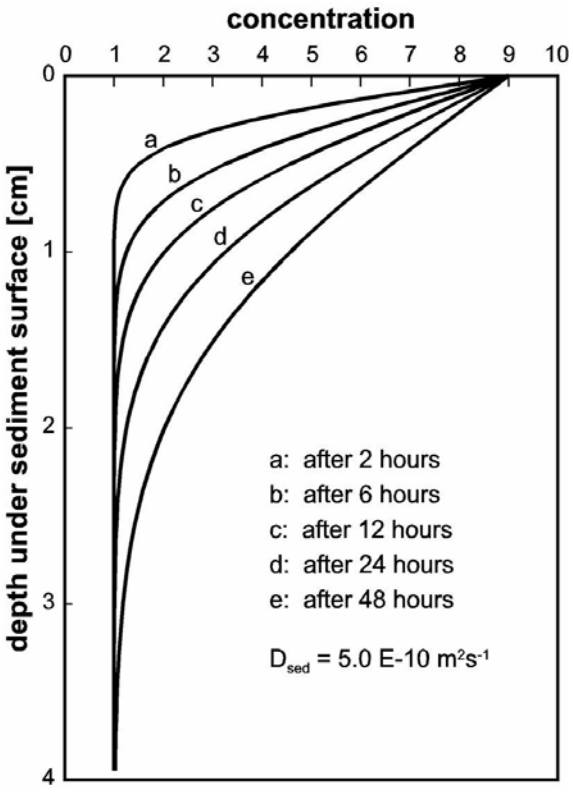

Fig. 3.3 Calculated non-steady state concentration profiles in pore water of a young sediment. It was assumed that the concentration of '1' has been previously constant in the pore water of the sediment as well as in the supernatant bottom water for a long period of time, so that a steady state situation was prevalent. Then the concentration of bottom water changed shortly to '9'. The concentration profiles a to e are non-steady states after 2 and up to 48 hours. The calculation of such non-steady state concentration profiles can be performed , for example, with the aid of the model program CoTAM (Hamer and Sieger 1994) or CoTReM (cf. Chap. 15).

3.2 Calculation of Diffusive Fluxes and Diagenetic Reaction Rates

3.2.1 Steady State and Non-Steady State Situations

In the preceding section and especially in all the following chapters, one pair of terms will assume extraordinary importance for describing and understanding biogeochemical processes: the steady state and non-steady state situation.

Let us first consider the steady state situation as its description is more straight forward in a model concept. In Figure 3.2c a concentration profile is shown in which a substance is continually consumed at a specific rate of reaction and within a reactive layer. At the same time, a constant concentration is prevalent in the bottom water above the sediment surface, an infinite reservoir as compared to the consumption in the sediment. It follows therefore that a constant concentration gradient exists between the sediment surface and the reactive layer, and thus everywhere the same diffusive flux. Such a concentration gradient is referred to as being in steady state. It remains in this condition as long as its determining factors - turn-over rates in the reactive layer, concentration at the sea-floor, dimension and properties of the space between the reactive layer and sediment surface - are not changed.

Any change of the conditions that is liable to exert any kind of influence on the concentration profile, terminates the steady state situation. A non-steady state emerges, which is a time-dependent situation occurring in the pore water. If the system remains unperturbed in the changed situation for a sufficient length of time, a new steady state situation can become established, different from the first and reflecting the novel configuration of conditions.

Strictly speaking, there are no real steady-state situations in nature. Even the sun had begun to shine at a certain time, the earth and, upon her, the oceans have come into existence at a certain time, and all things must pass sooner or later. Hence, the term referring to the steady-state condition also depends on the particular stretch of time which is under study, as well as on the dimension of the system, and, not least, on the accuracy of the measurements with which we examine the parameters that describe the system.

A given concentration in the pore water of a pelagic sediment, several meters below the sediment surface, can be measured today, next month, next year, and after 10 years. Within the margins of reasonable analytical precision, we will always measure just about the same value and rightfully declare the situation to be steady-state (That there are also exceptions to the rule may be concluded from the Examples 2 and 3 described in Section 15.3.2). At the same time, pore water concentrations in sedimentary surface areas near the same pelagic sediment could be subject to considerable seasonal variation (such as residual deposits of algal bloom periods) and thus be classified as being in a non-steady state.

A calculated example for pore water concentrations in a non-steady state condition is shown in Figure 3.3. Details concerning the calculation procedure will not be discussed here. The conceptual model employed will be described in Section 3.2.4, a suitable computer model is described in Chapter 15. A typical diffusion coefficient characteristic of young marine sediments and a characteristic porosity coefficient were used in the calculation.

In the calculated example shown in Figure 3.3 the assumption was made that a constant concentration of '1' has been prevalent for a long time in the pore water of the young sediment and in the bottom water above it. Then, the bottom water underwent a momentary change to yield a concentration of '9'. By means of diffusion, the new concentration gradually spreads into the pore water. After 2 hours it reaches a depth of less than 1 cm, after 48 hours, respectively, a depth of about 3 to 4 cm below the sediment surface. If the concentration of '9' remains constant long enough in the bottom water above the sediment, this concentration will theoretically penetrate into an infinitely great depth. To what extent, and into what depths of pore water, these concentrations are to be assigned to steady state or non-steady states can only be determined in each particular case, having its own concentration in the bottom water over a given period of time. At any rate, the allocation of one or the other state can only be done separately for each system, each parameter, and each time interval. Calculations as shown in Figure 3.3 are likely to produce valuable preliminary concepts, for evaluating real measured pore water profiles.

In the next example, the influence of seasonal variation in the bottom water lying above the sediment will be examined, as well as the resulting non-steady states in the pore water fraction. To this end, the following boundary conditions are selected: A substance concentration of '1' is supposed to be prevalent in the bottom water over one half year, afterwards the concentration changes to '10' for one half year, then it changes back to a value of '1', and so on, continually changing. Figure 3.4 shows the result of such an oscillatory situation after several years. The curve denoted 'a' demonstrates the situation in which the bottom water concentration was '1' after half a year; the curve denoted 'b' reflects the situation in which the bottom water concentration was '10' after half a year. It is evident that essential effects of such changes can only be observed down to a depth of less than 0.2 m below the sediment surface. In this model calculation, the effects of

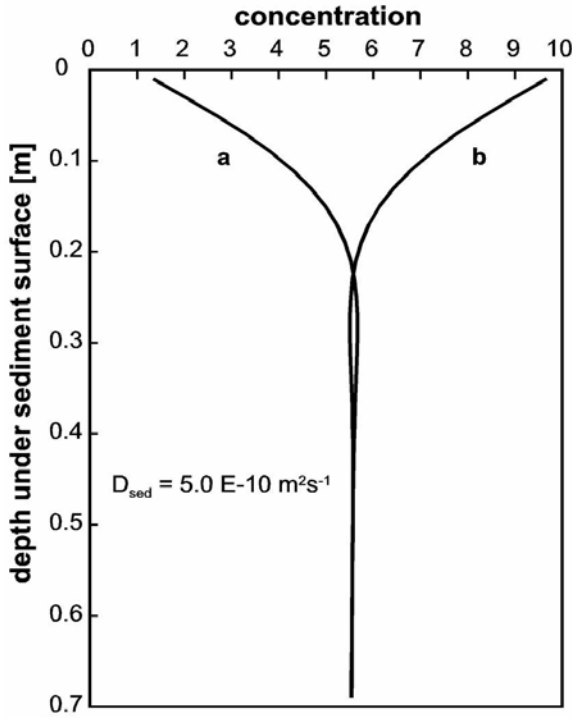

Fig. 3.4 Calculated non-steady state concentration profiles in the pore water of a young sediment. The calculation assumes that concentrations of '1' and '10' were prevailing alternately in the bottom water over the sediment, each over a period of half a year. After several years, the curve a. reflects the situation of concentration '1' at the end of one half year, whereas curve b. reflects the situation of concentration '10' at the end of one half year. The calculation of such non-steady state concentration profiles can be performed, for example, with the aid of the model programs EXPLICIT or CoTReM (cf. Chapter 15).

the preceding half year still remain visible in a depth between about 0.22 m and 0.35 m below the sediment surface. Below a depth of 0.4 m no further non-steady states can be seen, a constant and steady-state mean concentration of '5.5' prevails.

The conditions proposed in Figure 3.4 describe a very extreme situation. On the one hand, the half-yearly alternating concentrations differ by a whole order of magnitude, on the other hand, no transitory periods with intermediate concentrations were anticipated. Seasonal variations in nature usually display smaller concentration differences and are also likely to possess transitory intermediate concentrations. Both diminish the effects of non-steady state formation in sedimentary depths as were shown in the example of Figure 3.4.

Figure 3.4 also demonstrates clearly the effects of the analytical precision on differentiating steady state and non-steady states in pore water. In the theoretical calculation shown in Figure 3.4, the difference between both curves is still visible in form of a non-steady state at a depth between 0.22 and 0.4 m. However, if the possible errors are taken into consideration that occur during sampling and in the analytic treatment of pore water samples (Sects. 3.3 - 3.5), then there is likely to be no current parameter with which these differences could be discovered practically. Below a depth of 0.2 m, one would always measure the same concentration and consequently judge the situation as stationary, or as a steady state.

3.2.2 The Steady State Situation and Fick's First Law of Diffusion

According to Fick's first law of diffusion, the diffusive flux (J) is directly proportional to concentration gradient ($\partial C/\partial x$) under steady state conditions. The factor of proportionality is the temperature-dependent and substance-dependent diffusion coefficient (D^0):

$$J = -D^0 \cdot \frac{\partial C}{\partial x} \qquad (3.1)$$

The negative sign indicates that the diffusive flux runs in opposition to the gradient's direction from high concentrations to lower concentrations. In these terms, increasing concentrations in greater depths will yield negative gradients in the sediment along with an upwards directed positive flux, and vice-versa.

The relations shown in Equation 3.1 are only valid for free solutions, thus without the 'disturbing' sedimentary solid phase. The diffusion coefficient D^0 is only valid for infinitely dilute solutions. Boudreau (1997) and Iversen and Jørgensen (1993) have summarized the current state of knowledge concerning the application of the diffusion laws to the pore water volume of sediments, accomplished on the basis of an extensive literature survey, and have thoroughly discussed the general problem. As nothing further needs to be added at this point, the calculation of the values shown in the following Tables 3.1 and 3.2 were performed by using the relations published by Boudreau (1997). Table 3.1 contains the diffusion coefficients for a number of ions, gases, and uncharged complex compounds dissolved in seawater at various temperatures.

Looking at diffusion processes in the pore water volume of sediments, it must be taken into consideration that diffusion can only take place within the pore water volume (porosity ϕ), hence a diffusive flux can only be proportionally effective with regard to this spatial compartment. Beyond this limitation, the diffusion coefficient is distinctly lower in the pore water volume of a sediment (D_{sed}) than in free solution. The diffusive flux in the sediment (J_{sed}) is calculated as:

$$J_{sed} = -\phi \cdot D_{sed} \cdot \frac{\partial C}{\partial x} \qquad (3.2)$$

The diffusion coefficient in the pore water volume of sediments differs from the diffusion coefficient of free solutions in such a manner that diffusion in the pore water volume cannot follow a straight course, but must take 'deviations' around each single grain. The degree of deviation around particles is called tortuosity (θ). It describes the mean ratio between the real length of the pathway and the straight-line distance. Tortuosity can be quantified directly by measuring the electrical resistivity (R) (McDuff and Ellis 1979) and employing a related 'formation factor' (F).

$$F = R_s / R_f \qquad (3.3)$$

In this equation, R_s is the specific electrical resistivity for the whole system composed of sediment and pore water, and R_f denotes the electrical resistivity for pore water only. Since the electric cur-

Table. 3.1 Diffusion coefficient in free solution for sea-water at various temperatures. The calculations were performed on the basis of relations derived from a comprehensive literature study carried out by Boudreau (1997).

Ion	0 °C	5 °C	10 °C	15 °C	20 °C	25 °C
			D^{sw} [m^2s^{-1}]			
H^+	5.17E-09	5.89E-09	6.60E-09	7.30E-09	8.01E-09	8.69E-09
D^+	3.03E-09	3.68E-09	4.33E-09	4.97E-09	5.61E-09	6.24E-09
Li^+	4.21E-10	5.34E-10	6.45E-10	7.56E-10	8.66E-10	9.74E-10
Na^+	5.76E-10	7.15E-10	8.52E-10	9.88E-10	1.12E-09	1.26E-09
K^+	9.08E-10	1.10E-09	1.29E-09	1.47E-09	1.66E-09	1.84E-09
Rb^+	9.70E-10	1.17E-09	1.36E-09	1.56E-09	1.75E-09	1.94E-09
Cs^+	9.79E-10	1.17E-09	1.36E-09	1.55E-09	1.74E-09	1.93E-09
Ag^+	7.43E-10	9.11E-10	1.08E-09	1.24E-09	1.40E-09	1.57E-09
NH_4^+	9.03E-10	1.10E-09	1.29E-09	1.47E-09	1.66E-09	1.85E-09
Ba^{2+}	3.86E-10	4.68E-10	5.49E-10	6.30E-10	7.10E-10	7.88E-10
Be^{2+}	2.44E-10	3.10E-10	3.75E-10	4.39E-10	5.03E-10	5.66E-10
Ca^{2+}	3.42E-10	4.26E-10	5.09E-10	5.91E-10	6.72E-10	7.53E-10
Cd^{2+}	3.15E-10	3.85E-10	4.56E-10	5.25E-10	5.95E-10	6.63E-10
Co^{2+}	3.15E-10	3.85E-10	4.56E-10	5.25E-10	5.95E-10	6.63E-10
Cu^{2+}	3.22E-10	3.96E-10	4.69E-10	5.41E-10	6.13E-10	6.84E-10
Fe^{2+}	3.15E-10	3.84E-10	4.54E-10	5.22E-10	5.91E-10	6.58E-10
Hg^{2+}	3.19E-10	4.17E-10	5.13E-10	6.09E-10	7.04E-10	7.98E-10
Mg^{2+}	3.26E-10	3.93E-10	4.60E-10	5.25E-10	5.91E-10	6.55E-10
Mn^{2+}	3.02E-10	3.75E-10	4.46E-10	5.17E-10	5.88E-10	6.57E-10
Ni^{2+}	3.19E-10	3.80E-10	4.40E-10	4.99E-10	5.58E-10	6.16E-10
Sr^{2+}	3.51E-10	4.29E-10	5.08E-10	5.85E-10	6.62E-10	7.38E-10
Pb^{2+}	4.24E-10	5.16E-10	6.08E-10	6.98E-10	7.88E-10	8.77E-10
Ra^{2+}	3.72E-10	4.65E-10	5.57E-10	6.48E-10	7.39E-10	8.28E-10
Zn^{2+}	3.15E-10	3.85E-10	4.55E-10	5.24E-10	5.93E-10	6.60E-10
Al^{3+}	2.65E-10	3.46E-10	4.26E-10	5.05E-10	5.83E-10	6.61E-10
Ce^{3+}	2.80E-10	3.41E-10	4.02E-10	4.62E-10	5.22E-10	5.80E-10
La^{3+}	2.64E-10	3.28E-10	3.91E-10	4.53E-10	5.15E-10	5.76E-10
Pu^{3+}	2.58E-10	3.13E-10	3.69E-10	4.24E-10	4.79E-10	5.32E-10
OH^-	2.46E-09	2.97E-09	3.48E-09	3.98E-09	4.47E-09	4.96E-09
OD^-	1.45E-09	1.76E-09	2.07E-09	2.38E-09	2.68E-09	2.98E-09
$Al(OH)_4^-$	4.24E-10	5.37E-10	6.50E-10	7.62E-10	8.73E-10	9.82E-10
Br^-	9.51E-10	1.16E-09	1.36E-09	1.56E-09	1.76E-09	1.96E-09
Cl^-	9.13E-10	1.12E-09	1.32E-09	1.52E-09	1.72E-09	1.92E-09
F^-	5.98E-10	7.58E-10	9.17E-10	1.07E-09	1.23E-09	1.39E-09
HCO_3^-	4.81E-10	6.09E-10	7.37E-10	8.63E-10	9.89E-10	1.11E-09
$H_2PO_4^-$	3.82E-10	4.86E-10	5.90E-10	6.92E-10	7.94E-10	8.94E-10
HS^-	9.89E-10	1.11E-09	1.24E-09	1.36E-09	1.49E-09	1.61E-09
HSO_3^-	6.04E-10	7.34E-10	8.63E-10	9.91E-10	1.12E-09	1.24E-09
HSO_4^-	5.69E-10	7.13E-10	8.55E-10	9.96E-10	1.14E-09	1.27E-09
I^-	9.33E-10	1.13E-09	1.33E-09	1.53E-09	1.73E-09	1.92E-09

Ion	0 °C	5 °C	10 °C	15 °C	20 °C	25 °C
			D^{sw} [$m^2 s^{-1}$]			
IO_3^-	4.43E-10	5.61E-10	6.78E-10	7.93E-10	9.08E-10	1.02E-09
NO_2^-	9.79E-10	1.13E-09	1.28E-09	1.43E-09	1.58E-09	1.73E-09
NO_3^-	9.03E-10	1.08E-09	1.26E-09	1.44E-09	1.62E-09	1.79E-09
$Acetate^-$	4.56E-10	5.71E-10	6.84E-10	7.96E-10	9.08E-10	1.02E-09
$Lactate^-$	4.19E-10	5.32E-10	6.44E-10	7.54E-10	8.64E-10	9.72E-10
CO_3^{2-}	4.12E-10	5.04E-10	5.96E-10	6.87E-10	7.78E-10	8.67E-10
HPO_4^{2-}	3.10E-10	3.93E-10	4.75E-10	5.56E-10	6.37E-10	7.16E-10
SO_3^{2-}	4.31E-10	5.47E-10	6.62E-10	7.77E-10	8.91E-10	1.00E-09
SO_4^{2-}	4.64E-10	5.72E-10	6.79E-10	7.86E-10	8.91E-10	9.95E-10
$S_2O_3^{2-}$	4.58E-10	5.82E-10	7.06E-10	8.28E-10	9.50E-10	1.07E-09
$S_2O_4^{2-}$	3.75E-10	4.63E-10	5.49E-10	6.35E-10	7.20E-10	8.04E-10
$S_2O_6^{2-}$	5.04E-10	6.40E-10	7.75E-10	9.08E-10	1.04E-09	1.17E-09
$S_2O_8^{2-}$	4.64E-10	5.89E-10	7.12E-10	8.35E-10	9.57E-10	1.08E-09
$Malate^{2-}$	3.19E-10	4.05E-10	4.90E-10	5.74E-10	6.57E-10	7.39E-10
PO_4^{3-}	2.49E-10	3.16E-10	3.82E-10	4.48E-10	5.13E-10	5.77E-10
$Citrate^{3-}$	2.54E-10	3.22E-10	3.90E-10	4.57E-10	5.23E-10	5.89E-10
H_2	1.92E-09	2.36E-09	2.81E-09	3.24E-09	3.67E-09	4.10E-09
He	2.74E-09	3.37E-09	4.00E-09	4.63E-09	5.24E-09	5.85E-09
NO	1.02E-09	1.26E-09	1.49E-09	1.72E-09	1.95E-09	2.18E-09
N_2O	9.17E-10	1.13E-09	1.34E-09	1.55E-09	1.75E-09	1.96E-09
N_2	8.69E-10	1.07E-09	1.27E-09	1.47E-09	1.66E-09	1.85E-09
NH_3	9.96E-10	1.23E-09	1.45E-09	1.68E-09	1.90E-09	2.12E-09
O_2	1.00E-09	1.23E-09	1.46E-09	1.69E-09	1.91E-09	2.13E-09
CO	1.00E-09	1.24E-09	1.47E-09	1.69E-09	1.92E-09	2.14E-09
CO_2	8.38E-10	1.03E-09	1.22E-09	1.41E-09	1.60E-09	1.79E-09
SO_2	6.94E-10	8.54E-10	1.01E-09	1.17E-09	1.33E-09	1.48E-09
H_2S	9.17E-10	1.13E-09	1.34E-09	1.55E-09	1.75E-09	1.96E-09
Ar	8.65E-10	1.06E-09	1.26E-09	1.46E-09	1.65E-09	1.85E-09
Kr	8.38E-10	1.03E-09	1.22E-09	1.41E-09	1.60E-09	1.79E-09
Ne	1.31E-09	1.62E-09	1.92E-09	2.22E-09	2.51E-09	2.81E-09
CH_4	7.29E-10	8.97E-10	1.06E-09	1.23E-09	1.39E-09	1.56E-09
CH_3Cl	6.51E-10	8.01E-10	9.50E-10	1.10E-09	1.24E-09	1.39E-09
C_2H_6	6.03E-10	7.42E-10	8.80E-10	1.02E-09	1.15E-09	1.29E-09
C_2H_4	6.77E-10	8.33E-10	9.88E-10	1.14E-09	1.29E-09	1.44E-09
C_3H_8	5.07E-10	6.23E-10	7.40E-10	8.54E-10	9.69E-10	1.08E-09
C_3H_6	6.29E-10	7.74E-10	9.18E-10	1.06E-09	1.20E-09	1.34E-09
H_4SiO_4	4.59E-10	5.67E-10	6.76E-10	7.84E-10	8.92E-10	1.00E-09
$B(OH)_3$	5.14E-10	6.36E-10	7.57E-10	8.78E-10	9.99E-10	1.12E-09

rent in the pore water volume of sediments is bound to the presence of charged ions in solution, the same deviations are valid (cf. Sect. 2.1.2). The tortuosity (θ) is then calculated by applying the porosity (ϕ) to the equation according to (Berner 1980):

$$\theta^2 = \phi \cdot F \tag{3.4}$$

The diffusion coefficient in sediments (D_{sed}) can be calculated on the basis of a dimensionless tortuosity and the diffusion coefficient in free solutions of sea-water (D^{sw} in Table 3.1):

$$D_{sed} = D^{sw} / \theta^2 \tag{3.5}$$

If the tortuosity is not known on account of electric conductivity measurements and the 'formation factor' (F), its value may be estimated, a bit less accurately, by its empirical relationship to the porosity. About a dozen different empirical equations are known from literature. The most frequently used is Archie's Law (Archie 1942):

$$\theta^2 = \phi^{(1-m)} \tag{3.6}$$

The adaptation to specific data is done by means of (m) as long as parallel values are available for sediments obtained from direct measurements of their electrical conductivity. Boudreau (1997) shows, however, that this relation does not have any advantage as compared to:

$$\theta^2 = 1 - \ln(\phi^2) \tag{3.7}$$

Table 3.2 Tortuosity expressed in terms of a sediment's porosity. The calculation was performed by using the Equation 3.7 as published by Boudreau (1997).

ϕ	θ^2	ϕ	θ^2	ϕ	θ^2
0,20	4,22	0,44	2,64	0,68	1,77
0,22	4,03	0,46	2,55	0,70	1,71
0,24	3,85	0,48	2,47	0,72	1,66
0,26	3,69	0,50	2,39	0,74	1,60
0,28	3,55	0,52	2,31	0,76	1,55
0,30	3,41	0,54	2,23	0,78	1,50
0,32	3,28	0,56	2,16	0,80	1,45
0,34	3,16	0,58	2,09	0,82	1,40
0,36	3,04	0,60	2,02	0,84	1,35
0,38	2,94	0,62	1,96	0,86	1,30
0,40	2,83	0,64	1,89	0,88	1,26
0,42	2,74	0,66	1,83	0,90	1,21

This relation (Boudreau's law) has been used for the calculation of various porosity values prevalent in marine sediments as listed in Table 3.2.

By applying the contents of the Tables 3.1 and 3.2 as well as the relation expressed in Equation 3.5, the various examples of the following section are quantifiable. Notwithstanding, it should be emphasized that tortuosity values obtained by electrical conductivity measurements should always be, if available at all, favored to estimated values deduced on account of an empirical relation to porosity.

3.2.3 Quantitative Evaluation of Steady State Concentration Profiles

This section intends to demonstrate the application of Fick's first law of diffusion to some selected examples of concentration profiles which were derived from marine pore water samples. It needs to be stressed that all these calculations require that steady-state conditions are present. The calculation of non-steady state conditions will only be dealt with later in Section 3.2.4.

Figure 3.5 shows an oxygen profile measured *in-situ*. The part of concentration gradient exhibiting the highest inclination is clearly located directly below the sediment surface. This gradient of 22.1 mol $m^{-3}m^{-1}$ is identified in Figure 3.5 (cf. Sect. 12.2). A relatively high degree of porosity will have to be assumed for this sediment near the sediment surface. A porosity of $\phi = 0.80$ yields a tortuosity value (θ^2) of 1.45, according to Table 3.2. The diffusion coefficient for oxygen dissolved in free seawater at 5 °C is shown in Table 3.1 to amount to $D^{sw} = 1.23 \cdot 10^{-9}$ m^2s^{-1}. Applying Equation 3.5, it follows that the diffusion coefficient for oxygen in sediments is $D_{sed} = 8.5 \cdot 10^{-10}$ m^2s^{-1}. This yields the diffusive oxygen flux from the bottom water into the sediment $J_{sed,\,oxygen}$ as:

$$\begin{aligned} J_{sed,oxygen} &= -0.80 \cdot 8.5 \cdot 10^{-10} \cdot 22.1 \\ &= -1.5 \cdot 10^{-8}\ [\text{mol m}^{-2}\text{s}^{-1}] \end{aligned} \tag{3.8}$$

To arrive at less complicated and more imaginable figures, and in order to compare this value with, for instance, sedimentological data, we multiply with the number of seconds in a year ($365 \cdot 24 \cdot 60 \cdot 60 = 31{,}536{,}000$) and then we obtain:

$$\begin{aligned} J_{sed,oxygen} &= -1.5 \cdot 10^{-8} \cdot 31{,}536{,}000 \\ &= -0.47\ [\text{mol m}^{-2}\text{a}^{-1}] \end{aligned} \tag{3.9}$$

If we now assume that oxygen reacts in the sediment exclusively with C_{org} in a ratio of 106:138 as Froelich et al. (1979) have indicated (cf. Section 3.2.5), then we obtain the amount of C_{org} which is annually oxidized per m^2:

$$R_{ox,Corg} = 0.47 \cdot (106/138) \cdot 12 = 4.4\ [gC\ m^{-2}a^{-1}] \quad (3.10)$$

It must be pointed out that we have to differentiate very distinctly between two very different statements. On the one hand, the profile inescapably proves that 0.47 mol $m^{-2}a^{-1}$ oxygen are consumed in the sediment. On the other hand, the calculation that 4.4 g $m^{-2}a^{-1}$ C_{org} is equivalent to this amount requires that all oxygen is, in fact, used in the oxidation of organic matter. However, it is imaginable that at least a fraction of oxygen is consumed by the oxidation of other reduced inorganic solute species (e.g. Fe^{2+}, Mn^{2+}, or NH_4^+; cf. also with example shown in Fig. 3.8). There is indeed evidence that, depending on the specific conditions of the various marine environments, one or the other reaction contributes more or less to the consumption of oxygen. At any rate, this needs to be verified by other measurements, for instance, by recording the concentration profiles of the reducing solute species.

Figure 3.6 shows the concentration profile of dissolved sulfate obtained from the pore water of sediments sampled from the Amazon deep sea fan. The pore water was extracted by compression of sediment sampled with the gravity corer, and was immediately afterwards analyzed by ion-chromatography (compare Sects. 3.3 and 3.4). As compared to the previous example, a depth range comprising more than two orders of magnitude is dealt with here. The paths for diffusion are hence considerably longer in this example. Yet, the sulfate concentration in sea-water is also two orders of magnitude higher than the concentration of oxygen so that, in total, a similar gradient is formed nevertheless.

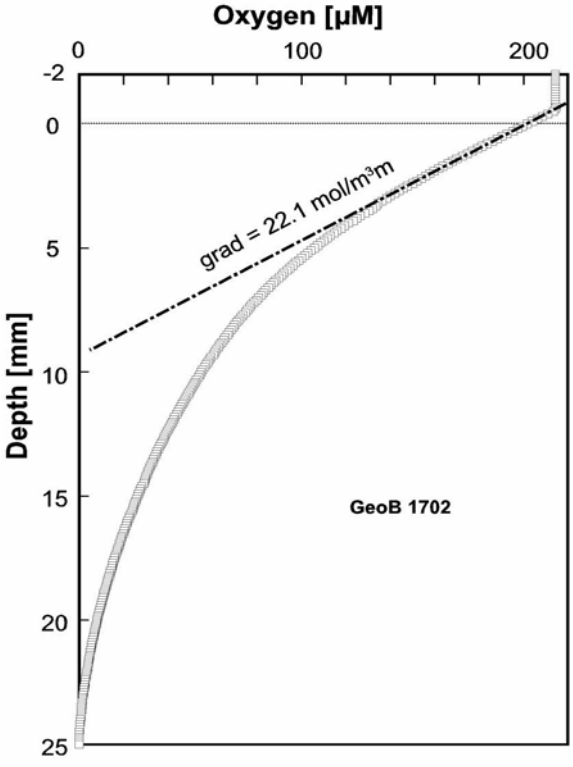

Fig. 3.5 A quite successful oxygen profile in a marine sediment. This profile was measured by Glud et al. (1994) in highly reactive sediments off the western shoreline of Africa using the 'Profilur' lander in situ. The most pronounced concentration gradient (chain line) lies directly below the sediment surface. Down to a depth of only about 25 mm below the sediment surface, the oxygen dissolved in pore water is entirely depleted.

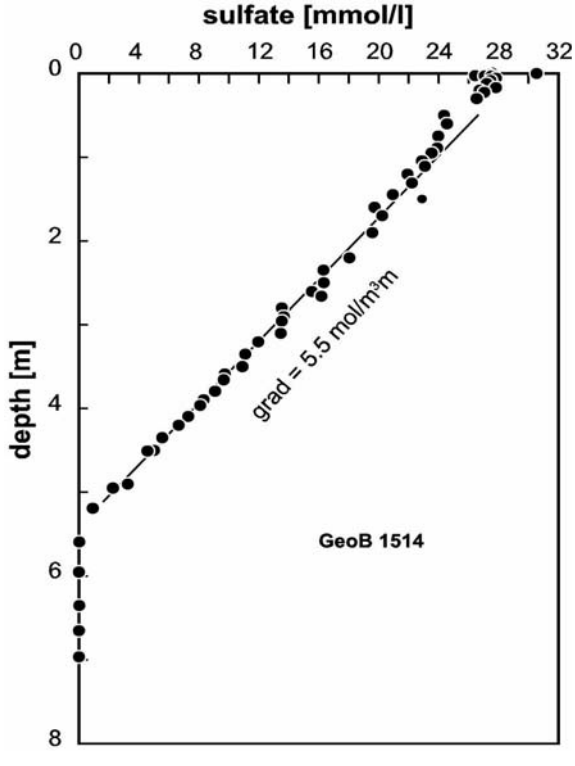

Fig. 3.6 Sulfate profile in pore water from sediments of the Amazon deep sea fan at a water depth of about 3500 m. A linear concentration gradient can be distinctly derived from the sediment surface down to a depth of about 5.4 m. The gradient change, and thus a change in the diffusive flux, is strongly limited to a depth interval of at the most 10 to 20 cm (after Schulz et al. 1994).

In this case a concentration gradient of 5.5 mol m^{-3} m^{-1} was derived as a mean value for the depths ranging from 0 to 5.4 m. Upon examining the curve in more detail, it is obvious that the gradient is less pronounced in the upper 2 meters which is probably explained by a somewhat higher porosity and a concurrently unchanged diffusive flux. As the discovered gradient within the sulfate profile is located distinctly deeper under the sediment surface than in the previous example, it is reasonable to assume a lower degree of porosity. A porosity of $\phi = 0.60$ yields, according to Table 3.2, a tortuosity value (θ^2) of 2.02. On consulting Table 3.1 we find that the diffusion coefficient for sulfate in sea-water at 5 °C is $D^{sw} = 5.72 \cdot 10^{-10}$ $m^2 s^{-1}$. Using Equation 3.5 it follows that the diffusion coefficient in the sediment amounts to $D_{sed} = 2.8 \cdot 10^{-10}$ $m^2 s^{-1}$. Thus, the diffusive sulfate flux from the bottom water into the sediment corresponds to $J_{sed,\ sulfate}$:

$$J_{sed,sulfate} = - 0.60 \cdot 2.8 \cdot 10^{-10} \cdot 5.5 = - 9.2 \cdot 10^{-10} \text{ [mol m}^{-2}\text{s}^{-1}\text{]} \quad (3.11)$$

To arrive at more relevant figures and for reasons of comparison with other sedimentologic data, we multiply this value with the number of seconds in one year (31,536,000) and obtain:

$$J_{sed,sulfate} = - 9.2 \cdot 10^{-10} \cdot 31{,}536{,}000 = - 0.029 \text{ [mol m}^{-2}\text{a}^{-1}\text{]} \quad (3.12)$$

If we assume that sulfate reacts in the sediment exclusively with C_{org}, in a ratio of 106:53 as Froelich et al. (1979) have reported, then for the amount of C_{org} that is annually oxidized per square meter amounts to:

$$R_{ox,Corg} = 0.029 \cdot (106/53) \cdot 12 = 0.70 \text{ [gC m}^{-2}\text{a}^{-1}\text{]} \quad (3.13)$$

It should be indicated at this point as well that the calculated diffusive sulfate flux from the bottom water into the sediment, and from there into a depth of about 5.4 m, is the unequivocal consequence of the profile shown in Figure 3.6. It also follows that this sulfate is degraded in the depth of 5.4 m within a depth interval of at the most 10 to 20 cm thickness. The calculated C_{org} amount that undergoes conversion again depends on the assumption made by Froelich et al. (1979) that indeed the whole of sulfate reacts with organic carbon. Several studies demonstrated that this must not be generally the case. For sediments obtained from the Skagerak, Iversen and Jørgensen (1985) showed that an essential proportion of sulfate is consumed in the oxidation of methane. At different locations of the upwelling area off the shores of Namibia and Angola, Niewöhner et al. (1998) could even prove that the entire amount of sulfate is consumed due to the oxidation of methane which diffuses upwards in an according gradient.

Figure 3.7 shows a nitrate profile obtained from sediments of the upwelling area off Namibia which is rather characteristic of marine pore water. The processes behind such nitrate profiles are now well understood. The details of these reactions are described in the chapters 5 and 6; here, they will be discussed only briefly as much is necessary for the comprehension of calculated substance fluxes.

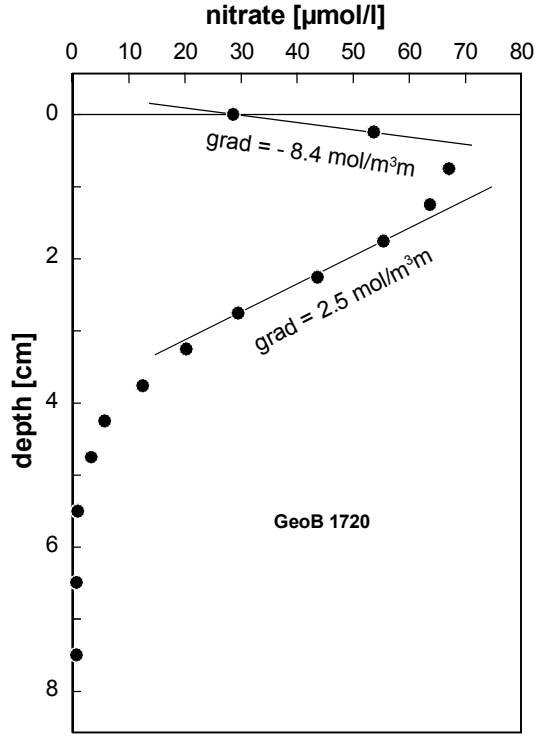

Fig. 3.7 Nitrate profile of pore water obtained from sediments of the upwelling area off the coast of Namibia. The profile displays the shape which is typical of nitrate profiles, with a maximum at a depth which is determined by the decomposition of organic material and the oxidized nitrogen released from it after having reacted with the dissolved oxygen. The gradients indicated document a flux upward into the bottom water and a flux downward into zones where nitrate functions as an electron acceptor in the oxidation of other substances.

The maximum at a specific depth below sea-level is the result of oxidation of organic material by the oxygen that diffuses into the sediment zone from above. Here, the nitrogen of the organic material is converted into nitrate. Mostly, a more pronounced gradient transports the major proportion of nitrate upwards into the bottom water. The smaller proportion travels downwards along a shallow gradient where it is finally consumed as an electron acceptor in the oxidation of other substances.

All these processes can be derived directly and quantitatively from Figure 3.7. Since they are bound to a sedimentary zone which lies very close to the surface, a high degree of porosity can be assumed. According to Table 3.2, the porosity ϕ = 0.80 corresponds to a tortuosity (θ^2) of 1.45. Table 3.1 shows that the diffusion coefficient for nitrate in free sea-water at 5 °C amounts to D^{sw} = $1.08 \cdot 10^{-9}$ $m^2 s^{-1}$. Applying Equation 3.5 yields a sedimentary diffusion coefficient of D_{sed} = $7.4 \cdot 10^{-10}$ $m^2 s^{-1}$. Hence, the diffusive nitrate flux from the sediment to the bottom water compartment is calculated as:

$$J_{nitrate,up} = - 0.80 \cdot 7.4 \cdot 10^{-10} \cdot (-8.4) = 5.0 \cdot 10^{-9} \text{ [mol m}^{-2}\text{s}^{-1}\text{]} \quad (3.14)$$

or as

$$J_{nitrate,up} = 5.0 \cdot 10^{-9} \cdot 31{,}536{,}000 = 0.16 \text{ [mol m}^{-2}\text{a}^{-1}\text{]} \quad (3.15)$$

The nitrate flux in a downward direction is calculated accordingly:

$$J_{nitrate,down} = - 0.80 \cdot 7.4 \cdot 10^{-10} \cdot 2.5 = - 1.5 \cdot 10^{-9} \text{ [mol m}^{-2}\text{s}^{-1}\text{]} \quad (3.16)$$

or as

$$J_{nitrate,down} = - 1.5 \cdot 10^{-9} \cdot 31{,}536{,}000 = - 0.047 \text{ [mol m}^{-2}\text{a}^{-1}\text{]} \quad (3.17)$$

The sum of both fluxes yields a minimal estimate value of the total nitrate concentration released from organic matter due to its reaction with oxygen. However, the real value for the total amount of released nitrate must be higher than the sum of both calculated fluxes. The gradient of the downward directed flux may be quite reliably calculated from numerous points, however, the more pronounced gradient of the flux leading upward into the bottom water consists only of two points, one of which merely represents the concentration in the bottom water whereas the other represents the pore water of the uppermost 0.5 cm of sediment. It is probably correct to assume that the gradient is more pronounced in closer proximity to the sediment surface, and hence the flux should also prove to be more enhanced. A more accurate statement would only be possible under *in-situ* conditions with a depth resolution similar to the oxygen profile shown in Figure 3.5. As for measurements performed under *ex-situ* conditions, a better depth resolution than shown in Figure 3.7 is very hard to obtain.

If we assume that the released nitrate exclusively originates from the oxidation of organic matter, and that the organic matter is oxidized in a manner in which the C:N ratio corresponds to the Redfield-ratio of 106:16 (cf. Sect. 3.2.5), then we can also calculate the conversion rate of organic matter on the basis of the nitrate profile:

$$R_{ox,Corg} = [\text{abs}(J_{nitrate,up}) + \text{abs}(J_{nitrate,down})] \cdot (106/16) \quad (3.18)$$

or by employing the values of the above example:

$$R_{ox,Corg} = (0.16 + 0.047) \cdot (106/16) = 1.37 \text{ [mol m}^{-2}\text{a}^{-1}\text{]} \quad (3.19)$$

or

$$R_{ox,Corg} = 16.5 \text{ [gC m}^{-2}\text{a}^{-1}\text{]} \quad (3.20)$$

At any rate, such a value might serve only as a rough estimation, since apart from the aforementioned error, the calculation procedure implicitly contains some specific assumptions. It has been already mentioned that the C:N ratio of the oxidized material is supposed to be (106/16 = 6.625). Publications of Hensen et al. (1997), however, indicate that especially in sediments with a rich abundance of organic matter a distinctly lower ratio of almost 3 is imaginable (cf. Chap. 6). It must also be considered that the measured profiles are not just influenced by diffusion in the surface zones, but also by the processes of bioturbation and bioirrigation (cf. Sect. 3.6.2).

In principle, the shape of the manganese profile shown in Figure 3.8 is not dissimilar to the nitrate profile of Figure 3.7. Here, we again identify the zones of maximum concentrations – in this particular case about 0.5 m below the sea-floor level – as the site of dissolved manganese release into the pore water. Again, a pronounced negative gradient transports the dissolved manganese up-

wards away from the zone of its release. This time, however, the substance flux does not reach up to the bottom water above the sediment, instead, very low manganese concentrations are measured at a depth which is only few centimeters below the sediment surface. A flat positive gradient leads a smaller fraction of the released manganese to greater depth where it is withdrawn from the pore water at about 14 to 15 m below the sediment surface.

Here as well, similar to the previously discussed example, both fluxes can be calculated. The upwardly directed flux from the manganese release zone ($J_{manganese,\ up}$) is obtained from the gradient (-0.5 mol $m^{-3}m^{-1}$), where in the upper zone the sediment possesses an assumed porosity of 0.80. Considering the values in Table 3.1 and 3.2, as well as the Equation 3.5, a sedimentary diffusion coefficient of $D_{sed} = 2.6 \cdot 10^{-10}$ m^2s^{-1} yields the following manganese flux:

$$J_{manganese,up} = - 0.80 \cdot 2.6 \cdot 10^{-10} \cdot (-0.5) = 1.0 \cdot 10^{-10} \text{ [mol m}^{-2}\text{s}^{-1}\text{]} \quad (3.21)$$

or

$$J_{manganese,up} = 1.0 \cdot 10^{-10} \cdot 31{,}536{,}000 = 3.2 \cdot 10^{-3} \text{ [mol m}^{-2}\text{a}^{-1}\text{]} \quad (3.22)$$

Likewise, the downward-directed manganese flux is calculated, however, taking a porosity degree of $\phi = 0.60$ into account and an accordingly calculated $D_{sed} = 1.9$ E-10 m^2s^{-1}:

$$J_{manganese,down} = - 0.60 \cdot 1.9 \cdot 10^{-10} \cdot 0.0084 = - 9.6 \cdot 10^{-13} \text{ [mol}^1\text{m}^{-2}\text{s}^{-1}\text{]} \quad (3.23)$$

or

$$J_{manganese,down} = - 9.6 \cdot 10^{-13} \cdot 31{,}536{,}000 = - 3.0 \cdot 10^{-5} \text{ [mol m}^{-2}\text{a}^{-1}\text{]} \quad (3.24)$$

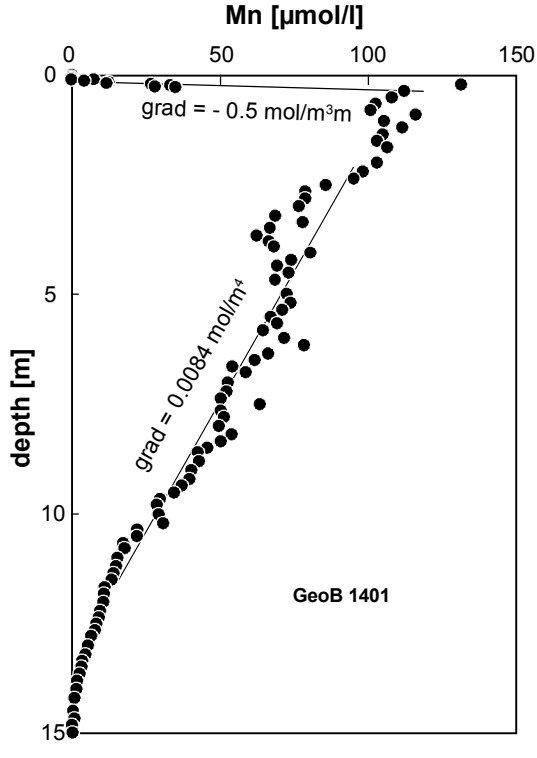

Fig. 3.8 A manganese profile in pore water of sediments off the Congo River estuary, in a water depth of approx. 4000 m. The profile is, in principle, quite similar to the profile of nitrate previously shown in Figure 3.7. Here, manganese is released into the pore water at a specific depth below the sediment surface. A gradient with a high negative slope leads most of the Mn^{2+} upwards; another gradient, positive and more level, conveys manganese into a precipitation zone, which was just included in the lowest core meter (between 14 and 15 m).

Again, both fluxes added together constitute the total release of dissolved manganese from the sediment into the pore water. Since the downward-directed flux is in this case almost two orders of magnitude lower than the upward-directed flux, it may be neglected considering the possible errors occurring in the determination of the upward stream. The release of manganese is equivalent to the conversion of oxidized tetravalent manganese into the soluble divalent manganese. Which substance is the electron donor in this reaction cannot be concluded from the manganese profile. It could be organic matter as proposed by Froelich et al. (1979). In this case we should not overlook the fact that the converted substance amounts are one order of magnitude lower than they are, for instance, in sulfate fluxes (Fig. 3.6), and more than two orders of magnitude lower than they are in the flux of oxygen. (Fig. 3.5). It should also be noted that upon reducing one mole of Mn(IV) to Mn(II) only two moles of electrons are exchanged, whereas it amounts to 4 moles of electrons per mole oxygen, and even 8 moles of electrons per mole sulfate. Even the 'impressive' gradient of the manganese profile shown in Figure 3.8 does not represent an essential fraction of the overall diagenetic processes in the sediment, involved in the oxidation of organic matter.

The upward-directed manganese flux does not reach into the bottom water, instead, the Mn^{2+} is re-oxidized in a depth of only few centimeters below the sediment surface. Generally, one would ex-

pect this re-oxidation to occur by the action of dissolved oxygen (cf. Chap. 11).

It is not within the scope of the present discussion to decide whether the variations in the concentration profile that were averaged upon calculating the gradient of 0.0084 mol $m^{-3}m^{-1}$ shown in Figure 3.8, merely reflect the inaccuracy pertinent to the sampling technique and/or the analytical procedure, or whether they represent discrete processes of their own. Since they do not vary independently, and since several points appear to constitute smaller minima and maxima, it may be suggested that these measurements do not simply represent analytical variations, but reasonable and true values. At any rate, the whole curve leads in its course to very low values that are reached at a depth of 14 m along with a distinct change of the gradient's slope. In many cases, a precipitation of Mn(II)-carbonate is to be expected. The identification of such diagenetic phases anticipated in geochemical modeling is discussed in more detail in Section 15.1.

3.2.4 The Non-Steady State Situation and Fick's Second Law of Diffusion

All examples of the preceding Sections 3.2.2 and 3.2.3 are strictly only valid under steady-state conditions when concentrations, and hence the gradients and diffusive fluxes, are constant over time. Fick's second law of diffusion is applicable in non-steady state situations:

$$\frac{\partial C}{\partial t} = D_{sed} \cdot \frac{\partial^2 C}{\partial x^2} \qquad (3.25)$$

The diffusion coefficient in free solution (D) or the diffusion coefficient in sedimentary pore water (D_{sed}) are used due to the conditions of the system. In contrast to Fick's first law of diffusion, the time co-ordinate (t) appears here next to the local co-ordinate (x). The concentrations and thus the gradients and fluxes are variable for these co-ordinates. Such a partial differential equation cannot be solved without determining a specific configuration of boundary conditions. On the other hand, most of the known solutions are without great practical value for the geochemist due to their very specifically chosen sets of boundary conditions that are seldom related to real situations.
In the following only one solution will therefore be presented in detail. The following boundary conditions are to be considered as valid: In the whole sediment profile below the sediment surface the same diffusion coefficient (D_{sed}) is assumed to prevail, the same concentration (C_0) prevails in the sediment's pore volume. After a certain point in time (t=0) the bottom water attains another concentration (C_{bw}) at the sediment surface. The concentrations ($C_{x,t}$) in the depth profile (co-ordinate x = depth below the sediment surface) at a specific time-point (t) are for these conditions described as:

$$C_{x,t} = C_0 + (C_{bw} - C_0) \cdot erfc\left\{x \Big/ \left(2 \cdot \sqrt{D_{sed} \cdot t}\right)\right\} \qquad (3.26)$$

The error function (erfc(a)), related to the Gauss-function, can be approximated according to Kinzelbach (1986) with the relation:

$$erfc(a) = \exp(-a^2) \cdot (b_1 \cdot c + b_2 \cdot c^2 + b_3 \cdot c^3 + b_4 \cdot c^4 + b_5 \cdot c^5) \qquad (3.27)$$

with:

$b_1 = 0.254829592$
$b_2 = -0.284496736$
$b_3 = 1.421413741$
$b_4 = -1.453152027$
$b_5 = 1.061405429$

and:

$$c = 1 / [1 + 0.327591117 \cdot \mathrm{abs}(a)]$$

for negative values for (a) it follows:

$$erfc(a) = 2 - erfc(a)$$

Figure 3.9 shows the graphical representation of the error function according to the approximation published by Kinzelbach (1986). This is the function complementary to the error function of Boudreau (1997):

$$erfc(a) = 1 - erfc(a) \qquad (3.28)$$

With this analytical solution of Fick's Second Law of Diffusion, the various curves in Figure 3.3 can now be calculated. On doing this, one will find that the outcome is exactly the same as in the corresponding calculations with the different numerical solutions presented in Chapter 15. Yet, the components of Figure 3.4, with the multiple change of the concentration in bottom water and the 'memory' of which is preserved over several cycles in the pore water fraction, is not accessible with this rather simple analytical solution.

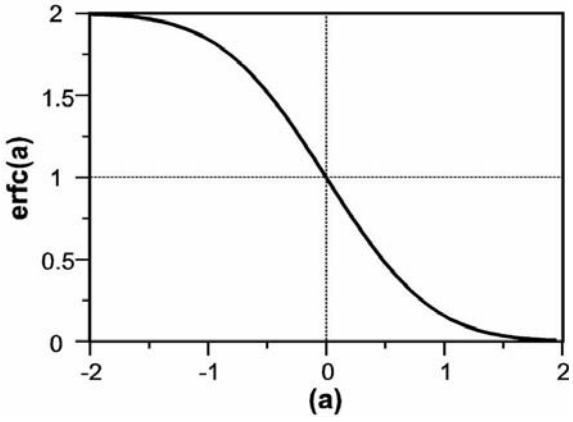

Fig. 3.9 Graphical representation of the error function in the approximated form after Kinzelbach (1986). This is the function complementary to the error function of Boudreau (1997). Additionally, in the form published by Boudreau (1997), the range of negative values for (a) is omitted, as this has little relevance for sediments.

Another example that can be assessed with this analytical solution results from the following considerations: At the beginning of the Holocene, about 10,000 years ago, the sea level rose more than 100 m as a result of thawing ice, which is equivalent to 3 % of the entire water column. This means that seawater had been previously about 3 % higher in concentration. If we assume a chloride concentration of 20,000 mg/l in the seawater today, and thus a mean concentration of 20,600 mg/l in seawater of the ice age, then we are able to calculate the non-steady state chloride profile in pore water with the application of the analytical solution of Equation 3.26.

From the result of this calculation (shown in Fig. 3.10) it follows that we will find just about one half of the ice age seawater concentration (20,300 mg/l) at a depth of 12 m below the sediment surface. If we consider that the reliability of our analytical methods lies at best somewhere around 1.5 %, the exemplary calculation reveals that the effect in pore water is almost at the limit of detection.

Other applications of such analytical solutions hardly make any sense, since, with the exception of chloride, practically all other parameters of pore water are strongly influenced by complex biogeochemical processes. In order to retrace these processes appropriately, analytical solutions for non-steady states in pore water are usually not sufficiently flexible. Hence, numeric solutions are mostly employed. These will be discussed later in Chapter 15 with regard to connection to biogeochemical reactions.

3.2.5 The Primary Redox-Reactions: Degradation of Organic Matter

Nearly all biogeochemical processes in young marine sediments during early diagenesis are directly or indirectly connected with the degradation of organic matter. This organic matter is produced by algae in the euphotic zone of the water column by photosynthesis. Usually, only a small part of the primary production reaches the sediment surface and of which only a small part is incorporated into the sediment where it becomes the driving force for most of the primary diagenetic redox-reactions (cf. Fig. 12.1).

The conceptual model for the degradation of organic matter in marine sediments was first proposed by Froelich et al. (1979). Although many more details, variations and specific pathways of these redox-reactions have become known in the meantime, this 'Froelich-model' of the primary redox-reactions in marine sediments is still valid

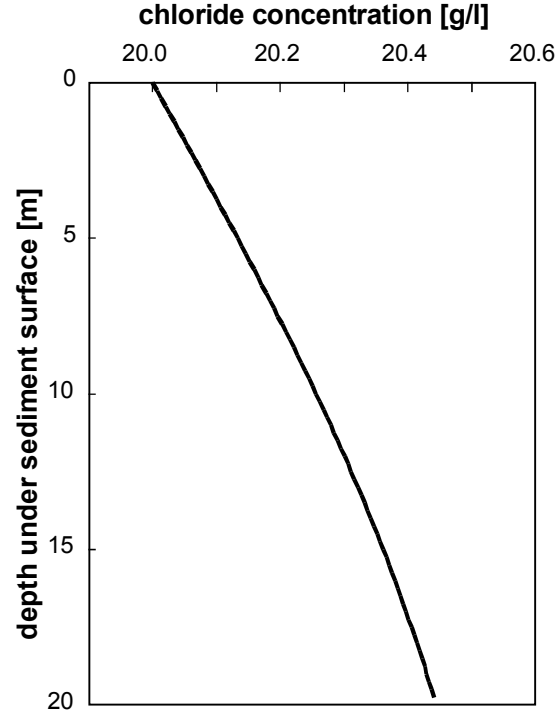

Fig. 3.10 Calculated concentration profile in the pore water of a marine sediment according to an analytical solution of Fick's Second Law of Diffusion. For reasons of simplification it was assumed that the seawater contained 3 % less chloride concentration since the beginning of the Holocene as a result of thawing ice. This lower concentration (20,000 mg/l) had enough time over 10,000 years to replace the higher concentration (20,600 mg/l) from the sediment.

(Fig. 3.11). Usually, these reactions are based on a very simplified organic matter with a C:N:P-ratio of 106:16:1 ('Redfield-ratio') as described by Redfield (1958) (cf. Sects. 5.4.4 and 6.2). The standard free energies for these model reactions are also listed in Figure 3.11 (cf. Sect. 5.4.1). The reactions in this figure are listed in order of declining energy yield from top to bottom.

Based on these reactions, a succession of different redox zones is established:

- Close to the sediment surface, dissolved oxygen is usually transported from the bottom water into the sediment either by molecular diffusion or as a result of biological activity. In this upper zone (the oxic zone), dissolved oxygen is the electron acceptor for the degradation of organic matter. Products of this reaction are carbonate, nitrate and phosphate derived from the nitrogen and phosphorus in the organic matter. For details of these reactions, see Chapter 6.

- Below the oxic zone follows a zone where manganese(IV) oxides in the solid phase of the sediment serve as electron acceptors. Products of this reaction are usually carbonate, nitrogen, phosphate and dissolved Mn^{2+}-ions in the pore water. These dissolved Mn^{2+}-ions are usually transported either by diffusion or by bio-activities to the oxid zone where manganese is re-oxidized and precipitates again as manganese(IV) oxide. These reactions belong to a manganese cycle, by which oxygen is transported into deeper parts of the sediment. For details of these reactions, see Chapter 11.

- Below this zone, nitrate serves as an electron acceptor, which is a product of the redox-

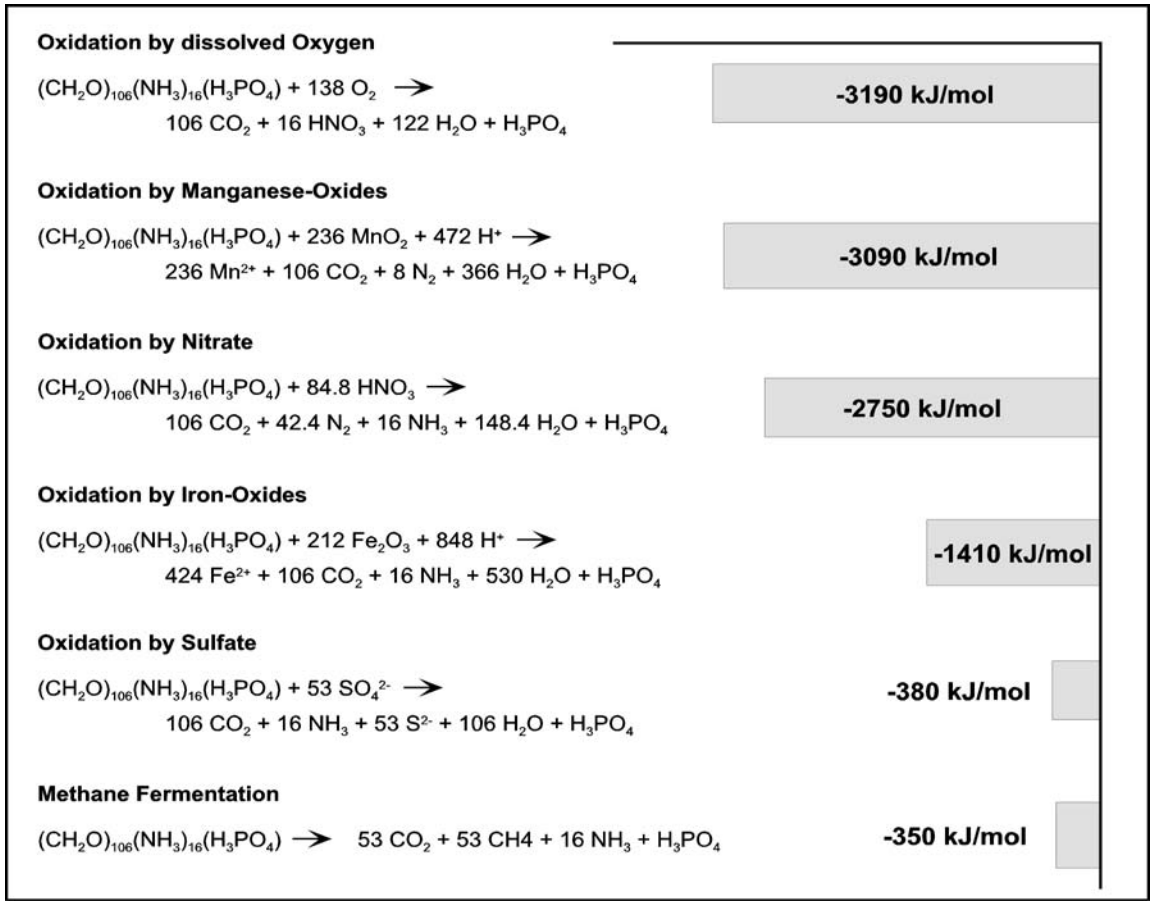

Fig. 3.11 Degradation of organic matter with different electron acceptors (Froelich et al. 1979). The columns represent the different amounts of resulting energy. The oxidation of organig matter by nitrate describes a reaction of the nitrate to elementary nitrogen and leaves the nitrogen of the organic matter as ammonium. Other reactions are possible (cf. section 6.3).

reactions in the oxic zone. Carbonate, phosphate and nitrogen, as well as ammonia are produced. The oxygen for the oxidation of organic matter in this zone is derived from the nitrate, produced in the oxic zone. In most cases, this process oxidizes at least one order of magnitude less organic matter than the reactions in the oxic zone. For details of these reactions, see Chapter 6.

- Below this zone, iron(III) oxides or iron(III) hydroxides in the solid phase of the sediments act as electron acceptors. For details of these reactions, see Chapter 7.

- Below this zone, dissolved sulfate serves as electron acceptor for the oxidation of organic matter, according to the 'Froelich-model'. Recent publications however showed that, in most cases, not organic matter is oxidized in this zone, but predominantly methane, which diffuses up from the deeper parts of the sediment (Niewöhner et al. 1998). For details of these reactions, see Chapter 8.

- The reaction with the lowest yield of standard free energy is methane fermentation with the products carbonate, methane, ammonia and phosphate. For details of these reactions, see Chapter 4.

3.3 Sampling of Pore Water for *Ex situ* Measurements

Ideally, one would prefer to analyze pore water exclusively under *in situ* conditions, as will be explained in Section 3.5, for the parameters that permit such procedure. The pressure change, and frequently the change of temperature as well, are usually coupled to *ex situ* measurement and exert a number of influences of varying potential. However, the *ex situ* measurement will certainly remain a necessity for quite a long time, with regard to most of the substances dissolved in pore water and especially for great depths below the sediment surface. This book is not the place to give a general review on sediment sampling techniques. Rather, the more common procedures for sediment sampling will be introduced with an emphasis put on pore water analysis. Then, the particularities, the possible errors as well as problems arising in the application of these sampling techniques, will be discussed.

The following section is concerned with the separation of the aquatic pore water phase from the solid sediment phase. As with all particularly problematic and error-inducing procedures, these various techniques have, depending on the case at hand, their specific advantages and disadvantages.

As a matter of course, one would want to analyze the obtained pore water as soon as it has been separated from the sediment to quantify the dissolved substances therein. In daily routine proceedings, compromises must be made since not all analyses can be carried out simultaneously, and since each and every analytical instrument is not present on board a ship. Thus, it will be necessary to describe the state of knowledge concerning pore water storage, transport and preservation.

3.3.1 Obtaining Samples of Sediment for the Analysis of Pore Water

A number of different techniques are available to withdraw samples from the marine sediment. Depending on the scientific question under study, a tool may be chosen that is either capable of taking the sample without harming the sediment surface or disturbing the supernatant bottom water (e.g. multicorer), or that punches out a large as possible sample from the sediment surface area (e.g. box corer), or one that yields cores from the upper less solid meters of the sediment which are as long as possible and most undisturbed (gravity corer, piston corer, box corer).

The Box Corer

The generic term 'box corer' denotes a number of tools of different size and design used in sampling marine sediments, mostly lowered from ships by means of steel wire rope to the bottom. All have a square or rectangular metal box in common which is pressed into the sediment by their own weight, or perhaps by additionally mounted weights. Upon lifting the tool from the sea-floor the first pull on the steel ropes is used to close the box by means of a shovel while it is still situated in the sediment. At the same time, an opening at the top is shut, more or less tightly, so that the bottom water immediately above the sediment is entrapped. The lateral dimensions of

small metal box corers are about 10 cm and they reach to that extent into the sediment. Larger box corers ('giant box corer') possess lateral dimensions and penetration depths of 50 cm, respectively.

Apart from the large sample volume that is collected, the giant box corer has the advantage that the *in situ* temperature is kept stable at least in the central zones of the sample, even if the sample is raised at the equator, from a depth of several thousand meters where the sediment is about 2° C cold. This is about the only advantage the box corer has with regard to the geochemical pore water analysis, whereas various disadvantages are to be considered. The shutter on top of the box corer is often not very tightly sealed, and thus the entrapped bottom water might become uncontrollably adulterated upon being raised upwards through the water column. On hoisting the loaded, heavy box corer out of the water, and during its later transportation, onto the deck of a ship, the sediment surface is mostly destroyed to an extent that at least the upper 1-2 cm become worthless for the subsequent pore water analysis.

The Multicorer

The multicorer is also employed from the ship using steel wire ropes and can also be used for all depths under water. On applying this tool, up to 12 plastic tubes (mostly acrylic polymers), each measuring a length of about 60 cm and about 5-10 cm in diameter, are simultaneously inserted approximately 30 cm into the sediment. As with the box corer, the first pull of the steel rope on lifting the appliance is used to seal the plastic tubes on both ends. These shutters are usually tight enough to ensure that the entrapped water will later represent the genuine bottom water.

Variations to the *in situ* conditions are caused in greater depths (about 1000 m and more) by the expansion of the pore water, which happens relative to the sediment, when the pressure diminishes. The uppermost millimeters of the profile are then distorted. Moreover, the temperature rise gives cause for disturbances upon raising the samples upwards out of great depths, in the course of which microbial activity is activated within the sediment sample, which is distinctly higher than under *in situ* conditions.

On the other hand, the multicorer provides, at present, the best solution for *ex situ* sampling of sediments from the sediment/water interface. The nitrate profile shown in Figure 3.7 was measured in pore water extracted from a sediment sample which had been obtained by using the multicorer. It shows clearly that the concentration profile can be measured in pore water with an almost undisturbed depth resolution of 0.5 cm per each sample. The reliable sampling technique using the multicorer also becomes evident upon comparing the *in situ* measured oxygen profiles (Holby and Riess 1996) with the *ex situ* measured oxygen profiles of a multicorer sample (Enneking et al. 1996). Both measurements (Figure 3.12) were conducted at the same location, at the same time, and lead to the same oxygen penetration depth and nearly identical oxygen concentration profiles. In both cases, the oxygen was measured with micro-electrodes.

Light-weight, High-momentum Gravity Corer

A light-weight, high-momentum gravity corer was first described by Meischner and Ruhmohr (1974) (cf. Figure 3.13). Somewhat modified variants

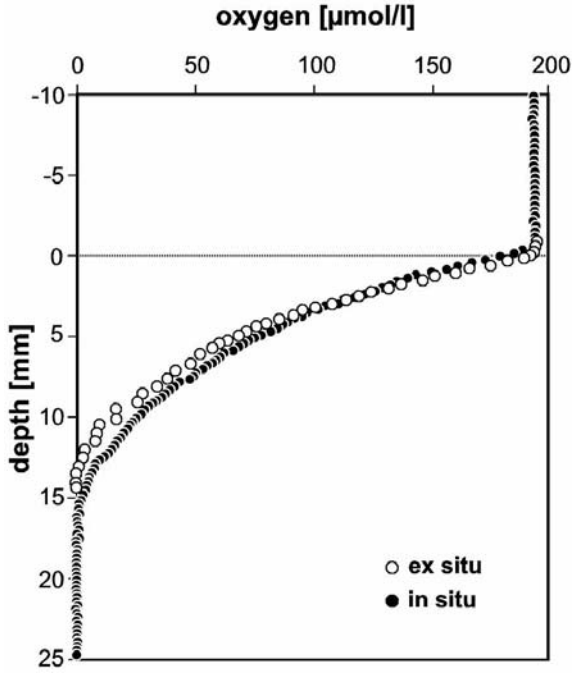

Fig. 3.12 *In situ* measured oxygen profile (dots, Holby and Riess 1996). In addition, an oxygen profile which was also measured ex situ with a micro-electrode is shown (circles, Enneking et al. 1996). The sample was obtained with a multicorer tube. Both profiles were measured in the course of the Meteor M 34/2 expedition at the same time and from the same location in an upwelling area off Namibia, at a depth of approx. 1,300 m below sea level.

made by various manufacturers are in use, whereby 'Rumohr corer' is a model frequently used. In most cases, a plastic tube (mostly an acrylic polymerization product) with a diameter of about 6 cm and a variable weight, is pressed 0.5 m to 1 m deep into the sediment. Upon pulling the tube out, the top aperture is shut whereby the bottom water that just covers the sediment becomes entrapped. The tube is not sealed at the bottom because (mostly) the closure at the top suffices to prevent the sediment from falling out. But, as soon as the high-momentum gravity corer is held out of the water, the bottom aperture of the tube must be sealed with an adequate rubber stopper.

The high-momentum gravity corer is most frequently used in shallow waters, on the shelf and from the decks of smaller ships, since it does happen from time to time that the bulk sample slides out of the bottom prior to its closure with the rubber stopper, and owing to the fact that the corer has only one tube that is filled with sample of sediment. In greater depths, and whenever a larger ship is available, the multicorer will be used in preference. Otherwise, the quality of the samples is entirely comparable. Furthermore, the high-momentum gravity corer is capable of extracting sample cores of up to 1 m in length.

The Gravity Corer and the Piston Corer

Upon using the gravity corer, a steel tube of about 13 cm in diameter is pressed between 6 m and 23 m deep into the sediment with the aid of a lead weight weighing about 3 - 4 t. Inside the steel tube, a plastic liner made of HD-PVC is situated that encompasses the core. Upon extraction from the sediment and raising the tube upwards through the water column, the tube's top aperture is kept shut by a valve. Below, another valve-like shutter - the core catcher - prevents the core material from falling out. Generally, cores of about 10 - 15 m in length are obtained in pelagic sediments, although at times they reach up to 20 m.

In a piston corer the same steel tubes and plastic liners are employed, but with a lighter lead weight. However, this corer is additionally equipped with a shear-action mechanism that moves a piston upwards through the tube when the tool is immersed into the sediment. The piston stroke produces a vacuum that facilitates the penetration of core into the tube. By using the piston corer, core lengths can be achieved which are frequently 20 - 30 m in length and thus several meters longer than the ones obtained with the gravity corer. Yet, it is observed that the cores obtained with the

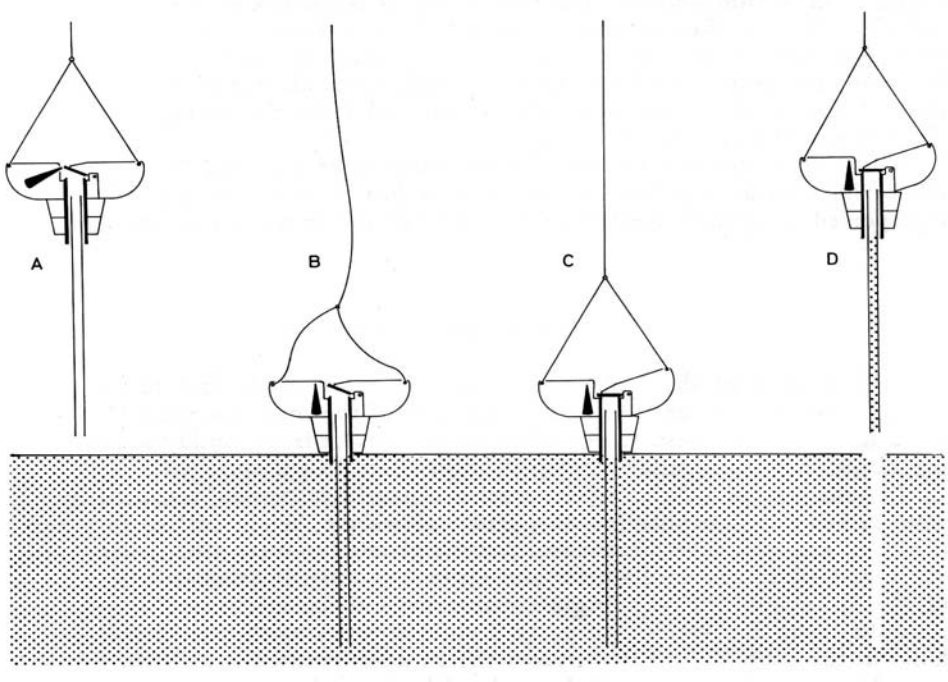

Fig. 3.13 Application of a high-momentum gravity corer (Meischner and Rumohr 1974) to obtain samples from marine sediments. The device can also be stationed on smaller vessels and is suited to extract almost unperturbed cores measuring 1 m in length to be applied in pore water analysis.

gravity corer and with the piston corer display the same stratigraphical depth zones of the sediment. It is therefore assumed that the cores sampled with the gravity corer are 'somewhat compressed' especially in the lower parts, whereas the piston corer produces cores that are 'somewhat extended' in length. How this comes into effect and what conclusions are to be drawn with regard to the pore water samples is yet completely uncertain. In the examined pore water profiles of sediments extracted with the gravity corer, there were no indications as to any noticeable compression to date.

Both sampling tools can only be operated from the decks of larger ships that are equipped with steel ropes and winches designed for managing weights of 10 - 15 tons. The author would personally always prefer using the gravity corer because its handling is easier, safer and faster; and because, especially in low latitudes, every minute counts in which the core is unnecessarily exposed to high temperatures on board the deck of the ship.

At least the upper 10 to 30 cm of the core length obtained with either tool is usually adulterated in that it is not appropriate for pore water analysis. The multicorer, high-momentum gravity corer, or at least the box corer should be employed in a parallel procedure to ensure that this layer will also be included as part of the sample. It should not be overlooked that, especially in the deep sea, sampling with two different tools 'at the same site' might imply a distance of several 100 m on the ocean floor. From this deviation considerable differences in pore water composition, and in some of the biogeochemical reactions close to sediment surface, are likely to result. Hence the specification as to 'same site' must be acknowledged with caution.

After the usage of either tool - the gravity corer and the piston corer - the sediment core obtained is immediately dissected into pieces of 1 m in length within the tube. Usually, the one meter long tubular pieces, tightly sealed with caps, are stored at *in situ* temperature prior to the subsequent further processing which is to be carried out as quickly as possible.

The Box-shaped Gravity Corer (Kastenlot)

In principle, the box-shaped gravity corer is not dissimilar to the above mentioned gravity corer. Here, a metal box with a core length of about 10 m and a lateral dimension of about 0.1 m up to 0.3 m is used instead of a steel tube with a plastic liner. The core box is shut by valves upon being pulled out of the sediment and is then hoisted upwards through the water column. The advantage of using the box-shaped gravity corer consists in providing a large core diameter, less perturbations due to the metal box's thinner walls, and by removing one side of the box it allows the sediment stratigraphy to be examined. The essential disadvantage in examining pore water samples consists in the fact that the core is distinctly less accessible, and that processing of the core under an inert atmosphere (glove box) is hardly feasible.

The Harpoon sampler

Sayles et al. (1976) have described a device that allows collection of pore water samples under *in situ* conditions. To achieve this, a tube is pressed about 2 meters deep into the sediment, like a harpoon. Then the pore water is withdrawn from various sections of the tube, through opened valves, and concomitantly passed through filters. The crucial step of separating sediment and pore water thus happens under *in situ* conditions. The obtained water samples are then ready to be analyzed *ex situ*. The concentrations which were measured by Sayles et al. (1976), however, do not differ greatly from those which were obtained 'from the same location' by expressing pore water under *ex situ* conditions.

Jahnke et al. (1982) used the same (or, at least a quite similar) tool in 4450 m deep waters of the equatorial Pacific, at approximately 0° to 10° N, and approximately 140° W (MANOP-site). Here, the distances between the locations in which the harpoon sampler was used and in which, for reasons of comparison, pore water was obtained by compression after the sampling was carried out with the box corer, amounted to 300 m to up to 3000 m. In measurements, which were corroborated several times, Jahnke et al. (1982) found similar concentrations of nitrate, nitrite, silica, pH, and manganese. Yet, the concentrations of $\sum CO_2$, alkalinity and phosphate were distinctly higher and displayed statistical significance.

3.3.2 Pore Water Extraction from the Sediment

In the following section, the separation of pore water from the sediment will be described. The necessary procedures will be described in the sequence in which they are employed. This is to

say, that we will begin with the filled tubes of the multicorer, the high-momentum gravity corer, or the meter-sized pieces of the gravity corer or piston corer. The entire processing steps described in the following for the core material should be performed at temperatures which should be kept as close as possible to the temperatures prevailing under *in situ* conditions.

In this context, the problem needs to be dealt with as to how long a tightly sealed core, which is exposed to the *in situ* temperature all the while, can be left to itself before it is processed without the occurrence of any essential perturbation in the pore water fraction. In order to extract pore water from a sediment core, such as is shown in Figure 3.1, and subsequently analyze and preserve it, even a practiced team would require several days. In most cases, a compromise needs to be found therefore, between the highest number of samples and most rapid processing.

A special situation prevailed in the case of the core shown in Figure 3.1, as the ship was cruising for a relatively long time after the core had been taken. Then the experiment was conducted that led to the results shown in Figure 3.1. The core was analyzed with an almost unusual high sampling density. As these procedures afforded plenty of time, and since it was unsure whether the pore water of the sediment core, which was stored at *in situ* temperature in the meantime, would change within the prospective processing time of ten days, the single pieces measuring one meter were intentionally *not* analyzed in a depth sequence, but in a *randomized* sequence. Thereby, the variations in the processing time had to become reflected as discontinuities in the corresponding data at the end of each meter interval. This had not been the case at either interval, from which it follows that a processing time of 10 days was obviously quite innocuous to the quality of the samples.

Analysis of Dissolved Gases

For some substances dissolved in pore water everything will be too late for a reliable analysis as soon as the sediment core lies freshly, but in a decompressed state, on the deck of the ship. This holds true predominantly for the dissolved gases.

In this respect, dissolved oxygen is relatively easy to manage, a circumstance which becomes evident upon comparing the *in situ* oxygen profile with the *ex situ* profile, both measured at the same sites (shown in Fig. 3.12). The reason for this similarity is that the relatively low concentrations, that are often below the saturation level, do not significantly assume a condition of oversaturation even after decompression. Notwithstanding, the results shown in Figure 3.12 reflect the situation too favourably, because differences of up to a factor of 2 were also observed between *in situ* and *ex situ* conditions with regard to the penetration depth of oxygen, and thus to the corresponding reaction rates as well. As to what extent these differences between *in situ* and *ex situ* conditions really exist, or whether such differences result from measurements carried out at not exactly identical sites, has not yet been sufficiently investigated.

The case is obviously similar for dissolved carbon dioxide whose concentration is essentially determined by the equilibrium of the aquatic carbonate phases. As for the alkalinity, no remarkable variations were found in measured values, even at high concentrations, when the measurements were performed successively on adjacent parts of the same sediment core (cf. alkalinity profile shown in Fig. 3.1).

The measurement of sulfide is much more troublesome, especially at high concentrations (It should be noted that H_2S is strongly toxic and that one can become quickly accustomed to its smell after prolonged presence in the laboratory. When working with sulfide-containing core material the laboratory should be ventilated thoroughly at all times!). As a general rule, everything already perceived by its smell is already lost to analysis. Since sulfide is readily analyzed by various methods in aqueous solution, most errors arise from decompression of the core and the subsequent separation of pore water from the sediment. As soon as decompression begins, a great quantity starts to degas, initially forming a finely distributed effervescence. In this condition, measurements can mostly still be carried out, however with less satisfactory results, provided that a specific volume of water-containing degassed sediment is punched out with a syringe and immediately brought into an alkaline environment (SAOB = Sulfur Anti-Oxidizing Buffer with pH > 13, after Cornwell and Morse 1987).

Even more difficult is the sampling and the analysis of sediments with a marked content of methane gas. In this particular case, a considerable amount of degassing of the sample occurs immediately upon decompression, thus not

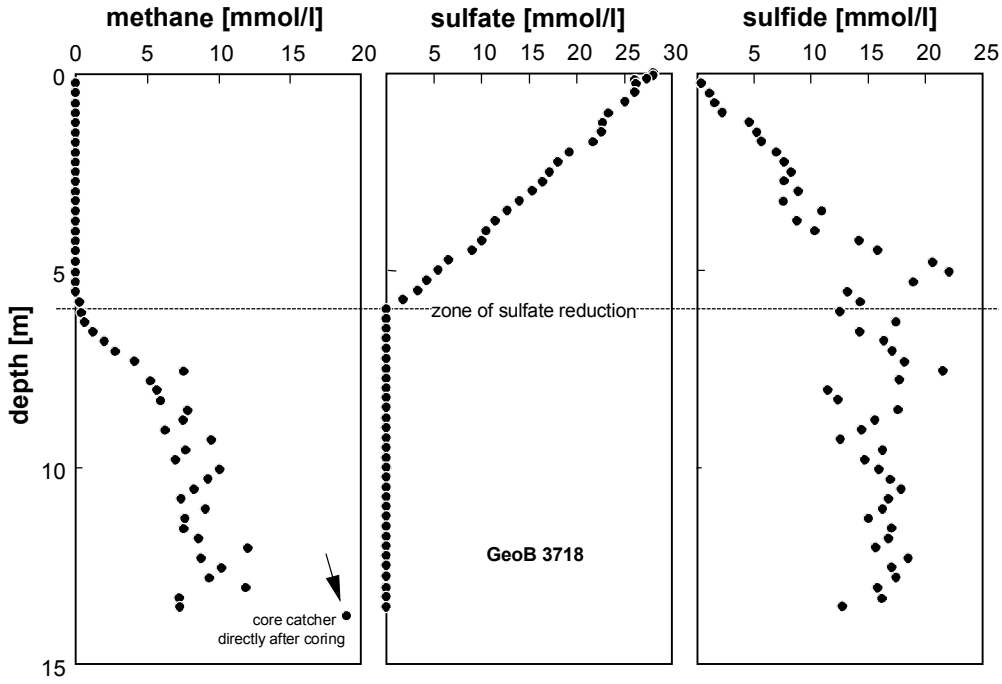

Fig. 3.14 Concentration profiles of pore water from anoxic sediments obtained from an upwelling area off Namibia at a water depth of approximately 1300 m. The analysis of sulfide and methane was carried out in samples that were punched out with syringes from small and quickly sawed-out 'windows' in the fresh sediment core. As for sulfide, these syringe-drawn samples were brought into an alkaline environment, whilst for methane analysis the samples were stored in head space vials for subsequent gas-chromatography analysis. The arrow points to a methane sample that originated from a sealed sediment core obtained by using a sample from the 'core catcher' (after Niewöhner et al. 1998).

permitting the measurement of the concentrations afterwards which are oversaturated under conditions of normal atmospheric pressure.

The results of measurements carried out on a core with high sulfide and methane concentrations are shown in Figure 3.14. The material was obtained in 1300 m deep water, in a high productivity zone of upwelling off the coast of Namibia. It can clearly be seen that in the depth zone of sulfate reduction, methane moving upwards meets with the downwards-diffusing sulfate, both substances displaying almost identical flux rates. These processes are dealt with more thoroughly in Chapter 8; at this point, just the sampling at the site of the core and the analytical sample treatment will be discussed.

As for both substances, sulfide and methane, concentrations found in the core are similar to that of sulfate. For the purpose of sampling, small 'windows' (2 x 3 cm) were cut into the plastic liners with a saw, immediately after the meter-long segments from the gravity corer were available. In each of these windows, 2-3 ml samples of fresh sediment were punched out with a syringe. For the determination of sulfide some of these sufficiently undisturbed partial samples were placed into a prepared alkaline milieu (see above, SAOB); for the determination of methane others were transferred directly to head space vials. The head space vials comprising a volume of 50 ml contained 20 ml of a previously prepared solution of 1.2 M NaCl + 0.3 M $HgCl_2$. The analysis of sulfide was performed by measuring the sample with an ion-selective electrode, whereas methane analysis was done in the gaseous volume of the headspace vials by gas-chromatography.

It is noticeable that the values in the profiles hardly scatter at the somewhat lower concentrations (about 4 mmol/l for methane and 7 mmol/l for sulfide, respectively). The values of the higher concentrations obtained in greater depths scatter more strongly and are altogether far too low. This became evident since the highest methane concentration is to be found in a sample that was not obtained from an extra sawed-out 'window', but from one that was previously taken directly from the core catcher at the lower open end of the core. As to the question concerning the potential

electron donor for sulfate reduction it was, however, of particular importance that methane could be reliably determined up to a concentration of 2-3 mmol/l, and that the upwards directed gradient reached into the zone of the reaction.

Opening and Sampling a Core under Inert Gas inside the 'Glove Box'

In order to extract the pore water from the sediment, the next step consists in opening, or rather cutting the meter-long segments previously excised from the sediment in a lengthwise fashion. In the case of multicorer or high-momentum gravity corer, the cores are pushed upwards by using an appropriate piston. Caution should be taken that anoxic sediments (easy to identify: if uncertain, everything that is not distinctly and purely brown in color) must not, by any means, come into contact with an oxygen-containing atmosphere in the course of sampling. Therefore the opening of the core segments must happen in an inert atmosphere, or, as the case may be, the core must be pushed from below into the 'glove box' where such an atmosphere is maintained. A 'glove box' that suits the purpose and that can also be easily self-made and adapted to the requirements of the prevailing conditions is described by De Lange (1988).

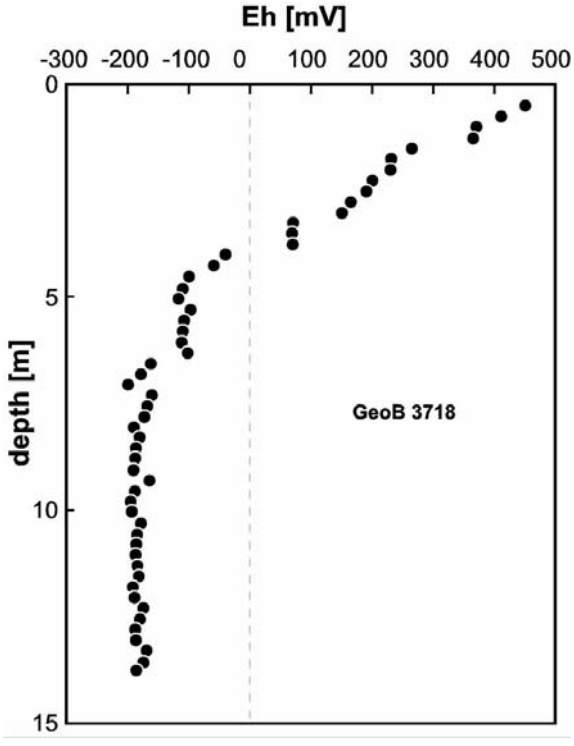

Fig. 3.15 Redox profile (E_H in mV) for the same core as shown in Figure 3.14. Values varying approximately +/- 30 mV must be allowed, whereas an otherwise plausible profile is measured in coherence to the prevailing redox processes.

The inert gases of higher molecular weight, as well as nitrogen, are suited for maintaining the desired inert gas atmosphere. As for nitrogen it must be considered that the least expensive version of the gas does not contain sufficiently low amounts of oxygen. Argon is often more useful, as ordinary argon that is used for welding usually has sufficiently low oxygen. A slight excess pressure in the 'glove box' maintains that, in the event of small leakage, the dissipation of gas might increase, yet the invasion of oxygen is securely prevented.

Measurement of E_H and pH with Punch-in Electrodes

In the glove box, the redox potential (E_H-value) and the pH value should be measured by applying punch-in electrodes directly to the freshly cut core surface. Suitable electrodes are available today from most suppliers because they are, for example, quite often used in the examination of cheese. However, there is a risk that the electrodes become damaged when larger particles or solidified kernels are present in the sediment sample.

The measurement of the pH-value is relatively easy to do since the function of the electrode can be checked repeatedly with the aid of appropriate calibration solutions. However it must merely be taken into consideration that the comparison with *in situ* measurements close to the sediment surface (cf. Sect. 3.5) may not necessarily lead to corroborated values, because the decompression within the core material has an immediate effect on the pH-value as well.

The redox potential (E_H-value in mV) is considered as a quite troublesome and controversial parameter, with regard to the actual measurement and to its consequences as well. The electrodes available for this purpose cannot be checked with calibration solutions. The occasionally mentioned calibration solutions that function on the basis of divalent and trivalent Fe-ions are not satisfactory, since they actually just confirm the electrode's electric functioning and, at the same time, 'shock' the electrode to such a degree that it may remember the value of the calibration solution for several days to come. The method of choice can

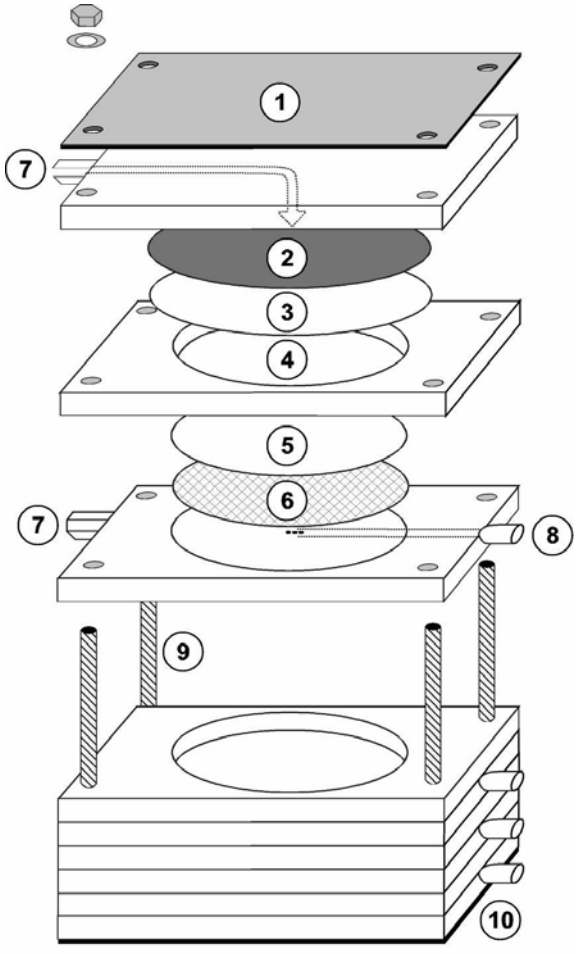

Fig. 3.16 Extractor used for the preparation of pore water from low density sediments (modified after Schlüter 1990).

only consist of using well polished Pt-electrodes and of being continually aware of the plausibility and variation of the measured values. Whenever necessary, the electrode must be substituted for another well-polished Pt-electrode. Useful recommendations as to the redox potential and its measurement are described by Kölling (1986, 2000) and by Seeburger and Käss (1989). A compilation of fundamentals, processes and applications of redox measurements in natural aquatic systems was published by Schüring et al. (2000). A measured E_H-profile is shown in Figure 3.15 for the same core as was shown in the previous Figure 3.14. It can be seen that the values scatter by approximately +/- 30 mV, but that otherwise a reasonable profile has been measured that is likely to contribute to an understanding of the redox processes occurring in the sediment.

Extraction of Pore water

For extracting pore water from the sediment, various authors have developed appliances that all have a common design (e.g. Reeburgh 1967; De Lange 1988; Schlüter 1990). In each case, a sediment sample volume of 100 - 200 ml is transferred into a container made of PE or PTFE which has on the bottom side a piece of round filter foil (pore size: 0.1 - 0.2 µm) measuring 5-10 cm in diameter. On top, the sample is sealed with a rubber cover onto which argon or nitrogen is applied at a pressure of 5-15 atm. The sediment sample is thus compacted and a part of the pore water passes downwards through the filter layer. By this method, a pore water sample comprising 30 - 50 ml can easily be obtained from the water-rich and less solid layers lying close to the sediment surface (Figure 3.16).

It might make sense, in case of anoxic sediments, to load the extractor in an inert atmosphere, or even better, to carry out the whole procedure in the glove box under these conditions. This becomes inevitable if, for instance, divalent iron is to be analyzed. The question of how fast this pore water sample needs to be analyzed for single constituents, will be discussed further in Section 3.4.

Certain losses of CO_2 from the sample into the inert atmosphere of the glove box, and due to that, an increase of pH and a precipitation of calcite seem to be inevitable. Only the combined *in situ* measurement of pH, CO_2 and Ca^{2+} will lead to a reliable measurement of the calcite-carbonate-system.

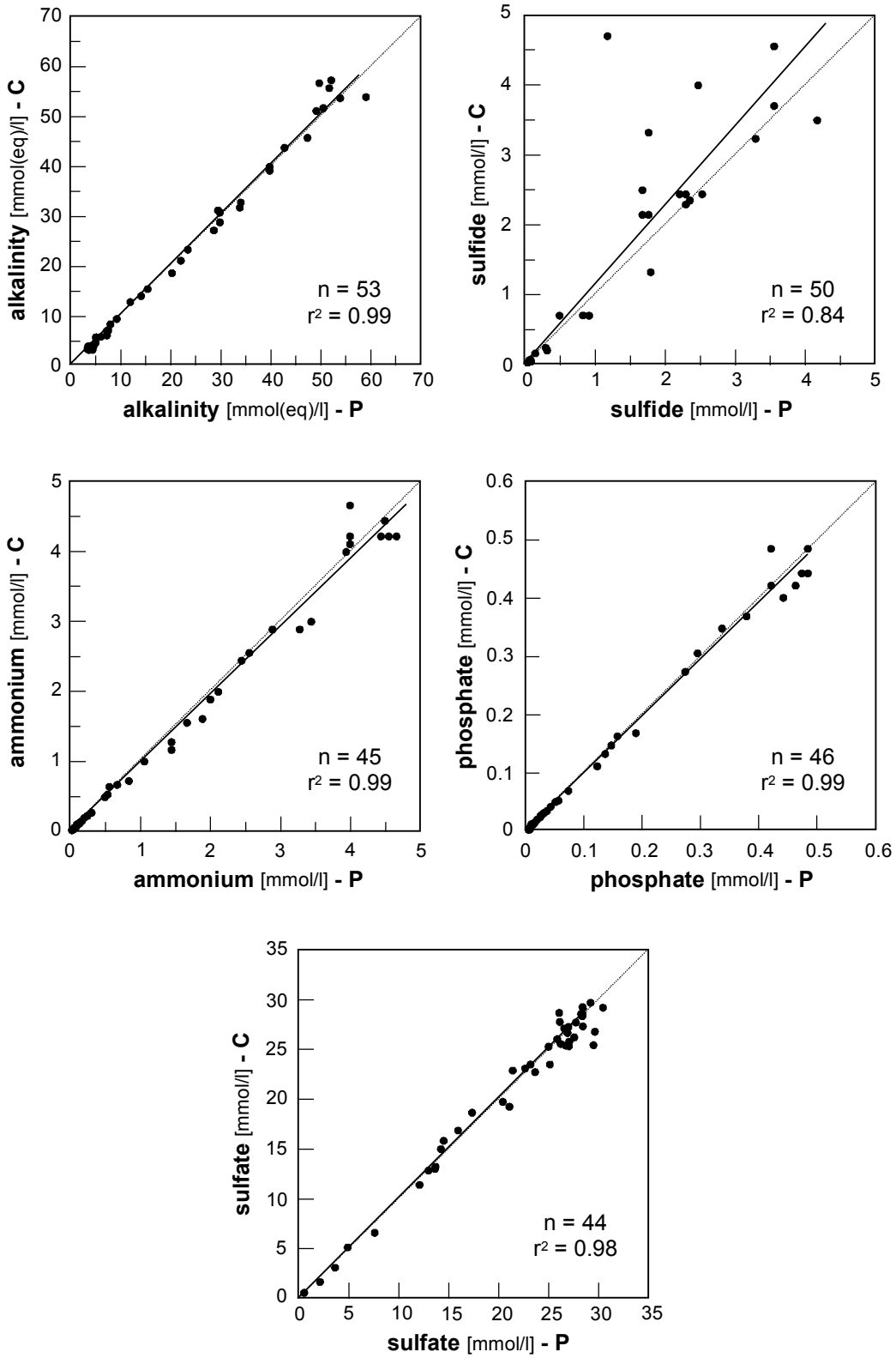

Fig. 3.17 Comparison of analyses after the preparation of pore water by compression and centrifugal extraction. In principle, there are no observable differences. The larger variation of the sulfide values might be attributed to the decompression of the core and/or might have occurred upon mounting the sediment into the press or into the centrifuge (after Schulz et al. 1994).

It should be noted that the choice of the filter used in the extraction procedure will determine what will be evaluated as dissolved constituent and what will be evaluated as particle or solid sedimentary phase. The entire field of colloids which had not yet been investigated thoroughly for marine sediments will therefore be either evaluated as part of the solid phase, or as dissolved constituents, depending on the analytical method employed, for instance, whenever this fraction is eliminated by the addition of hydrochloric acid. With respect to the available and customary methods, a lot of work still remains to be done on this subject.

Centrifugal Extraction of Pore water

Centrifugal extraction of pore water from sediments is a procedure not very frequently performed although it appears rather easy at first examination. Anoxic sediments must be loaded into tightly sealed centrifugation tubes, to be filled and capped under the inert atmosphere conditions of a glove box. But as these plastic tubes are often not sufficiently air-tight, the invasion of ambient air might affect the sample. Moreover, a cooling centrifuge must be regularly employed, since heating the sediment above the *in situ* temperature is by no means desirable. According to the opinion of most workers, the operation of a centrifuge on board a ship is rather troublesome and, most frequently, leads in various ways to the reception of high repair bills.

In the course of centrifugation, the sediment will be compacted in such a manner that a supernatant of pore water can be decanted. Generally, less pore water is gained as compared to pressure exertion. At any rate, the water must be passed through a filter possessing a pore-size of 0.1 to 0.2 µm. As for anoxic sediments, all these steps must be carried out inside the glove box and under an inert atmosphere. The measurements comparing centrifugal extraction and pressing techniques, which have been done so far, indicate that both methods yield quite identical values (see Fig. 3.17).

Whole Core Squeezing Method

A simple method of pore water preparation from a sediment core that is still kept in a plastic liner has been described by Jahnke (1988). In this method, which is also suitable for employing on anoxic sediments, holes are drilled into the tubes used in the multicorer, high-momentum gravity corer, or for a partial sample derived from the box corer. These holes are sealed prior to core sampling with plastic bolts and O-rings. As soon as the tube is filled with the sediment core, the device is mounted solidly permitting a piston from above and below to hold the core into position. Then, the prepared drainage outlets are opened and sample ports mounted to them, through which the pore water is drained off and passed through a filter. If the core is compressed either by the mechanical force of the pistons, or by infusion of gas, the filtered pore water runs off through the prefixed apertures and can be collected without coming into contact with the atmosphere, provided that such precautions were taken. Jahnke (1988) compares concentration profile examples of pore water obtained by the application of this method with pore water extracted centrifugally. Within the margins of attainable precision, these profiles must be conceived as truly 'identical'.

Pore-Water Extraction with Rhizons

Rhizons were originally developed to gain pore water samples which were then used to analyze the moisture of water in unsaturated soils (Meijboom and van Nordwijk 1992). A rhizon is supposed to function like an artificial root of a plant, hence its name is derived from *'rhiza'*, the Greek word for root. The device consists of thin tubes of various lengths (several cm) measuring approx. 2.5 mm in diameter. They are closed on one end and possess a connector on the other, over which a negative pressure is built up inside the tube. The tube material consists of a hydrophilic porous polymer, with a pore diameter of about 0.1µm. The actually quite instable tube is reinforced by an inserted piece of wire made of inert metal or durable plastic, allowing it to easily penetrate the soil or a sediment from the outside. In case of hard soils or sediments, a hole must first be punctured with a similarly shaped piece of metal or durable plastic.

The special property of the hydrophilic porous polymer is that, after short soaking in water, it becomes permeable to water - but not to air - once a vacuum is applied inside. Wherever the rhizon and the pore water come into contact, the negative pressure will draw the water into the interior, without allowing air to enter or destroy the vacuum. The water thus drawn inside will be simul-

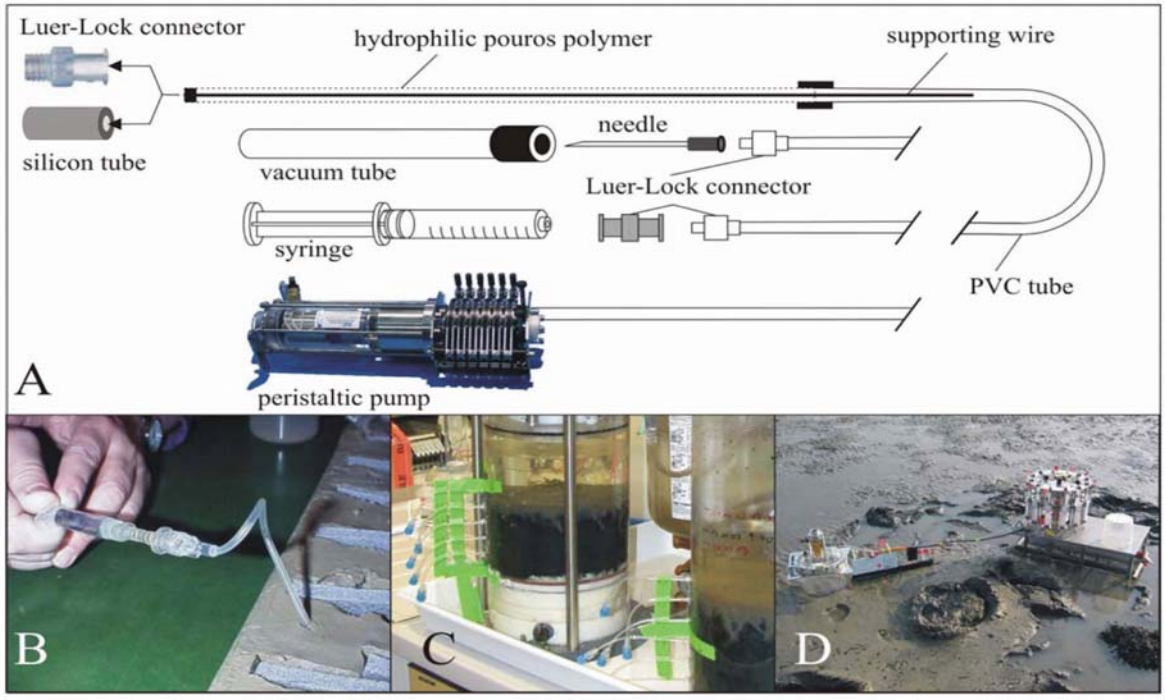

Fig. 3.18 Extraction of pore water from marine sediments with rhizons. (A) Basic construction of a rhizon including three different techniques to apply a vacuum. (B) Insertion into an opened core section. (C) Insertion into a multicorer core. (D) Application in the intertidal flat region, from the sediment surface (from: Seeberg-Elverfeldt et al. 2005).

.

taneously filtered through the 0.1µm wide pores, permitting its analysis without further treatment.

Seeberg-Elverfeldt et al. (2005) applied rhizons for the first time in marine environments and obtained very good results. Figure 3.18 shows two different application modes. The upper part of Figure (A) outlines three different possibilities how the vacuum may be generated. First, the outside connector of the rhizon can be equipped with a hypodermic needle which is punctured through a rubber seal into a previously evacuated glass vessel. This glass vessel will later contain the pore water being drawn into it. The vacuum can also be generated by means of a disposable syringe or a peristaltic pump. The lower part of Figure 3.18 demonstrates various modes of application, (B) on an open core section, (C) laterally inserted into a multicorer tube through small apertures, and (D) directly inserted into a naked sandflat sediment at low tide.

Previous applications of rhizons produced pore-water analyses which were very similar to those of compressed pore-water samples, except for the phosphate concentrations which were significantly higher when rhizons were used. This agrees with the observations made by Jahnke et al. (1982) upon drawing *in situ* samples with a harpoon sampler (cf. Section 3.3.1) and indicates that using rhizons to extract pore water obviously comes closer to the conditions *in situ* than by pressing or centrifugation. The method of extracting pore water with rhizons not only seems to be easier, but better as well.

Rhizons are manufactured and distributed by Rhizosphere Research Products (Dolderstraat 62, NL-6706 JG Wageningen, The Netherlands) or Eijkelkamp (P.O. Box 4, NL-6987 ZG Giesbeek, The Netherlands). Their price is markedly higher as compared to filters used for pressing pore water out of a sediment sample, however, they can be used more than just once. Special sizes and connectors will be supplied, if a larger number of pieces is ordered.

Sediments as yet Impossible to Sample

Whatever has been said so far as to the separation of pore water from sediments holds true only for fine-grained material that is, in most cases, still quite rich in water. Fortunately, this is what most marine sediments and almost all deep-sea sediments are. However, sediments consisting of pure sand might

give rise to problems (e.g. sands from the shelf or purely foraminiferal sands on the mid-ocean ridge). The reason for this is, first of all, that these sediments cannot be compacted by pressure exertion or centrifugation. Consequently, practically no water can be obtained from them at all. It is of even more importance that these sediments possess a high degree of permeability so that as soon as the corer is raised out of the water, the pore water (and sometimes the core material as well) is spilled out from the bottom. A simple method for the extraction of pore water from coarse, sandy material by centrifugation is described by Saager et al. (1990). However, this technique does not solve the problem of how to bring a specimen of sand and its pore water into a centrifuge unperturbed. Only the water which is present at the sampling site at a certain point in time can be collected, even if the abovementioned rhizons are applied. However, it must not be the same water which had been *in situ* at this location.

In situ measurements of pH-values and oxygen with the aid of landers are certainly still possible (cf. Sect. 3.5). But since the thin electrodes are likely to break off upon examining such material, these sediments are not very much favoured. Fortunately, this particular sediment type often contains only a small amount of decomposable organic matter, so that the biogeochemical processes of diagenesis do not display reaction rates as high as other sediment types. Upon sparing these sediments, the pore water geochemist usually suffers no great loss.

3.3.3 Storage, Transport and Preservation of Pore Water

In this section, the vessels in which the pressed or centrifuged pore water is kept until the time for analysis arrives will be briefly discussed. In Section 3.4 it will also be considered, in connection with the analytical methods, how much time one may allow to pass between pore water preparation and analysis. Hence the decision depends on whether immediate analysis is necessary, or whether the analyses can be made at a later time, provided that an appropriate preservation of the material has been accomplished.

Vessels, Bottles

Bottles made of polyethylene have proven to be quite useful for the storage of filtered pore water samples. In most cases the disposable 20 ml PE-bottles which are used in scintillation measurements are very much suited to the purpose. These bottles need not be cleaned prior to use, but are just briefly rinsed with the first milliliters that run out of the press or the rhizon. A second use does not really make sense considering the low price of these bottles and the obligatory amount of work effort and detergent to be invested in their cleaning. If several bottles are to be used for the storage of one and same sample, for instance when the sample volume is rather large due to water-rich sediments, precautions should be taken to be sure that the entire sample amount is homogenized prior to the analytical measurements, since differences in contrations between the first and the last drop of pore water are possible.

Preservation of Pore water Samples

Only the alkali-metals, sulfate, and the halogenides do not require any preservation of the samples prior to their analytical measurement at a later date. Otherwise, pore water samples that are not to be analyzed immediately can be preserved with regard to some dissolved substances, allowing a delayed analysis.

The concentrations of most cations - as long as different valences of iron, for instance, are not to be determined - are measurable after a longer period of time when the samples' pH is lowered by the addition of acid (mostly HNO_3) to a value of at least pH 2 or pH 3. Care should be taken that a sufficient amount of 'suprapur' quality acid is added. The required amounts can vary considerably depending on the alkalinity of the sample. Usually, concentrated acid will be used in order to prevent unnecessary dilution of the sample. It is also important that the sample has been previously passed through a filter of 0.1 - 0.2 µm pore-size, since the acid will dissolve all particles (and certainly the colloids that pass the filter as well).

As for the substances that are altered in their concentration by microbial activity, the toxification of sample is recommended. Mercury (II) salts are not very much favored since the handling of these extremely toxic substances - which are toxic also to man - requires special precaution measures. Chloroform is banned from most laboratories because it is considered as particularly carcinogenic. Thus, only the solvent TTE (trifluorotrichloro-ethane) remains which is frequently used in water analyses. The addition of one droplet usually suffices since only a small but sufficient proportion dissolves whereas the rest

remains at the bottom phase of the bottle. Even though the compound is not as toxic in humans as those previously mentioned, no one would think of pipetting the sample thus (or otherwise) treated by mouth. It is anticipated that these toxified samples have a shelf-life of about 4 weeks.

Previously, water samples were often frozen. This procedure is not at all suited for marine pore water because mineral precipitations might occur. These precipitations do not become soluble upon thawing the samples, hence the pore water samples have become irreversibly damaged.

3.4 Analyzing Constituents in Pore Water, Typical Profiles

This section does not claim to re-write the analytical treatment of sea water anew, nor is it intended to present this aspect as a mere recapitulation of facts which will be far from being complete. This task would by far exceed the possibilities and, above all, the scope of this book. However, analytical methods are subject to continual improvement and relatively fast changes so that many of the methods to be introduced here would soon become outdated. Therefore, only a short account of the current methods will be given, especially of those that demand comment on the specificity to marine pore water.

The analytical details of methods that are currently used in the examination of marine pore water can be looked up in the internet under the following address:

http://www.geochemie.uni-bremen.de

We will take it upon ourselves to continually update the internet page, to evaluate the suggestions we receive for improvement, and eventually make this information available to other researchers.

If we take for granted that, in each single case, the determination of oxygen dissolved in marine pore water, as well as the measurement of the pH-value, E_H-value, and certainly the measurement of the temperature as well, has already been performed, the following sequence of single analytical steps is applied to the pressed or centrifuged pore water samples:

- The titration of alkalinity must be carried out as quickly as possible, i.e., within minutes or maximally within one hour, as a replacement to the direct determination of carbonate. Especially when high alkalinity values are present (maximal values up to 100 mmol(eq) l^{-1} are known to occur in pore water, whereas sea water contains only about 2.5 mmol(eq) l^{-1}), the adjustment to atmospheric pCO_2 might induce too low alkalinity values due to precipitation of calcite within the sample.

- If sampling for methane and sulfide has been performed as described above (see Sect. 3.3.2 'Analyses of Dissolved Gases'), the analytical measurement of the already preserved samples does not have to take place immediately within the first few minutes. Yet, the analysis should not be deferred for more than a couple of hours.

- Analyzing compounds that are sensitive to microbial action (phosphate, ammonium, nitrate, nitrite, silica) should always be completed approximately within one day, if the samples were not preserved by the addition of TTE (trifluorotrichloroethane). Even in its preserved state, it is not recommended to store the sample for longer than four weeks. Storage is best in the dark at about 4°C; freezing the samples is not recommended.

- The determination of sulfate and halogenides is not coupled to any particular time. It must be ascertained that no evaporation of the sample is likely to occur. Other instances of sample perturbation are not known. Storage is best at about 4°C; freezing the samples is not recommended.

Photometrical Determinations, Auto-Analyzer

Most procedures for photometric analysis of sea water samples were described by Grasshoff et al. (1999). Owing to the quicker processing speed, and especially the need to apply lower amounts of sample solution, one would generally employ the auto-analyzer method to this end. The method is also described in the aforementioned textbook. The auto-analyzer can be either self-built or may be purchased from diverse commercial suppliers as a ready-to-use appliance. The analysis of marine pore water is generally characterized by small sample volumes and, as for some parameters, concentrations that are distinctly different from

sea water. Allowing for these limitations, the recipes summarized under the above internet-address have proven quite useful for the determination of phosphate, ammonium, nitrate, nitrite, and iron(II) in pore water.

Figure 3.1 shows the characteristic profiles of ammonium and phosphate concentrations that were measured by photometrical analysis of pore water obtained from reactive sediments possessing a high amount of organic matter. Both parameters demonstrate quite similarly shaped curves compared to alkalinity. Here, the ratio of the concentrations derived from both profiles lies close to the C:N:P Redfield-ratio of 106:16:1 and clearly documents their release into the pore water due to the decomposition of organic matter. A typical photometric nitrate profile in reactive sediment zones near the sediment surface is shown in the quantitative evaluation of fluxes and reaction rates presented in Figure 3.7.

Alkalinity

Usually, alkalinity is actually the ultimate parameter that is subject to a procedure of 'genuinely chemical' titration, in this regard as a proxy parameter for carbonate. A new spectrophotometric method for the determination of alkalinity was proposed by Sarazin et al. (1999). Mostly, alkalinity will be, for reasons of simplification, set equal to the total carbonate concentration, although a number of other substances in pore water will contribute to the titration of alkalinity as well. Most geochemical model programs (cf. Chap. 15) foresee the input of titrated alkalinity as an alternative to the input of carbonate. The model program will than calculate the proportion allocatable to the different carbonate species.

Another problem arising from titration of alkalinity in a pore water sample usually consists in the fact that samples with very small volumes cannot easily be used. Most ocean chemists will be accustomed to the titration of a volume of 100 ml, or at least 10 ml. Under certain circumstances, a pore water sample obtained from a definite depth might contain in total not more than 10 ml, hence, at best, merely 1 ml needs to be sacrificed for the titration of alkalinity. This requires that markedly pointed and thin (thus easily breakable) pH-electrodes are used. These are immersed, together with an electronically controlled micropipette, into a small vial so that a tiny magnetic stirrer bead still has enough room to fit inside as well.

Mostly, an adequate amount of 0.001 M hydrochloric acid will be added to a previously pipetted volume of 1 ml, thus the pH will be brought to a value of about 3.5. Since the dilution of the pre-pipetted volume must be considered, the alkalinity (Alk) is calculated according to the following equation:

$$Alk = [(V_{HCl} \cdot C_{HCl}) - 10^{-pH} \cdot (V_0 + V_{HCl}) \cdot f_{H^+}^{-1}] \cdot V_0^{-1} \quad (3.29)$$

in which V_{HCl} describes the volume of added hydrochloric acid, C_{HCl} represents the molality of the added hydrochloric acid, pH denotes the pH value the solution attains after the addition of hydrochloric acid, V_0 is the pre-pipetted sample volume, and f_{H^+} the activity coefficient for H^+-Ions in solution. The activity coefficient f_{H^+} can be determined according to the method described by Grasshoff et al. (1999), or calculated by employing a geochemical model (e.g. PHREEQC, cf. Chap. 15). The Equation 3.29 was also formulated in the first edition of the textbook published by Grasshoff et al. (1983) [equation 8-25 on page 108]. It must be pointed out that a very misleading error has unfortunately found its way into the equation in this reference. This error is hardly noticeable when low concentrations are prevalent in ocean water, or when the sample volumes are comparably large. In the case of high concentrations in combination with small sample volumes, however, alkalinity values will be calculated that are prone to an error of more than a factor of 2. For this reason, the equation is presented here in its correct form.

Flow Injection Analysis

A very interesting method to analyze total carbon dioxide and ammonium in pore water was introduced by Hall and Aller (1992). In this method, a sample carrier stream and a gas receiver stream flow past one another, separated only by a gas-permeable PTFE (Teflon®) membrane. For determining the total CO_2 , the sample carrier stream consists of 10-30 mM HCl. To this stream, the sample in a volume of about 20 µl is added via a HPLC injection valve. The carbon dioxide traverses the PFTE membrane and enters the gas receiver stream which, in this case, consists of 10 mM NaOH. The CO_2 taken up by the gas receiver stream causes an electrical conductivity change that can be determined exactly in a micro-sized continous flow cell.

For the analysis of ammonium, the sample carrier stream consists of 10 mM NaOH + 0.2 M Na-citrate. This converts ammonium into NH_3-gas which penetrates the PTFE membrane and travels into the gas receiver stream, in this case consisting of 50 µm HCl. Here as well, an electric conductivity cell is used for the measurements. To provide a steady and impulse-free flow of the solutions, a multichannel peristaltic pump is used. The flow rates in both cases were set to approx. 1.4 ml min^{-1}.

These very reliable and easy to establish analytical procedures for the determination of these two important parameters of marine pore water are of special interest, because they require only small sample amounts and because a reliable analysis is obtained over a broad range of concentrations.

Ion-selective Electrodes

Ion-selective electrodes were accepted in water analysis only with great reluctance, despite of the advantages that had been expected on their introduction about 20 years ago. The reasons for this were manifold. The analytical procedure is inexpensive only at first sight. As has been confirmed for some electrodes (especially when its handling is not always appropriate), aging sets in soon after initial use which becomes noticeable with decreased sensitivity, low stability of measured values, and prolonged adjustment times.

With regard to marine pore water, ion-selective electrodes were successfully applied in the determination of fluoride (standard addition method) and in the analysis of sulfide within a mixture of sediment and pore water processed into SAOB-buffer (cf. Sect. 3.3.2). Figure 3.1 shows a typical profile of fluoride measured with an ion-selective electrode in pore water. The total sulfide profile shown in Figure 3.14 was measured in the way described above, by using an ion-selective electrode. The measured values occasionally display considerable variations, probably on account of the sediment's decompression and thereafter they might be produced upon withdrawing the sample from the core. They do not necessarily come about during the course of the analytical measurement.

Ion-Chromatography

The analysis of chloride and sulfate in marine pore water samples after an approximately 20-fold dilution is a standard method for normal ion-chromatography (HPLC), so that no further discussion is needed here. Considering the very dilute sample solution and the low sample amount required in ion-chromatography, the applied quantity of pressed or centrifuged pore water is negligibly small. However, the high background of chloride and sulfate which is due to the salt content in sea water prevents, with or without dilution, the determination of all other anion species by ion-chromatography. The sulfate profiles measured with this method are shown in the Figures 3.1, 3.6, and 3.14. Since the chloride profiles are mostly not very interesting, because they reflect practically no early diagenesis reactions at all, they can be consulted for control and eventually for correction of the sulfate profiles, whenever analytical errors have emerged in the course of their concomitant determination, e.g. due to faulty dilutions, or mishaps occurring in the injection valve of the machinery.

ICP-AES, AAS, ICP-MS

Generally the alkali metals (Li, Na, K, Rb, Cs), the alkali earth metals (Mg, Ca, Sr, Ba) and other metals (e.g. Fe, Mn, Si, Al, Cu, Zn, Cr, Co, Ni) are determined in the acid-preserved pore water samples. Analytical details depend on the special conditions provided by the applied analytical instruments ICP-AES (Inductively Coupled Plasma Atomic Emission Spectrometer), ICP-MS (Inductively Coupled Plasma Mass Spectrometer), or AAS (Atomic Absorption Spectrometer) of the respective laboratory. A discussion of details is not appropriate in this chapter. In most cases dilutions of 1:10 or 1:100 will be measured depending on the salt content in marine environments, so that the required sample amounts are rather low.

Gas-Chromatography

The quantification of methane with the aid of gas chromatography (FID-detection) is an excellent standard method, which therefore does not need any further discussion. The main importance is the immediate withdrawal of a sediment/pore water sample as already mentioned in Section 3.3.2. This sample is placed into a 50 ml-headspace vial with a syringe in which the sample is combined with 20 ml of a prepared solution of 1.2 M NaCl + 0.3 M $HgCl_2$. After equilibrium is reached in the closed bottle between the methane concentration in the

gaseous phase and its concentration present in aqueous solution (at least one hour), the gas phase is ready to be sampled by puncturing the rubber cap that seals the vial with a syringe.

3.5 *In-situ* Measurements

The desire to measure the properties of a natural system, or profiles of properties, *in situ*, appears to be obvious whenever the system becomes subject to a change as a result of the sample collection procedure. In principle, this is applicable to many aquatic geosystems. Especially where solid and aquatic phases come together in a limited space, this boundary constitutes the site of essential reactions. Such a site is the surface boundary between bottom water and sediment. An essential biogeochemical process of early diagenesis is exemplified by the permeation of oxygen into the young sediment by diffusion, but also by the activity of organisms. The oxygen in the sediment reacts in many ways (cf. Chaps. 5 and 6). In part, the oxygen is depleted in the course of oxidizing organic matter, in part, upon re-oxidizing various reduced inorganic species (e.g. Fe^{2+}, Mn^{2+}).

In organic-rich and highly reactive sediments, the depletion of oxygen previously imported by means of diffusion already occurs in the uppermost millimeters of the sediment (cf. Sect. 3.5). However, these organic-rich and young sediments are mostly extremely rich in water (porosity values up to 0.9) and very soft, so that every sample removal will most likely induce a perturbation of the boundary zone which is, in a crucial way, maintained by diffusion.

Moreover, the actively mediated import of oxygen into the young sediment, which runs parallel to diffusion, and which is transported by the organisms living therein, will function 'naturally' only as long as these organism are not 'unnaturally' treated. Any interference caused by sampling is certain to be regularly coupled to a change of temperature, pressure and the quality of the bottom water, and thus means a change in the 'normal' living conditions. Here as well, it is of special interest to measure the active import of oxygen into the sediment governed by biological activity *in situ*. (cf. Sect. 3.6). An overview of the literature references and the state of knowledge related to the *in situ* measurement methods and techniques applied to capture the biogeochemical processes in the water/sediment transition zone has been provided by Viollier et al. (2003).

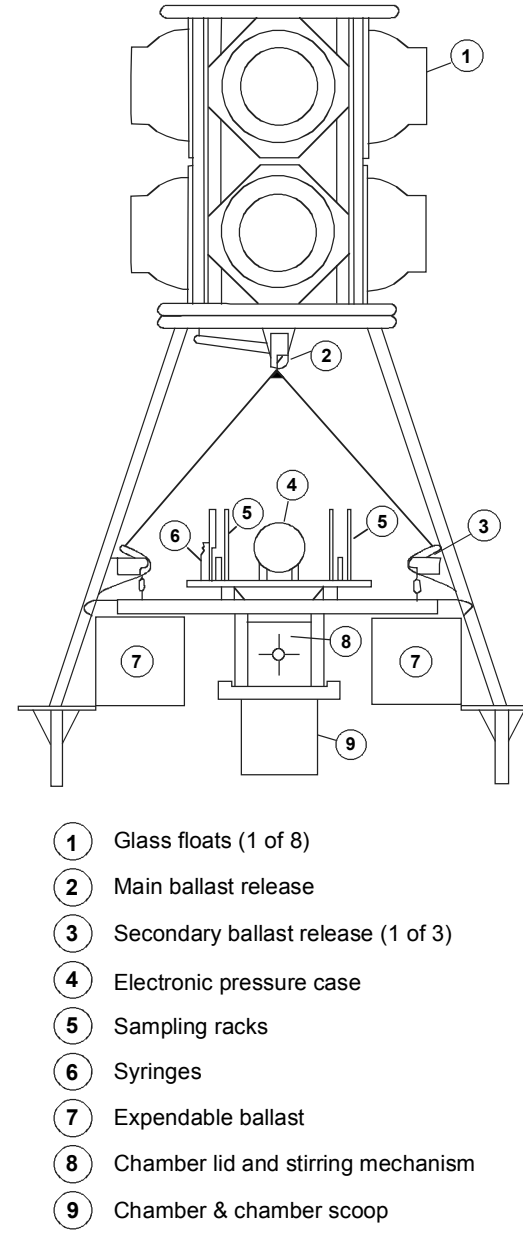

Fig. 3.19 Schematic representation of a Lander System which is also used in the deep sea. The machinery sinks freely, without any attachment, to the ocean floor where it carries out measurements and returns back to the surface after the release of ballast. The depicted version stands about 2-3 m in height. It is designed to conduct incubation experiments at the ocean floor, yet similar landers are used to record/monitor in situ microprofiles of the oxygen concentration through the sediment/bottom water boundary layer. The perspective shows only two of the three feet upon which the lander stands (after Jahnke and Christiansen 1989).

Lander Systems

In some very shallow waters the *in situ* measurement at the sediment/bottom water boundary might be achieved from a ship, or by using light diving equipment. However, so-called 'Lander systems' have been developed for applications in greater depths and, above all, in the deep sea. Lander systems are deployed from the ship and sink freely, without being attached to the ship, down to the ocean floor where they softly 'land'. Standing on the bottom of the ocean they conduct measurements (profiles with microelectrodes), experiments (*in situ* incubations), and/or remove samples from the sediment or the bottom water. When the designated tasks are completed, ballast is released and the whole system emerges back to the surface to be taken on board.

The lander technique described above is, especially in the deep sea, more easily outlined in brief theory than to put into operation, as the involved workers need to invest a considerable amount of construction effort and operational experience in the lander systems so far used.

The problems which cannot be discussed here in detail consist of, for example, deploying the device into the water without imparting any damage to it, conducting the subsequent performance of sinking and landing at the proper speed, keeping the lander in a proper position, recording and storing the measured values, the timing of ballast release and thus applying the correct measure of buoyancy all the way up to the ocean's surface, and finally, the lander's retrieval and ultimate recovery on board of the ship. The correct performance of the *in situ* measurements is not even mentioned in this enumeration. In Figure 3.19 such an appliance is shown according to Jahnke and Christiansen (1989) which is very similar to the lander used by Gundersen and Jørgensen (1990) as well as Glud et al. (1994). A survey and comparative evaluation of 28 different lander systems is given by Tengberg et al. (1995) who also delivers an historical account on the development of landers. One of the first publications

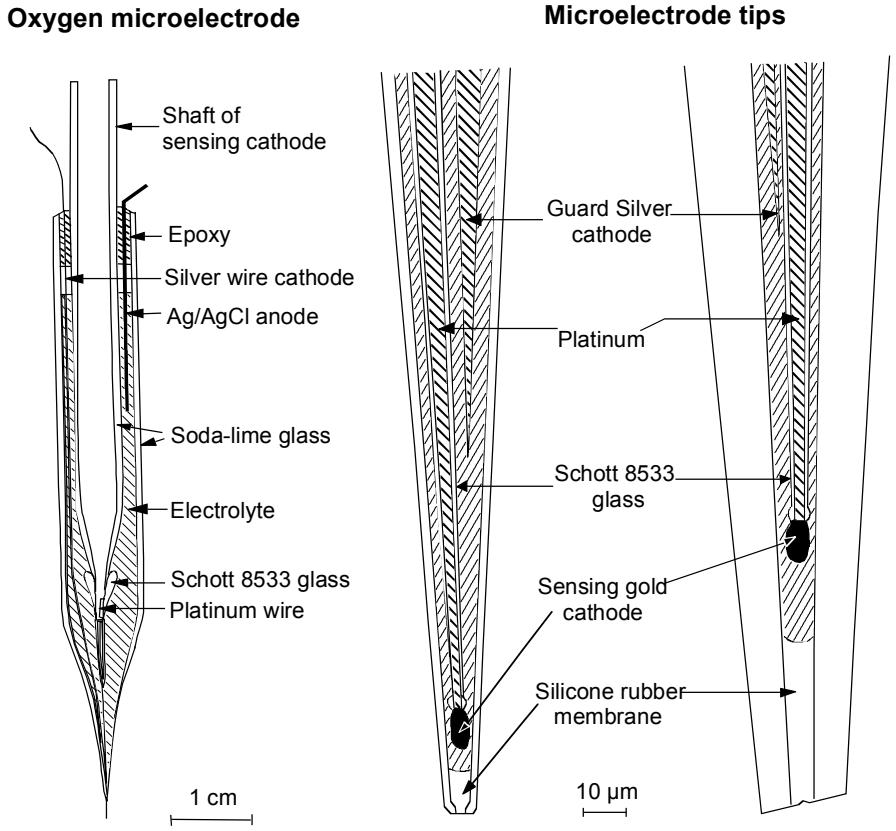

Fig. 3.20 Construction of an oxygen electrode equipped with a Guard-cathode (after Revsbech, 1989).

on the measurements of oxygen microprofiles in sediment/bottom water boundary layers of the deep sea is the report by Reimers (1978). Jørgensen and Revsbech (1985), subsequently, Archer et al. (1989) and Gundersen and Jørgensen (1990) were the first to measure a diffusive boundary layer using landers. The first *in situ* incubations using a lander were carried out by Smith Jr. and Teal (1973).

Profiles with Microelectrodes

A profile measured *in situ* with an oxygen microelectrode has already been presented and quantitatively evaluated in Figure 3.5. Such measurements became feasible only after oxygen electrodes had been developed that could measure oxygen concentrations at the sediment/bottom water boundary layers with a depth resolution of about 20 to 50 µm. It is also important to note that the measurement is carried out without being influenced by the oxygen depletion of the electrode. The development of the electrodes is closely linked to the name of N.P. Revsbech (Aarhus, Denmark) and is described in the publications of Revsbech et al. (1980), Jørgensen and Revsbech (1985), Revsbech and Jørgensen (1986), Revsbech (1989) and Kühl and Revsbech (2001).

The basic construction principle underlying the function of an oxygen microelectrode is shown in Figure 3.20, after a publication by Revsbech (1989). It is evident that such an electrode cannot be built without considerable practiced skill and experience - and they have to be either self-made or purchased at a rather high price. It is furthermore evident that such microelectrodes are extremely sensitive and break easily as, when they either hit a rather solid zone in the sediment, contain slight imperfections from manufacturing, or are handled with the slightest degree of ineptitude.

A construction unit is shown in Figure 3.21 that permits the integration of microelectrodes in a lander along with the necessary mechanical system, the electronic control and data monitoring equipment. It is of utmost importance that this unit is built into the lander in such a manner that the measurements will begin above the sediment surface, then insert the electrodes deep enough into the sediment, allowing later derivations of the essential processes from the concentration profile. This requires, among other pre-requisites, the correct estimation as to how deep the feet of the lander will sink into the sediment. If the sediment is firmer than expected, only the bottom water might be measured; whereas, if the sediment is softer than expected, the profile might begin within the sediment. Thus,

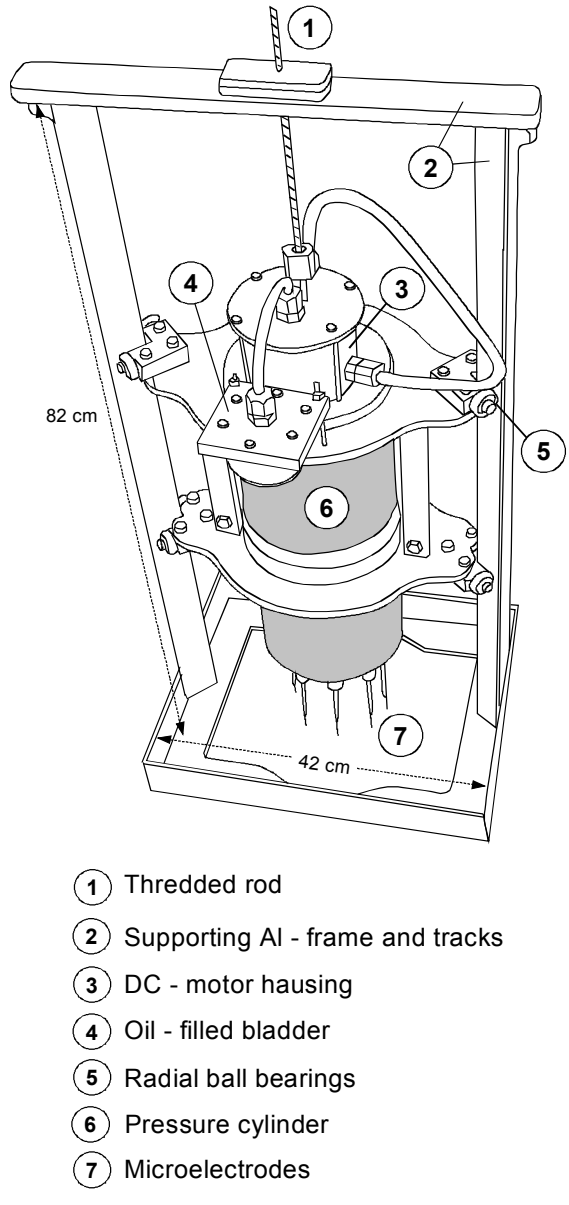

Fig. 3.21 Schematic representation of the mechanic and electronic unit applied to microelectrodes in a lander system. The round pressure cylinder contains the electronic control equipment and the data monitoring device, to the bottom of which various vertically positioned microelectrodes are mounted. The entire cylinder is lowered with the aid of a stepper motor and a corresponding mechanical system in pre-adjustable intervals so that the electrodes begin measuring in the bottom water zone and then become immersed into the sediment (after Reimers 1978).

much experience and many aborted profiles stand behind those profiles which are now shown in Figures 3.5 and 3.22.

By using such electrodes it is now possible to describe a diffusive boundary layer at the transition zone between the sediment and the bottom water with a sufficient degree of depth resolution (Fig. 3.22). This layer characterizes a zone which lies directly over the sediment and is not influenced by any current. Instead, a diffusion controlled transport of material characterizes the exchange between bottom water and sediment. This layer which possesses a thickness of 0.2 - 1 mm still belongs to the bottom water with regard to its porosity (100 % water), but due to its diffusion controlled material transport, it belongs instead to the sediment. In both oxygen profiles shown on the left in Figure 3.22, the location of the diffusive boundary layer is indicated. Above this layer, the bottom water is agitated, resulting in an almost constant oxygen concentration. A constant gradient is found within this layer because this is where only diffusive transport takes place, but no depletion of oxygen occurs. It may be of interest in this regard that the better known diffusion coefficient for water (D^{sw} in Equation 3.5 and in Table 3.1) must be applied for this diffusive transport, and not the diffusion coefficient for the

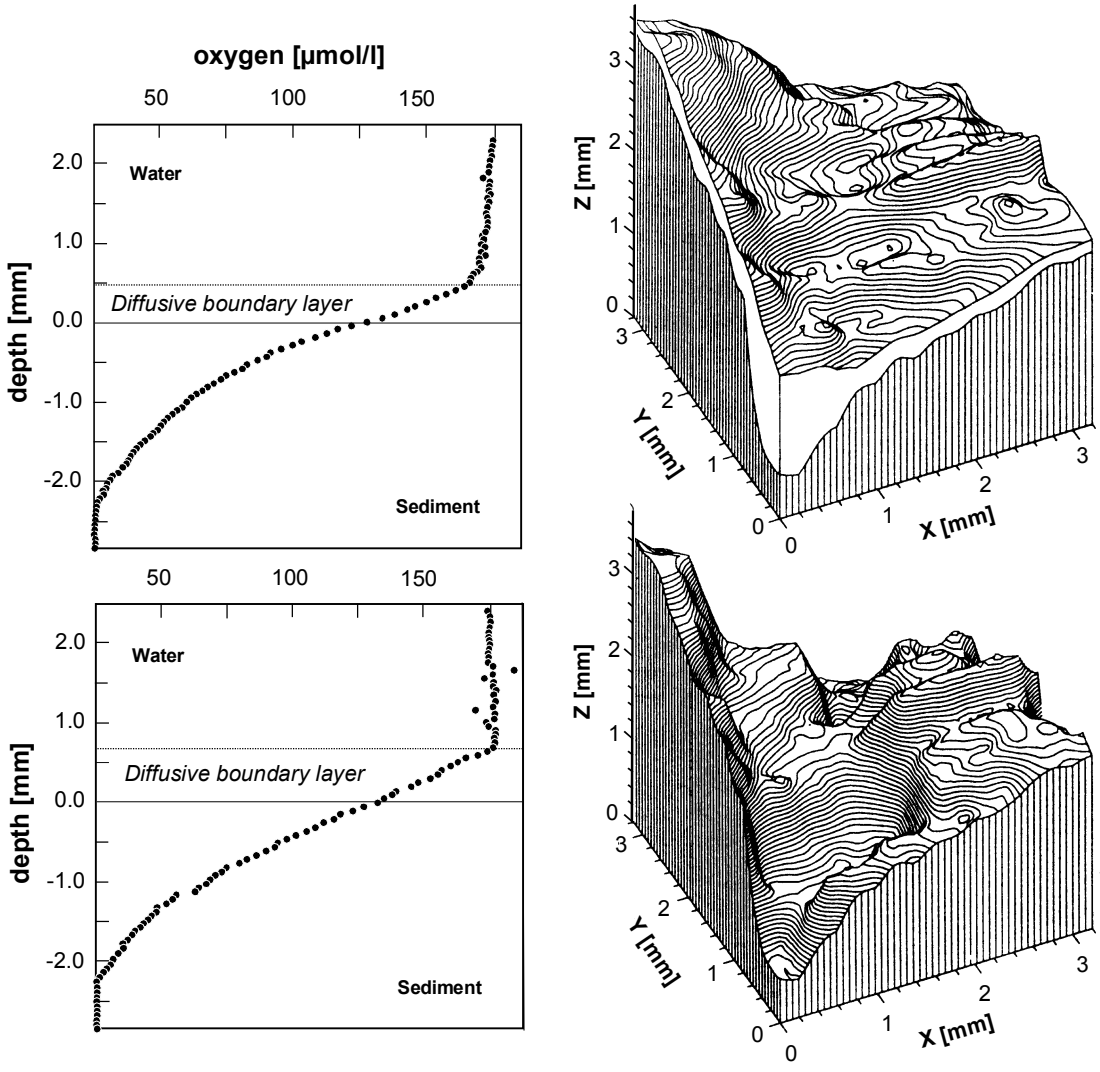

Fig. 3.22 Diffusive boundary layer at the sediment/bottom water transition measured with oxygen microelectrodes. Profiles are shown in both representations on the left. The two representations on the right show the respective spatial patterns. In the above right corner, the surface is shown, whereas the subsurface of the diffusive boundary layer is shown below (after Gundersen and Jørgensen 1990).

sediment (D_{sed}). Since the entire diffusive transport from the bottom water to the sediment crosses this transitory layer, measurements within the layer allow for especially reliable estimations of the oxygen consumption in the sediment.

To date, extremely good results have been obtained with oxygen microelectrodes in sediments with high reaction rates, because the essential processes can be analyzed only here, with profiles most often reaching a few centimeters into the sediment. The lower ends of these profiles are frequently marked by breakage of the electrodes. In sediments displaying less vigorous turnovers, the measurement mostly includes just one single oxygen concentration gradient, not reaching into the penetration depth for oxygen.

Less frequently, pH-profiles are published in literature when compared to the oxygen profiles. The details as to their shapes and their underlying processes are not yet sufficiently understood. Additionally, a reliable calibration under the given pressure conditions has not been accomplished for *in situ* pH-measurements. Consequently, only relative values are measured within one profile. Electrodes measuring H_2S can also be built as microelectrodes. However, they are only suited for *in situ* measurements when H_2S reaches close enough to the sediment surface.

Optodes

Apart from the great advantages of electrodes - they have practically opened a domain of the aquatic environment which was previously not accessible to measurement - the disadvantages should be mentioned as well. On the one hand, only the three aforementioned types are applicable (O_2, pH, H_2S), on the other hand, these electrodes are commercially available only at a rather high price or must be self-made. The manufacturing of one electrode demands - if one has the necessary experience – half a day up to one full day of labor. Additionally, the electrodes tend to break easily. Thus, in the experimental work that led to the publication by Glud et al. (1994) about 50 to 60 (!) microelectrodes were 'used up'.

It therefore appears to be reasonable to look for other methods and other measurement principles. Such an alternative principle consists of the construction of the optode (by analogy: electrodes as functioning electrically, optodes functioning optically). The basic principle (Fig. 3.23) consists of the conductance of light possessing a specific wavelength (450 nm) via glass fibers to the site of measurement. The tip of the glass fiber is surrounded by a thin layer of epoxy resin that contains a dye (ruthenium(II)-tris-4,7-diphenyl-1,1-phenanthroline).

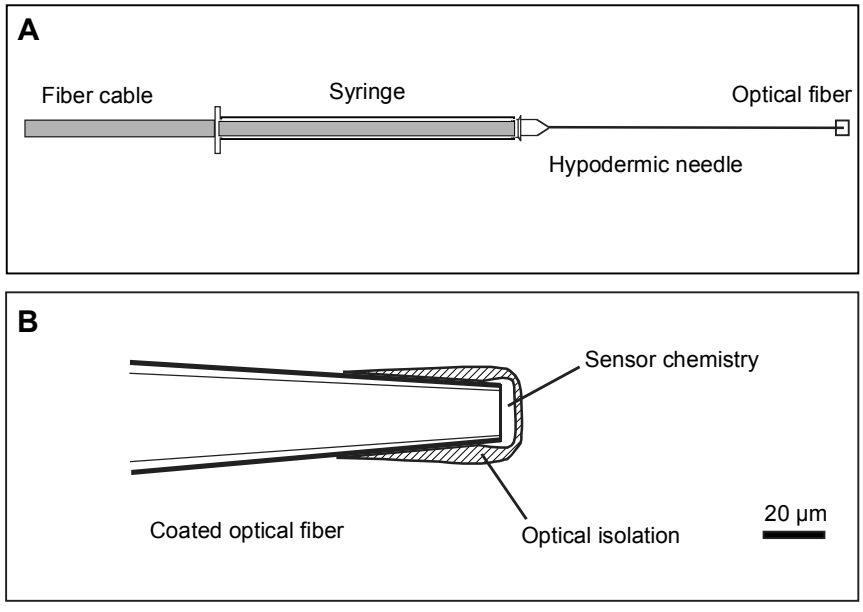

Fig. 3.23 Schematic representation of an oxygen microoptode. One end of the glass fiber can be mounted into a steel cannula for protection and stabilization (A). At the site of measurement, the tip of the glass fiber is surrounded by a thin layer of epoxy resin (B) which contains a fluorescent dye. The fluorescence properties of the dye depend on the concentration of the compound to be measured (after Klimant et al. 1995)

The dye emits a fluorescent light at a different wavelength (610 nm). The intensity of this fluorescence depends on the concentration of the substance to be measured that penetrates into the resin by diffusion, directly at the site of measurement. The construction of such microoptodes, and the first results of measuring oxygen at the sediment/bottom water boundary were described by Klimant et al. (1995, 1997), Glud et al. (1999) and Kühl and Revsbech (2001). According to Klimant et al. (1995), optodes can be developed for a number of substances (e.g. pH, CO_2, NH_3, O_2). As yet, this new technology has only been applied to oxygen measurements, i.e. in the form of the microoptode. Presumably, the construction details and the alchemy of the fluorescent dyes will still be the object of current development.

So-called planar optodes were developed in recent years, which, for example, allow us to draw two-dimensional maps showing the oxygen distribution in a sediment. The fluorescence induced by oxygen can be measured and made visible on a particularly processed stretch of foil (e.g. Glud et al. 2001).

in-situ Incubations

The diffusive input of oxygen into the sediment contributes to only one part of the whole oxygen budget. An input of oxygen into the sediment conducted by macroscopic organisms must be considered to occur especially in the sediments of shallow waters, and when the proportion of organic matter in the sediment is high. These proces-

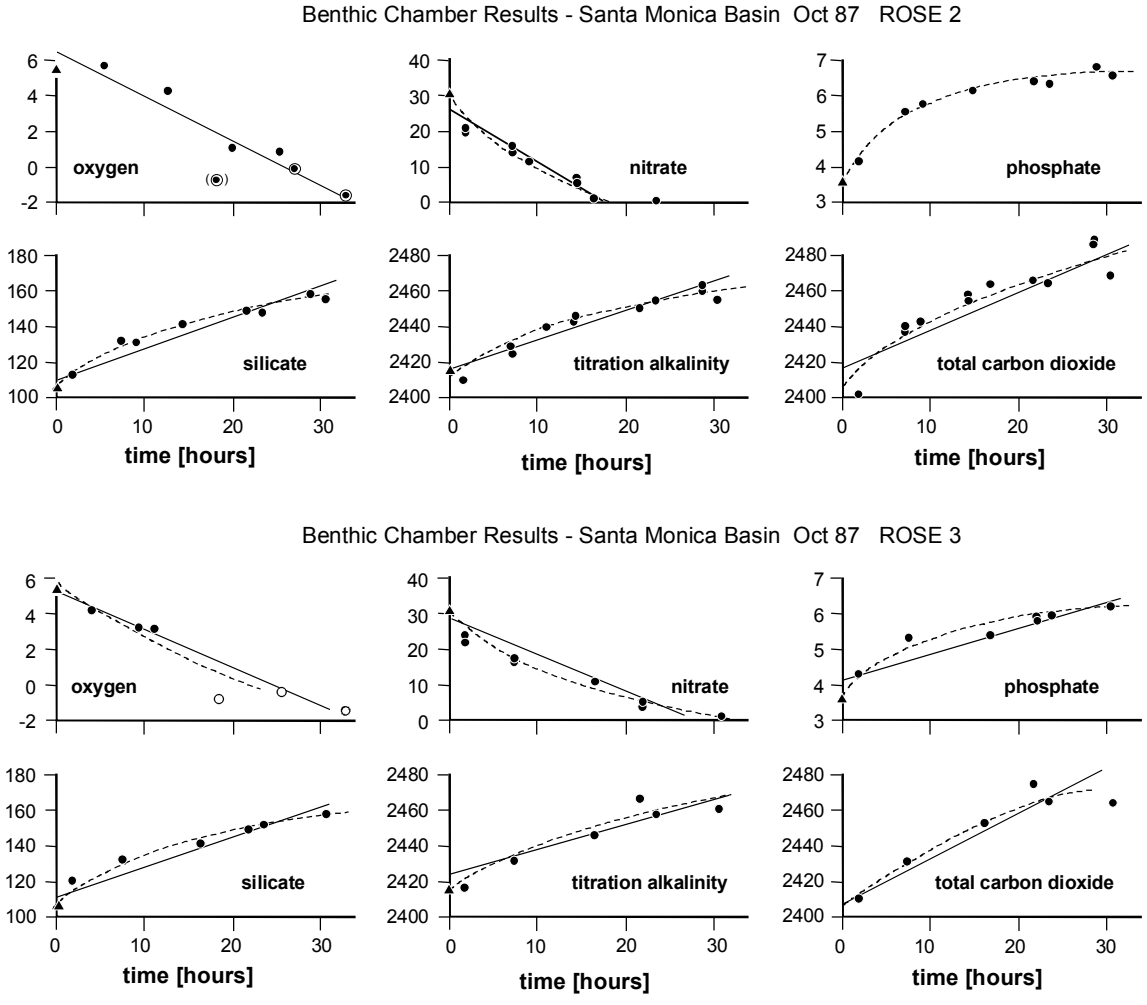

Fig. 3.24 Results of in situ incubation measurements. In both examples, a depletion of oxygen and nitrate and a concomitant release of phosphate, silica, and carbonate was observed in incubation time lasting 30 hours. The concentration unit is µmol/kg, alkalinity is expressed in µmol(eq)/kg. (after Jahnke and Christiansen 1989).

ses will be discussed more thoroughly in the following Section 3.6 concerned with bioirrigation.

The total oxygen consumption at the transition between sediment and bottom water is measured in so-called incubation experiments which are best to be carried out under *in situ* conditions. To this end, a distinct area of the sediment surface area (usually several dm^2) is covered with a closed box in such a manner that a part of the bottom water is entrapped. Inside the closed box, the concentrations of oxygen and/or nutrients are repeatedly measured over a sufficient length of time. The total exchange of substances is deduced from the measured concentration changes in relation to the volume of entrapped bottom water and the area under study.

Figure 3.24 shows the result of such an *in situ* experiment taken from a study conducted by Jahnke and Christiansen (1989). The sediment's uptake of the electron acceptors oxygen and nitrate is easy to quantify, as well as the concomitant release of phosphate, silica, and carbonate into the bottom water.

Glud et al. (1994) also carried out *in situ* incubation experiments in the upwelling area off the coast of Namibia and Angola, in a parallel procedure to their recording diffusion controlled oxygen profiles by means of microelectrodes. Thus, they were able to obtain values for the sediment's total oxygen uptake and, at about the same site, simultaneously measured the exclusively diffusion-controlled oxygen uptake. The ratio of total uptake and diffusive uptake yielded values between 1.1 and 4. The higher ratios were coupled to the altogether higher reaction rates observable in organic-rich sediments at shallower depths. Similarly a good correlation between the difference of total oxygen uptake minus diffusive oxygen uptake on the one hand, and the abundance of macroscopic fauna on the other hand was observed.

Peepers, Dialysis, and Thin Film Techniques

At first glance, dialysis would appear to be a very useful technique for obtaining pore water samples under *in situ* conditions which can be analyzed for nearly all constituents. Different types of 'peepers' are presently used which can be pressed into the sediment from the sediment surface. Such a peeper usually consists of a PE-column 0.5 - 2 m long with 'peepholes' on its outside. Cells filled with de-ionized water inside the peeper are allowed to equilibrate via dialysis through a filter membrane with the pore water outside the peeper. However, an equilibration time of many days or even a few weeks may be necessary if a volume of fluid greater than 5 - 10 cm^3 is necessary for analysis and if a small peephole is required in order to achieve a certain depth resolution. This

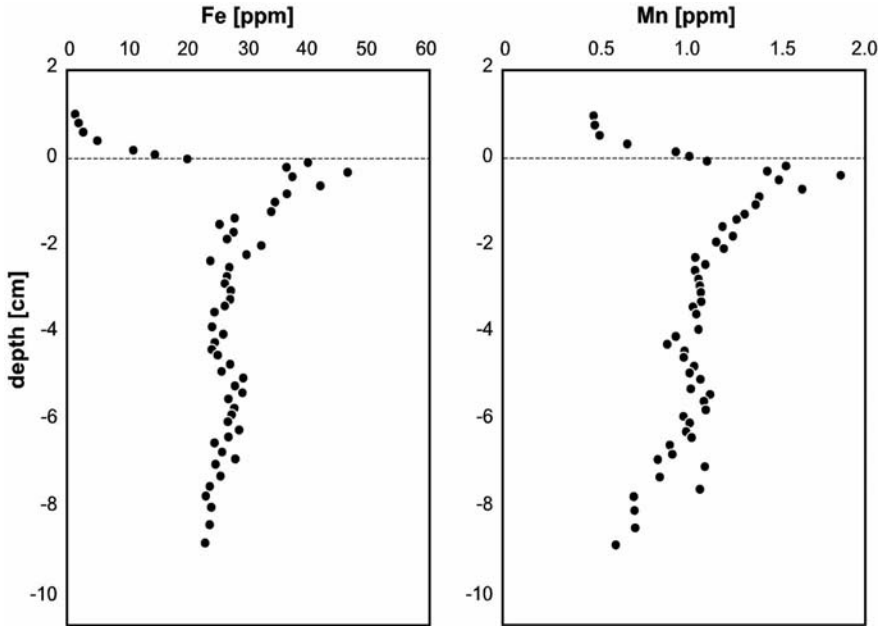

Fig. 3.25 Concentration-depth profiles for Mn and Fe through the sediment/water interface. For these measurements, a DET gel was deployed for 24 hours in situ. (after Davison et al. 1994)

restricts the use of dialysis-peepers to shallow water environments where diving is possible, and thus makes it especially useful in tidal areas. It should be pointed out that dialysis does not simply result in the sampling of pore water under *in situ* conditions. Only those aquatic species that are small enough to pass through the membrane can find their way through the peephole into the cell. The species distribution is therefore dependent on the nature of the membrane used. A review of different techniques is given by Davison et al. (2000). More relevant to the study of deep sea sediments are *in situ* techniques using the diffusive equilibration in thin films (DET) and diffusive gradients in thin films (DGT) (Davison et al. 1991; Davison and Zhang 1994; Davison et al. 1997; Davison et al. 2000).

Figure 3.25 shows concentration-depth profiles for Mn and Fe through the sediment/water interface with a depth resolution which would be impossible to obtain using any other technique. Measurements such as these have resulted in meaningful measurements of reaction rates within the uppermost layers of young sediments and of diffusive fluxes of various metals through the sediment/water interface for the first time. However, the preparation of the thin films, and their handling under field conditions is still quite troublesome and much work needs to be undertaken to further develop these techniques. Nonetheless, this seems to be a most promising approach for obtaining reliable *in situ* determinations of elements in sediment pore waters.

3.6 Influence of Bioturbation, Bioirrigation, and Advection

For the pure geochemist it would be most convenient if this chapter would close at this point. The concomitance of diffusive transport and reactions determinable on the basis of gradient alterations - although they are rather numerous - results in a sufficiently sophisticated system of pore water and sediment, quite well understood and calculable. For deeper zones below the sediment surface, beyond approximately 0.5 to 1 m, a description of the system in terms of diffusion and reactions probably seems to be quite acceptable, with a certain degree of accuracy obtained. The closer the zones under study are located to the sediment surface, the more inhomogeneities and non-steady state conditions become of quantitative importance. These are mainly determined by the activity of organisms living in the sediment.

Depending on whether the effect on the sediment or the pore water is considered, this phenomenon is referred to as bioturbation or bioirrigation, respectively. Advection (sometimes also called convection) is the term used for the motion of water coupled to a pressure gradient which partly overlaps with bioirrigation, when permeabilities are influenced by the habitats of the organisms. At the end of this section, model concepts will be outlined that allow for a quantitative description of this heterogeneous, yet very reactive domain of the sediment.

Bioturbation

Bioturbation refers to the spatial rearrangement of the sediment's solid phase by diverse organisms, at least temporarily living in the sediment. This process implies that all sedimentary particles in the upper layers, which are inhabited by macroorganisms, are subject to a continual

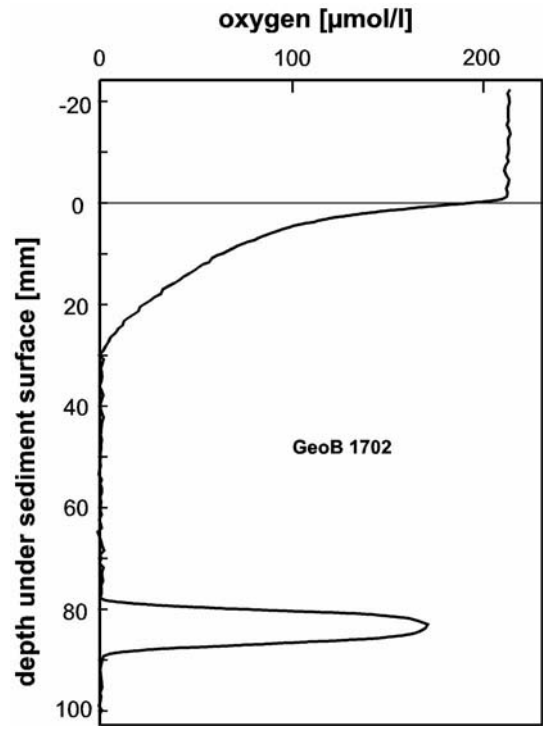

Fig. 3.26 In situ measurement of an oxygen profile in a water depth of 3100 m, off the mouth of the Congo River. The microelectrode detected an open cavity flooded with oxygen-rich bottom water in a depth between 80 mm and 90 mm below the sediment surface (after Glud et al. 1994).

transfer, i.e. seen in the long run, are integrated into a permanent cycle. From the publications of many authors (e.g. Aller 1988, 1990, 1994; Dicke 1986) it can be concluded that this layer, essentially influenced by bioturbation, generally reaches 5 to 10 cm, rarely even up to 15 cm, below the sediment surface. Only when a sediment particle has reached a greater depth in the course of continued sedimentation, will the 'recycling' process become a rare event until it ultimately comes to a final standstill.

This continued recycling of the sediment's solid phase is of great importance for a number of geobiochemical processes. By the action of this cycle, the electron donor (organic matter) and the electron acceptors (e.g. iron and manganese oxides) of the biogeochemical redox processes in the sediment are continually procured from the sediment surface. The results obtained by Fossing and Jørgensen (1990) can only be understood when considerably more sulfate is chemically reduced in the upper layers of the sediment than is accounted for by the sedimentation rate of directly imported organic matter. The re-oxidation of once released sulfide back to sulfate, which is also of importance in this regard, can only proceed when the oxides of iron and manganese, the electron acceptors, are continually supplied from the surface in an oxidized state, and return there in a chemically reduced form. Such a cycle has been described for iron and manganese, for instance, by Aller (1990); Van Cappellen and Wang (1996) as well as Haese (1997).

Bioirrigation

The process in which living organisms in the sediment actively transport bottom water through their habitats is known as bioirrigation. In this process, oxygen-rich water is usually pumped into the sediment, and water with less oxygen is pumped out. Figure 3.26 which is derived from the publication by Glud et al. (1994) demonstrates an oxygen profile measured in situ with the aid of a microelectrode. The electrode recorded a normal profile reaching about 30 mm below the sediment surface. Beyond, from about 30 mm to 80 mm below the sediment surface, the oxygen concentration was practically zero, whereas an open cavity was detected between 80 and 90 mm flooded with oxygen-rich bottom water.

In the publications submitted by Archer and Devol (1992), a comparative study on the purely diffusive oxygen flux (based on measurements with microelectrodes) and the total oxygen flux (based on incubations) was conducted for the shelf and the continental slope off the State of Washington. In a similar study, Glud et al. (1994) investigated the continental slope off Angola and Namibia. It was shown that the flux induced by bioirrigation was several times larger than the diffusive flux. However, such high fluxes only occur in densely populated sediments, mostly on the shelf. For deep sea conditions the total oxygen uptake was only slightly higher than the diffusive oxygen uptake of the sediment.

Advection of Pore Water

Except for bioirrigation, advection within the pore water fraction may only result from pressure gradients. Advection is sometimes referred to as convection, yet the terms are used rather synonymously. There are, in principle, three different potential causes leading to such pressure gradients, and thus to an advective flux:

- Sediment compaction and a resulting flow of water towards the sediment surface.
- Seafloor areas with warmer currents and a resulting upward-directed water flow, that corresponds with water flows directed downwards at other locations.
- Currents in bottom water that induce pressure differences at luv and lee sides of uneven patches on the sedimentary surface.

The first case can be quite easily assessed quantitatively on the basis of porosity measurements: one might imagine a fresh and water-rich deposited sediment column and observe the compaction as a further descent of the solid phase relative to the water that remains at the same place. Hence, the upwards directed advective flux results as the movement of water relative to the further sinking sediment. If the sediment exhibits a water content of approximately 0.9 at its surface, and even a value of 0.5 in several meters depth, and provided that the boundary between sediment and bottom water moves upwards due to the accumulation of new sediment, then it will inevitably follow that the compaction induces an advective flux which will not exceed values similar to the rate of sedimentation. As for deep sea

sediments, this process can produce values in the range of a few centimeters per millennium.

Some examples for the second case were provided by Schultheiss and McPhail (1986). By using an analytical instrument that freely sinks to the ocean floor, they were able to measure pressure differences between pore water, located 4 m below the sediment surface, and the bottom water directly. At some locations, deep sea sediments of the Madeira Abyssal Plain displayed pressure differences of about 0 Pa, at other locations, however, the pressure in pore water 4 m below the sediment surface was significantly lower (120 or 450 Pa) than in bottom water. With regard to the porosity (ϕ) and the permeability coefficient of the sediment (k), the advective flux is calculated according to the following equation:

$$v_a = \left(k \cdot \frac{\Delta p}{\Delta x} \right) \Big/ \phi \qquad (3.30)$$

In this equation, known as the *Darcy Equation*, and which is applied in hydrogeology for calculating advective fluxes in groundwater, v_a[m s^{-1}] denotes the velocity with which a particle/solute crosses a definite distance in aqueous sediments. Δp refers to the pressure altitude measured in meters of water column (10^5 Pa = 1 bar $\approx$ 750 mm Hg $\approx$ 10.2 m water column); and Δx [m] is the distance across which the pressure difference is measured. In the example shown above (ϕ = 0.77, k = $7 \cdot 10^{-9}$ m s^{-1}), this distance amounts to 4 m. Insertion into Equation 3.30 yields:

$$v_a = \left(7 \cdot 10^{-9} \cdot \frac{0.012}{4} \right) \Big/ 0.77 = 2.7 \cdot 10^{-11} \text{ [m s}^{-1}\text{]} \qquad (3.31)$$

or:

$$v_a = 0.86 \text{ [mm a}^{-1}\text{]}$$

Applying the other value specified by Schultheiss and McPhail (1986) as 450 Pa, a velocity of v_a = 3.2 [mm a^{-1}] ensues. (These authors end up with the same values, yet they do so by using a different, unnecessarily complicated procedure for calculation). Such values would thus be estimated as one, or rather two orders of magnitude greater than those resulting from compaction. Actually, such values should distinctly be reflected by the concentration profiles in pore water. However, despite of the huge number of published profiles, this consequence has not yet been demonstrated.

Upon applying the Darcy Equation 3.30 which is designed for permeable, sandy groundwaters, we must take into consideration that this equation is only applicable to purely laminar fluxes. Furthermore, it does not account for any forces effective near the grain's surface. A permeability value of k = $7 \cdot 10^{-9}$ m s^{-1} implies that grain size of the sediment particles is almost identical to clay. Within such material, the forces working on the grain surfaces impose a limitation on the advective flux, so that the calculation of Equation 3.31, based on the pressure gradient, will surely lead to a considerable overestimation of the real advective flux.

The third case, a pressure gradient induced by the bottom current and a supposed advective movement of the pore water, is of importance mainly on the shelf where shallow waters, fast currents, an uneven underground, and high permeability values in coarse sediments are encountered. Ziebis et al. (1996) as well as Forster et al. (1996) were able to demonstrate by *in situ* measurements and in flume experiments that the influence of bottom currents may be indeed crucial for the superficial pore water of coarse sand sediments near to the coast.

At flow rates of about 10 cm s^{-1} over an uneven sediment surface (mounds up to 1 cm high), the oxygen measured by means of microelectrodes had penetrated to a maximum depth of 40 mm, whereas a penetration depth of only 4 mm was measured under comparable conditions when the sediment surface was even (Fig 3.27). Huettel et al. (1996) were able to show in similar flume experiments that not only solutes, but, in the uppermost centimeters, even fine particulate matter was likewise transported into the pore water of coarsely grained sediments. Similar processes with marked advective fluxes are, however, not to be expected in the finely grained sediments predominant in the deep sea.

Advection of Sediment

An advection of the sediment's solid phase does not, at first sight, seem to make any sense, because it implies - in contrast to bioturbation - a movement of sediment particles which favor a specific direction. There is no known process that describes an advection of a solid phase, instead, the definition of such a process actually only

results from the definition of the position of the system of coordinates, and thus already indicates the model boundary conditions which will be later dealt with in more detail. If the zero-point of the coordinate-system is set by definition to the boundary between sediment and bottom water, it follows that the coordinate-system will travel upwards with the velocity of the sedimentation rate. Concomitantly, this also implies that sediment particles move downwards relative to the coordinate-system with the velocity of the sedimentation rate. This definition may appear somewhat formalistic, at first, but it becomes more real and relevant from a quantitative point of view when diagenetic reactions are studied. Then most turnovers are limited by the solid phase components that are introduced into the system by this form of 'advection'.

Conceptual Models

Conceptual models and their applications will be discussed in more detail in Chapter 15 where computer models will be presented and examples taken from various fields of application will be calculated. At this point, conceptual models will just be mentioned in brief summary and will contain the most essential statements of this chapter.

- The description of the diffusive transport by Fick's first and second law of diffusion includes the transport of soluble substances in pore water, which is not mediated by macroorganisms. In this regard, diffusive fluxes are always produced by gradients; and fluxes are always reflected by gradients. Upon assessment of concentration profiles with respect to material fluxes, it needs to be considered whether the depth zones of the investigated profile are sufficiently (quasi) stationary with regard to the studied parameter. Non-steady state conditions are appropriately described only by Fick's second law of diffusion.

- If no biogeochemical processes can be found in sediments at all, the pore water should display constant concentrations from the top down in a stationary way. Any reactions taking place in the pore water fraction, or between pore water and solid phase, will become visible as a change of the involved concentration gradients extending across the depth zone; any changes of the concentration gradients document the processes in which pore water has been involved.

- In principle, bioturbation as a macrobiological process should not be described in terms of easily manageable model concepts as can be done for molecular diffusion. Only if it is assured that the expansion of a given volume under study is large enough, and/or provided that the time-span necessary to make the

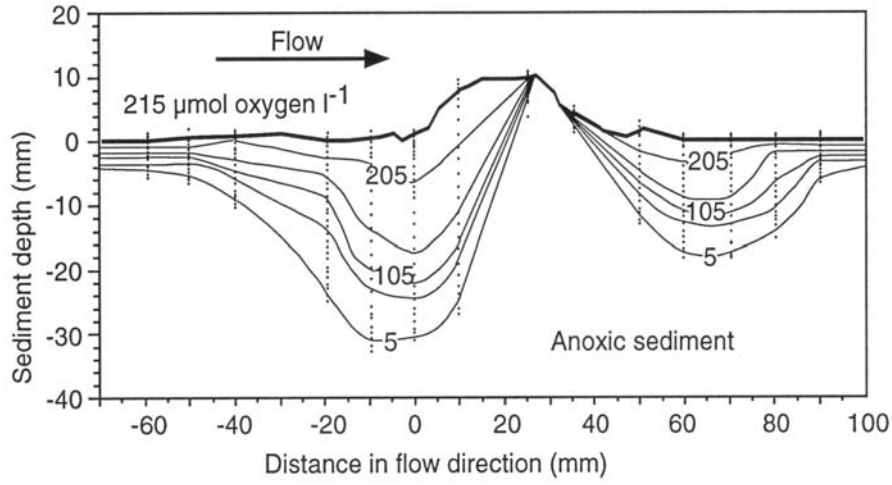

Fig. 3.27 Advective flow of pore water induced by bottom water flow and documented by O_2 penetration into the sediment around a small sediment mound (after Ziebis et al. 1996).

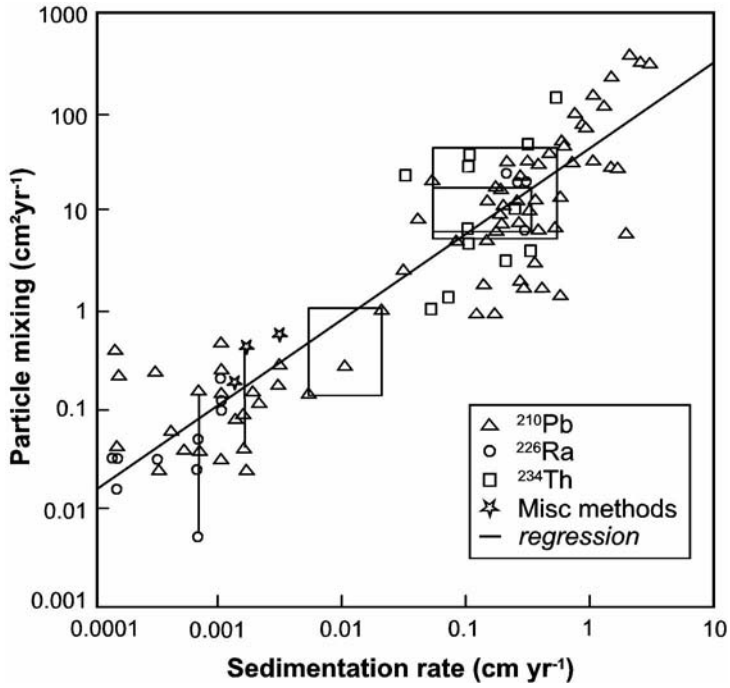

Fig. 3.28 Biodiffusion coefficients (particle mixing) in relation to their empirically determined dependence on the rate of sedimentation (after Tromp et al. 1995).

observation is sufficiently long, can we conceive of the bioturbation processes, on average, as identically effective at all places. In such cases, a model concept of 'biodiffusion' is frequently applied in which Fick's laws of diffusion are applied upon introducing an analogous 'biodiffusion coefficient'. Aller and De Master (1984) reported on having determined ^{234}Th and ^{210}Pb and drew conclusions using a model concept of bioturbation. Figure 3.28 shows an empirically determined biodiffusion constant according to Tromp et al. (1995) in its dependence on the sedimentation rate. Deep sea sediments with sedimentation rates in the range of 0.001 and 0.01 cm a^{-1} yield biodiffusion coefficients in the range of 0.1 and 1 cm^2a^{-1}, or, upon applying the dimensions contained in Table 3.1, values that lie between $3 \cdot 10^{-13}$ and $3 \cdot 10^{-12}$ m^2s^{-1}. Such biodiffusion coefficients are thus more than one order of magnitude smaller then the coefficients of molecular diffusion in sediment pore waters. The bioturbation process (= biodiffusion) is therefore without immediate relevance for pore water because, if we judge the matter realistically, its effects are by far less than the accuracy of the molecular diffusion coefficient. Bioturbation (= biodiffusion) is, however, very important for the dynamics and the new organization of the sediment's solid phase. By this mechanism, and adjunct biogeochemical reactions, bioturbation consequently also exerts an indirect but nevertheless important influence on the distribution of concentrations in pore water.

- Upon introducing a related coefficient, Fick's laws of diffusion have also been applied to bioirrigation. However, this surely reflects a rather poor model concept. Figure 3.26 already showed this in two ways: firstly, this process is indeed of relevance and applicable to pore water. Secondly, both processes, molecular diffusion and biorrigation, take place simultaneously and are effective in parallel action at the same location. A workable model concept to deal with bioirrigation is therefore still missing.

- The advection of pore water has the same order of magnitude as the sedimentation rate

and is, therefore, compared to molecular diffusion, not of great importance. However, advection as a model concept in itself may be quite easily included into computer models by the employment of the Darcy Equation 3.30. The advection of the sediment's solid phase results from the formal logic that the zero-point of the system of coordinates is always defined at the sediment surface, and that the sediment particles stream downward relative to the coordination system. This process is of great importance for balancing the diagenetical effects in the sediment.

3.7 Signals in the Sediment Solid Phase

As already described in the introductory section to this Chapter, the 'classic geological' approach to the processes of diagenesis was distinguished by the examination of the sediment's solid phase. And whenever a reconstruction of diagenetic processes in previous sediments - which nowadays consist of rock and have lost their original pore water content a long time ago -, is attempted, one will have to resort to an investigation of the solid phase. Analyzing the solid phase element profiles is much more reliable than is the case with pore water concentration profiles. However, the interpretation of such element profiles proves to be much more difficult, since the signals of the entire consecutive diagenetic processes interfere with those of sedimentation. Some of the element profiles measured in sediments can only be interpreted on account of the new understanding of diagenetic processes which was gained, in particular, after many pore water analyses had been carried out during the last two decades. The ratios of the sedimentary contents primarily originating from sedimentation compared to those originating from diagenetic processes might differ greatly from each other, depending on the element, the sedimentation area, and the type of diagenesis. In such case, it is always advisable to initially perform an estimative, rough calculation of the contents measured in the sediment in relation to the contents potentially altered in the sediment by the processes of diagenesis.

3.7.1 Analysis of the Sediment's Solid Phase

A variety of different analytical approaches lead to the profiles of sedimentary element contents. The two essential and most commonly used methods are nowadays the following:

- Laborious, yet very reliable, is the complete extraction of the dried, mortared and homogenized sediment sample using appropriate acids. Usually a microwave pressure extraction in a closed system composed of PTFE or a similarly inert and resistant material is applied for this purpose nowadays. With this method, all the sedimentary constituents are dissolved without exception by applying various mixtures of HF, HCl and HNO_3 ($HCLO_4$ can be avoided in most cases) at temperatures between 250 and 260 °C and a pressure ranging from 30 to 50 bars. In the ultimately received, slight nitric solution - hydrofluoric acid is left to evaporate in the course of the procedure - practically all elements (including the rare earth elements) can then be analyzed markedly above their limit of detection by atom absorption spectrometry (AAS), optical plasma emission spectrometry (ICP-OES) and/or plasma mass spectrometry (ICP-MS).

- X-ray fluorescence spectroscopy (XRF) is much easier in its performance but by no means as reliable particularly in case of low element contents. Here, the dried, mortared and homogenized samples can be used directly as powder, or better in this shape of pressed tablets, or even better still, as molten tablets. With this method, good detection limits are obtained for most of the quantitatively relevant elements, the access to trace metals, however, is not feasible to the same extent as in complete extraction and subsequent analysis of the extract solution.

The following comparison illustrates the greatly differing time and work effort associated with these two methods:

In order to analyze the quantitative element profiles, consisting of approximately 250 samples derived from one single core which was extracted with the gravity corer, several weeks are required for drying, mortaring, homogenization, weighing,

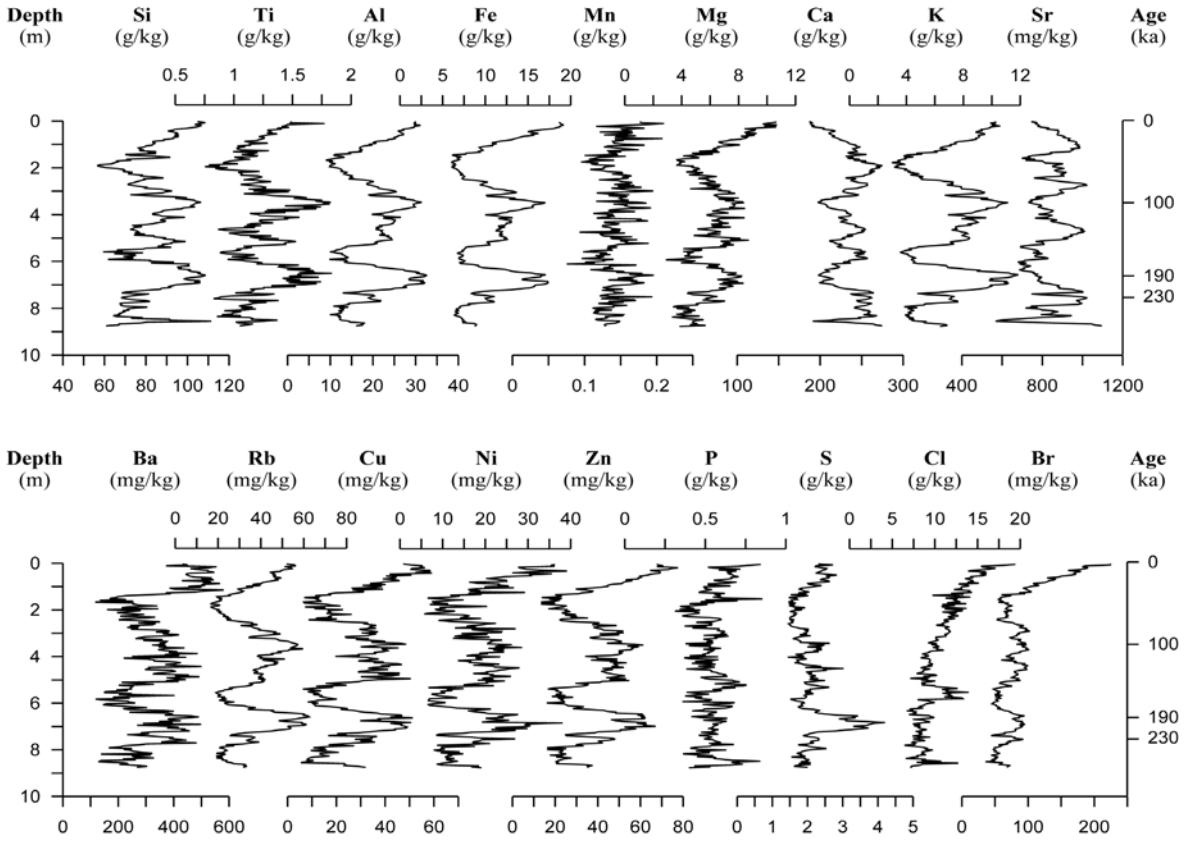

Fig. 3.29 Profile of the elemental contents within a sediment core which was obtained from a depth of 1952 m in the Cape Basin. Analysis was performed with a transportable X-ray fluorescnce anayzer (XRF) on board of a research vessel. Results were obtained within 24 hours after extracting the core (Wien et al. 2005a).

chemical extraction and analysis - provided that all steps of extraction and analysis are automated.

The element profiles of a sediment core from the Cape Basin (Wien et al. 2005a), which is shown in Figure 3.29, were obtained with a trans-portable XRF on board of a research vessel, the results were obtained within a period of 24 hours after core extraction with the gravity corer.

The energy-dispersive analysis was conducted with polarized X-rays. Powdered samples were measured because of the short processing time desired in this case, although lower detection limits and measured values displaying less scattering would certainly have been obtained by applying pressed or even molten tablets. An essential further improvement of the quality of measurements would have been accomplished if the more laborious wavelength-dispersive X-ray fluorescence (WDX), currently not available as transportable device, had been applied instead of the energy-dispersive X-ray fluorescence (EDX).

3.7.2 Interpretation of Element Profiles

The profiles of elemental contents shown in Figure 3.29 may serve as an example to briefly discuss the informational content, i.e. the various signals in these profiles. Core GeoB 8301 shown here originated from the Cape Basin at 34°46.0′S and 17°41.5′E and a water depth of 1952 m. The following signals can be distinctly recognized in the element profiles:

- The profiles of Ti, Al, Fe, K, Rb and also, to a limited extent, Mg are obviously determined by an input of terrestrial substance which is consequential to erosion. The curves which are very similar to each other represent the intensity and the type of erosion on the continent, formation and degradation of soil, as controlled by climate changes.
- The elements Ba, Cu, Ni und Zn produced similar curves, somewhat overlain by disturbing measurement variances. However, espe-

cially in the case of barium at a depth of somewhat more than 1 m below the sediment surface, a much steeper rise of the measured values is recognizable than is characteristic of the other elements also controlled by terrestric processes. A similar steep rise at this depth is otherwise only encountered by strontium which is predominately controlled by marine processes. Various authors conceive barium as a proxy parameter of paleoproductivity in the surface water of oceans (e.g. Kasten et al. 2001). Also the elements copper, nickel and zinc which produced curves similar to barium reach the sediment when they are bound to organic matter, and thus create similar imprints in the sediment.

- The earth alkali metals calcium and strontium are almost exclusively determined by marine routes of entry. They predominately reach the sediment in the shape of calcareous shells originating from perished marine organisms. In this case, various organisms contain slightly different amounts of strontium, while others incorporate strontium to a variable degree, a process which depends on the surrounding temperature. For this core, and other sediment cores obtained from the Cape Basin, it could be demonstrated that a profile of the Sr/Ca ratio matched perfectly with the corresponding $\delta^{18}O$-curve (SPECMAP curve, Imbrie et al. 1984), permitting an immediate deduction of an age model (cf. Wien et al. 2005b).

- The two elements in this core, calcium and strontium, were not even essentially influenced by diagenesis. Wherever the sediment's pCO_2 and concentration of dissolved carbonate changes in course of the degradation of organic matter, the respective dissolution/precipitation reactions of carbonate minerals can also be concomitantly determined (Pfeifer et al. 2002, Wenzhöfer et al. 2001).

- Large parts of the silicon curves show a resemblance to the elements which are introduced from land. This element obviously also reaches the marine sediment on similar routes of entry. However, individual peaks display a similarity to the elements which are controlled by marine conditions and thus provide evidence in favor of biogenic opal as the route of entry, which is also quantitatively relevant.

- Sulfur reaches the sediment essentially only by means of diagenetic processes. Here, the fixation of sulfate-bound sulfur in the form of barite in the sulfate-methane transition (SMT) zone produces an interesting signal, but is quantitatively irrelevant on account of the low barium concentrations in the pore water. Sulfur precipitates in much greater amounts in shape of sulfide (Mackinawite FeS, pyrite FeS_2) wherever sulfide resulting from the reduction of sulfate comes into contact with divalent iron by means of diffusion. In the core shown in Figure 3.29 this obviously proceeded at a depth of about 7 m below the sediment surface over a relatively long period of time.
- The two halogens Cl and Br also provide some interesting pieces of information. Since a high concentration of chlorine prevails in ocean water, but is practically not involved in any diagenetic processes, chlorine can make its way into the XRF sample only by means of pore water extraction. The curve of chlorine shown in Figure 3.29 represents the porosity of the sediment material so precisely that its concentration could be reconstructed. This influence can also be seen in the case of bromine which is, however, overlain by a similar signal of nearly the same intensity as those of the elements Ba, Cu, Ni, Zn which are controlled by organic matter.

3.7.3 Correlation of Sediment Cores by the Contents of Elements

A stratigraphic correlation of different sediment cores only makes sense if the element applied in a correlation of a given core is practically not influenced by any diagenetic process at all, and when its curve is practically only influenced by its input into the sediment.

Diagenetic influences would not be coupled to the stratigraphy, but would reach various depths at various locations instead, totally independent of the diagenetic processes. Especially suited for correlations are elements that do not display too low concentrations and whose input into the sediment is essentially determined by one single route of entry. This can be, for example, either one of elements aluminum or iron for the terrestrial input, or calcium or strontium for the marine

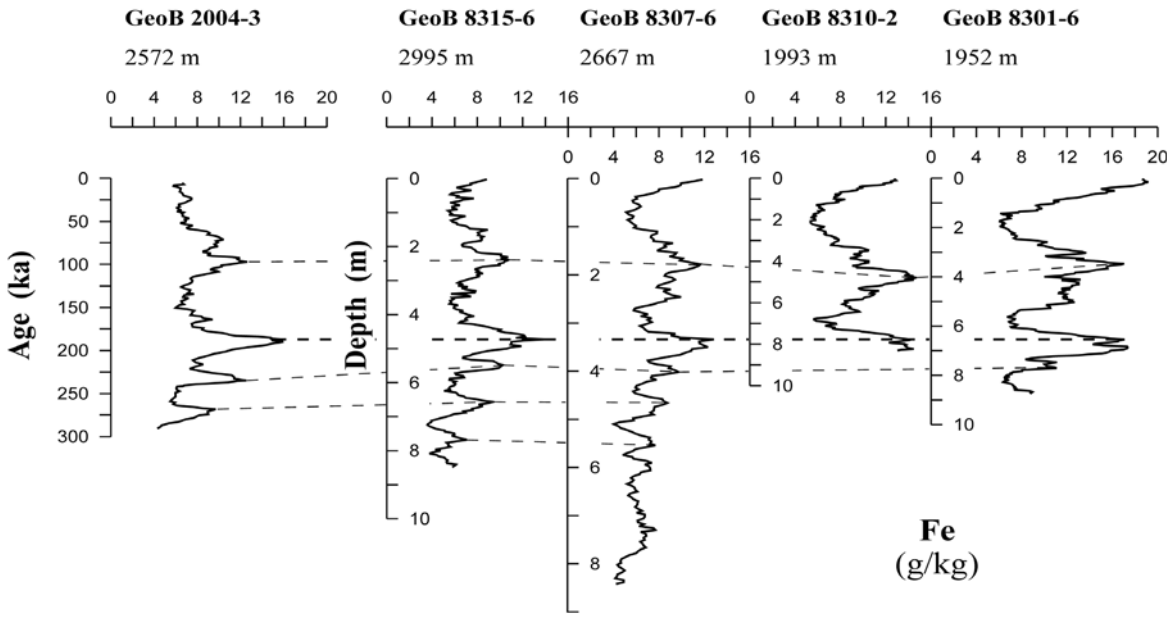

Fig. 3.30 Corelation of various sediment cores from the Cape Basin by means of sedimentary iron content profiles. This method permitted a safe projection of an age model available for one core to several other cores. (Wien et al. 2005a).

input. In Figure 3.30, core GeoB 8301 from the Cape Basin, shown in Figure 3.29, is correlated with several other cores derived from the Cape Basin by means of their iron profiles. Since a reliable age model was available for one of these cores (GeoB 2004), it could therefore also be applied to the other cores.

Graphical representations of element profiles frequently also show the ratios of elements. Above, the Sr/Ca ratio was mentioned as an example, along with its correlation with the SPECMAP curve in a certain sea area (Wien et al. 2005b). Especially popular is the representation of elemental contents reported as element/aluminum ratios. In this case, it is assumed that aluminum depends exclusively on a terrestrial route of entry. The element/aluminum ratio reveals the deviation of a given element from the behavior displayed by aluminum. An element/titanium ratio is used for the same purpose, however, it is not applied as often on account of the fact that titanium is not as reliable as aluminum and more difficult to analyze.

However, such element/aluminum or element/titanium ratios should never be applied in general and only with caution, as such procedure in fact systematically removes the terrestrial input signal from the data and, with it, all information which is attached to this course and running parallel to it. A good approach is given if only the marine signal is to be examined, and somebody has started it at some time. Some workers may be encountered occasionally who, as a matter of principle, looking at their data study nothing but the element/aluminum ratios anymore. They will never learn anything about the terrestrial routes of input, because they simply will never see them. Studying the element/titanium ratios is particularly nonsensical in this regard. The ratio of one element to another should only be used, if it is exactly known why this ratio is studied, which part of the statement is underscored, and which one will be suppressed.

Acknowledgements

This is contribution No 0330 of the Research Center Ocean Margins (RCOM) which is financed by the Deutsche Forschungsgemeinschaft (DFG) at Bremen University, Germany.

3.8 Problems

Problem 1

Which of the following parameters have to be measured in the fresh sediment, which as soon as possible in squeezed or centrifuged pore water, which after preservation within some weeks, and which without any preservation even after long time: alkalinity, ammonia, chloride, manganese, nitrate, oxygen, pH-value, potassium, sodium, sulfate, sulfide, total iron?

Problem 2

In Figure 3.14 a sulfate reduction zone is documented by measured profiles of sulfate and methane in pore water. Estimate the diffusive methane flux [mol $m^{-2}a^{-1}$] and use for the calculation the more reliable profile of sulfate concentrations. Use a temperature of 5°C and a sediment porosity of $\phi = 0.7$.

Problem 3

Figure 3.12 shows two very similar profiles of oxygen concentrations in pore water. Estimate the total oxygen consumption of the sediment and the rate of DIC production [mol $m^{-2}a^{-1}$]. Assume a C:N:P ratio of 106:16:1 for the organic matter. Use a temperature of 5°C and a sediment porosity of $\phi = 0.7$.

Problem 4

For which type of sediments, for which parameters, and for which steps of sampling, pore water extraction, and analyses a glove box with an inert gas atmosphere is necessary? Which inert gas would you prefer? Explain your decisions.

Problem 5

The contents of different elements in the sediment solid phase are determined by their different pathways into the sediment and by diagenetic processes. Which elements mainly document a marine input, which elements document a terrestrial input, which elements are mainly influenced by diagenetic processes?

References

Aller, R.C. and DeMaster, D.J., 1984. Estimates of particle flux and reworking at the deep-sea floor using 234Th/238U disequilibrium. Earth and Planetary Science Letters, 67: 308-318.

Aller, R.C., 1988. Benthic fauna and biogeochemical processes in marine sediments: The role of burrow structures. In: Blackburn, T.H. and Sørensen, J. (eds), Nitrogen cycling coastal marine environments. SCOPE. Wiley & Sons Ltd., pp. 301-338.

Aller, R.C., 1990. Bioturbation and manganese cycling in hemipelagic sediments. Phil. Trans. R. Soc. Lond., 331: 51-68.

Aller, R.C., 1994. The sedimentary Mn cycle in Long Island Sound: Its role as intermediate oxidant and the influence of bioturbation, O2, and Corg flux on diagenetic reaction balances. Journal of Marine Research, 52: 259-293.

Archer, D., Emerson, S. and Smith, C.R., 1989. Direct measurements of the diffusive sublayer at the deep sea floor using oxygen microelectrodes. Nature, 340: 623-626.

Archer, D. and Devol, A., 1992. Benthic oxygen fluxes on the Washington shelf and slope: A comparison of in situ microelectrode and chamber flux measurements. Limnology and Oceanography, 37: 614 - 629.

Archie, G.E., 1942. The electrical resistivity log as an aid in determining some reservoir characteristics. Trans. Am. Inst. Min. Metall., 146: 54 - 62.

Berner, R.A., 1980. Early diagenesis: A theoretical approach. Princton Univ. Press, Princton, NY, 241 pp.

Boudreau, B.P., 1997. Diagenetic models and their impletation: modelling transport and reactions in aquatic sediments. Springer, Berlin, Heidelberg, NY, 414 pp.

Cornwell, J.C. and Morse, J.W., 1987. The characterization of iron sulfide minerals in anoxic marine sediments. Marine Chemistry, 22: 193-206.

Davison, W., Grime, G.W., Morgan, J.A.W. and Clarke, K., 1991. Distribution of dissolved iron in sediment pore waters at submillimetre resolution. Nature, 352: 323-324.

Davison, W. and Zhang, H., 1994. In situ speciation measurements of trace components in natural waters using thin-film gels. Nature, 367: 546-548.

Davison, W., Zhang, H. and Grime, G.W., 1994. Performance characteristics of gel probes used for measuring the chemistry of pore waters. Environmental Science & Technology, 28: 1623-1632.

Davison, W., Fones, G.R. and Grime, G.W., 1997. Dissolved metals in surface sediment and a microbial mat at 100 µm resolution. Nature, 387: 885-888.

Davison, W., Fones, G., Harper, M., Teasdale, P. and Zhang, H., 2000. Dialysis, DET and DGT: in Situ Diffusional Techniques for Studying Water, Sediments and Soils, In: In Situ Chemical Analysis in Aquatic Systems, J. Buffle and G. Horvai, Eds.: Wiley, pp 495-569.

De Lange, G.J., 1988. Geochemical and early diagenetic aspects of interbedded pelagic/turbiditic sediments in two North Atlantic abyssal plains. Geologica Ultraiectina, Mededelingen van het Instituut vor Aardwetenschappen der Rijksuniversiteit te Utrecht, 57, 190 pp.

De Lange, G.J., Cranston, R.E., Hydes, D.H. and Boust, D., 1992. Extraction of pore water from marine sediments: A review of possible artifacts with pertinent examples from the North Atlantic. Marine Geology, 109: 53-76.

De Lange, G.J., 1992a. Shipboard routine and pressure-filtration system for pore-water extraction from suboxic sediments. Marine Geology, 109: 77-81.

De Lange, G.J., 1992b. Distribution of exchangeable, fixed, organic and total nitrogen in interbedded turbiditic/pelagic sediments of the Madeira Abyssal Plain, eastern North Atlantic. Marine Geology, 109: 95-114.

De Lange, G.J., 1992c. Distribution of various extracted phosphorus compounds in the interbedded turbiditic/pelagic sediments of the Madeira Abyssal Plain, eastern North Atlantic. Marine Geology, 109: 115-139.

Dicke, M., 1986. Vertikale Austauschkoeffizienten und Porenwasserfluß an der Sediment/Wasser Grenzfläche. Berichte aus dem Institut für Meereskunde an der Univ. Kiel, 155, 165 pp.

Enneking, C., Hensen, C., Hinrichs, S., Niewöhner, C., Siemer, S. and Steinmetz, E., 1996. Poor water chemistry. In: Schulz, H.D. and cruise participants (eds), Report and preliminary results of Meteor cruise M34/2 Walvis Bay-Walvis Bay, 29.01.1996 - 18.02.1996. Berichte, Fachbereich Geowissenschaften, Univ. Bremen, 78: 87-102.

Forster, S., Huettel, M. and Ziebis, W., 1996. Impact of boundary layer flow velocity on oxygen utilisation in coastal sediments. Mar. Ecol. Prog. Ser., 143: 173-185.

Fossing, H. and Jørgensen, B.B., 1990. Oxidation and reduction of radiolabeled inorganic sulfur compounds in an estuarine sediment, Kysing Fjord, Denmark. Geochimica et Cosmochimica Acta, 54: 2731-2742.

Froelich, P.N., Klinkhammer, G.P., Bender, M.L., Luedtke, N.A., Heath, G.R., Cullen, D., Dauphin, P., Hammond, D. and Hartman, B., 1979. Early oxidation of organic matter in pelagic sediments of the eastern equatorial Atlantic: suboxic diagenesis. Geochimica et Cosmochimica Acta, 43: 1075-1090.

Glud, R.N., Gundersen, J.K., Jørgensen, B.B., Revsbech, N.P. and Schulz, H.D., 1994. Diffusive and total oxygen uptake of deep-sea sediments in the eastern South Atlantic Ocean: in situ and laboratory measurements. Deep-Sea Research, 41: 1767-1788.

Glud, R.N., Klimant, I., Holst, G., Kohls, O., Meyer, V., Kühl, M. and Gundersen, J.K., 1999. Adaptation, Test and in situ Measurements with O_2 Micropt(r)odes on Benthic Landers. Deep Sea Research, 46: 171-183.

Glud, R.N., Tengberg, A., Kühl, M., Hall, P.O.J. and Klimant, I., 2001. An in situ instrument for planar O_2 optode measurements at benthic interfaces. Limnol. Oceanogr., 46: 2073-2080.

Grasshoff, K., Kremling, K. and Ehrhardt, M., 1999 (1st edition 1983). Methods of Seawater Analysis. 2nd edition, Wiley-VCH, Weinheim, NY, 600 pp.

Gundersen, J.K. and Jørgensen, B.B., 1990. Microstructure of diffusive boundary layer and the oxygen uptake of the sea floor. Nature, 345: 604-607.

Haese, R.R., 1997. Beschreibung und Ouantifizierung frühdiagenetischer Reaktionen des Eisens in Sedimenten des Südatlantiks. Berichte, Fachbereich Geowissenschaften, Univ. Bremen, 99, 118 pp.

Hall, P.O.J. and Aller, R.C., 1992. Rapid, small-volume, flow injection analysis for CO_2 and NH_4^+ in marine and freshwaters. Limnology and Oceanography, 35: 1113-1119.

Hensen C., Landenberger H., Zabel M., Gundersen J.K., Glud R.N. and Schulz H.D. (1997) Simulation of early diagenetic processes in continental slope sediments off Southwest Africa: The copmputer model CoTAM tested. Marine Geology, 144: 191-210

Holby, O. and Riess, W., 1996. In Situ Oxygen Dynamics and pH-Profiles. In: Schulz, H.D. and cruise participants (eds), Report and preliminary results of Meteor cruise M34/2 Walvis Bay-Walvis Bay, 29.01.1996 - 18.02.1996. Berichte, Fachbereich Geowissenschaften, Univ. Bremen, 78: 85-87.

Huettel, M., Ziebis, W. and Forster, S., 1996. Flow-induced uptake of particulate matter in permeable sediments. Limnology and Oceanography, 41: 309-322.

Imbrie, J., Hays, J.D., Martinson, D.G., McIntyre, A., Mix, A.C., Morley, J.J., Pisias, N.G., Prell, W.L. and Shackleton, N.J., 1984. The orbital theory of Pleistocene climate: Support from a revised chronology of the marine $\delta^{18}O$ record. In: Berger, A.L., Imbrie, J., Hays, J., Kukla, G. Saltzman, B., Reidel, D. (Eds.) Milankovitch and Climate. Dordrecht. 1: 269-305

Iversen, N. and Jørgensen, B.B., 1985. Anaerobic methane oxidation rates at the sulfate-methane transition in marine sediments from Kattegat and Skagerrak (Denmark). Limnology and Oceanography, 30: 944-955.

Iversen, N. and Jørgensen, B.B., 1993. Diffusion coefficients of sulfate and methane in marine sediments: Influence of porosity. Geochimica et Cosmochimica Acta, 57: 571-578.

Jahnke, R.A., Heggie, D., Emerson, S. and Grundmanis, V., 1982. Pore waters of the central Pacific Ocean:

nutrient results. Earth and Planetary Science Letters, 61: 233-256.

Jahnke, R.A., 1988. A simple, reliable, and inexpensive pore-water sampler. Limnology and Oceanography, 33: 483-487.

Jahnke, R.A. and Christiansen, M.B., 1989. A free-vehicle benthic chamber instrument for sea floor studies. Deep-Sea Research, 36: 625-637.

Jørgensen, B.B. and Revsbech, N.P., 1985. Diffusive boundary layers and the oxygen uptake of sediments and detritus. Limnology and Oceanography, 30: 111-122.

Jørgensen, B.B., Bang, M. and Blackburn, T.H., 1990. Anaerobic mineralization in marine sediments from the Baltic Sea-North Sea transition. Marine Ecology Progress Series, 59: 39-54.

Kasten, S., Haese, R.R., Zabel, M., Rühlemann, C. and Schulz, H.D., 2001. Barium peaks at glacial terminations in sediments of the equatorial Atlantic Ocean – relict of deglacial productivity pulses?. Chemical Geology, 175: 635-651.

Kinzelbach, W., 1986. Goundwater Modeling - An Introducion with Sample Programs in BASIC. Elsevier, Amsterdam, Oxford, NY, Tokyo, 333 pp.

Klimant, I., Meyer, V. and Kühl, M., 1995. Fiber-oxic oxygen microsensors, a new tool in aquatic biology. Limnology and Oceanography, 40: 1159-1165.

Klimant, I., Kühl, M., Glud, R.N. and Holst, G., 1997. Optical Measurement of Oxygen and Temperature in Microscale: Strategies and Biological Applications. Sensors and Actuators B 38: 29-37.

Kölling, M., 1986. Vergleich verschiedener Methoden zur Bestimmung des Redoxpotentials natürlicher Gewässer. Meyniana, 38: 1-19.

Kölling, M., 2000. Comparison of Different Methods for Redox Potential Determination in Natural Waters. In: Schüring et al. (Eds.): Redox – Fundamentals, Processes and Applications. Springer, Berlin, Heidelberg etc., pp. 42-54.

Kühl, M. and Revsbech, N.P., 2001. Biogeochemical Microsensors for Boundary Layer Studies, In Boudreau, B.P. and Jorgensen, B.B. (Eds.) The Benthic Boundary Layer - Transport Processes and Biogeochemistry. Oxford University Press, pp. 180-210.

McDuff, R.E. and Ellis, R.A., 1979. Determining diffusion coefficients in marine sediments: A laboratory study of the validity of resistivity technique. American Journal of Science, 279: 66-675.

Meijboom, F.W. and van Nordwijk, M., 1992. Rhizon Soil Solution Samplers as artificial roots. In: Kutschera, L., Hübl, E., Lichtenegger, E., Persson, H. and Sobotnik, M., (Eds.): Root Ecology and its practical Application.- Proc 3rd ISSR Symp., Verein für Wurzelforschung, Klagenfurt, Austria; pp. 793-795.

Meischner, D. and Rumohr, J., 1974. A Light-weight, High-momentum Gravity Corer for Subaqueous Sediments. Senckenbergiana marit., 6: 105-117.

Niewöhner, C., Hensen, C., Kasten, S., Zabel, M. and Schulz, H.D., 1998. Deep sulfate reduction completely mediated by anaerobic methane oxi-dation in sediments of the upwelling area off Namibia. Geochimica et Cosmochimica Acta, 62: 455-464.

Pfeifer K., Hensen C., Adler M., Wenzhöfer F., Weber B. and Schulz H.D., 2002. Modeling of subsurface calcite dissolution, including the respiration and reoxidation processes of marine sediments in the region of equatorial upwelling off Gabon. Geochimica and Cosmochimica Acta, 66: 4247-4259

Redfield, A.C., 1958. The biological control of chemical factors in the environment. Am. Sci., 46: 206-226.

Reeburgh, W.S., 1967. An improved interstitial water sampler. Limnology and Oceanography, 12: 163-165.

Reimers, C.E., 1987. An in situ microprofiling instrument for measuring interfacial pore water gradients: methods and oxygen profiles from the North Pacific Ocean. Deep-Sea Research, 34: 2019 -2035.

Revsbech, N.P., Jørgensen, B.B. and Blackburn, T.H., 1980. Oxygen in the sea bottom measured with a microelektrode. Science, 207: 1355-1356.

Revsbech, N.P. and Jørgensen, B.B., 1986. Microelectrodes: Their use in microbial ecology. Advances in Microbial Ecology, 9: 293-352.

Revsbech, N.P., 1989. An oxygen microsensor with a guard cathode. Limnology and Oceanography, 34: 474-478.

Saager, P.M., Sweerts, J.P. and Ellermeijer, H.J., 1990. A simple pore-water sampler for coarse, sandy sediments of low porosity. Limnology and Oceanography., 35: 747-751.

Sarazin, G., Michard, G. and Prevot, F., 1999. A rapid and accurate spectroscopic for alkalinity measurements in sea water samples. Wat. Res., 33: 290-294.

Sayles, F.L., Mangelsdorf, P.C., Wilson, T.R.S. and Hume, D.N., 1976. A sampler for the in situ collection of marine sedimentary pore waters. Deep-Sea Research, 23: 259-264.

Schüring, J., Schulz, H.D., Fischer, W.R., Böttcher, J. and Duijnisveld, W.H.M. (Eds.), 2000. Redox – Fundamentals, Processes and Applications. Springer, Berlin, Heidelberg etc., 251 pp.

Schlüter, M., 1990. Zur Frühdiagenese von organischem Kohlenstoff und Opal in Sedimenten des südlichen und östlichen Weddelmeeres. Berichte zur Polarforschung, Bremerhaven, 73, 156 pp.

Schultheiss, P.J. and McPhail, S.D., 1986. Direct indication of pore-water advection from pore pressure measurements in Madeira Abyssal Plain sediments. Nature, 320: 348-350.

Schulz, H.D., Dahmke, A., Schinzel, U., Wallmann, K. and Zabel, M., 1994. Early diagenetic processes, fluxes and reaction rates in sediments of the South Atlantic. Geochimica et Cosmochimica Acta, 58: 2041-2060.

Seeberg-Elverfeldt, Schlüter, M. and Kölling, M. 2005. Rhizon sampling of porewaters near the sediment-water interface of aquatic systems. Limnol. Oceanogr. Methods 3: 361-371.

Seeburger, I. and Käss, W., 1989. Grundwasser - Redoxpontentialmessung und Probennahmegeräte. DVWK-Schriften, Bonn, 84, 182 pp.

Smith, K.L.J. and Teal, J.M., 1973. Deep-sea benthic community respiration: An in-situ study at 1850 meters. Science, 179: 282-283.

Tengberg, A., De Bovee, F., Hall, P., Berelson, W., Chadwick, D., Ciceri, G., Crassous, P., Devol, A., Emerson, S., Gage, J., Glud, R., Graziottini, F., Gundersen, J., Hammond, D., Helder, W., Hinga, K., Holby, O., Jahnke, R., Khripounoff, A., Lieberman, S., Nuppenau, V., Pfannkuche, O., Reimers, C., Rowe, G., Sahami, A., Sayles, F., Schurter, M., Smallman, D., Wehrli, B. and De Wilde, P., 1995. Benthic chamber and profiling landers in oceanography - A review of design, technical solutions and function. Progress in Oceanography, 35: 253-292.

Tromp, T.K., van Cappellen, P. and Key, R.M., 1995. A global model for the early diagenetisis of organic carbon and organic phosphorus in marine sediments. Geochimica et Cosmochimica Acta, 59: 1259-1284.

Van Cappellen, P. and Wang, Y., 1996. Cycling of iron and manganese in surface sediments: a general theory for the coupled transport and reaction of carbon, oxygen, nitrogen, sulfur, iron, and manganese. American Journal of Science, 296: 197-243.

Viollier, E., Rabouille, C., Apitz, S.E., Breuer, E., Chaillou, G., Dedieu, K., Furukawa, Y, Grenz, C., Hall, P., Janssen, F., Morford, J.L., Poggiale, J.-C., Roberts, S., Shimmield, T., Taillefert, M., Tengberg, A., Wenzhöfer, F. and Witte, U., 2003. Benthic biogeochemistry: state of the art technologies and guidelines for the future of in situ survey. Journal of Experimental Marine Biology and Ecology, 285/286: 5-31.

Wenzhöfer F., Adler M., Kohls O., Hensen C., Strotmann B., Boehme S. and Schulz H.D., 2001. Calcite dissolution driven by benthic mineralization in the deep-sea: In situ measurements of Ca^{2+}, pH, pCO_2 and O_2. Geochimica et Cosmochimica Acta, 65: 2677-2690

Wien, K., Wissmann, D., Kölling, M. and Schulz, H.D. 2005a. Fast application of X-ray fluorescence spectrometry aboard ship: how good is the new portable Spectro Xepos analyser. Geomarine Letters, in press.

Wien, K., Kölling, M., and Schulz, H.D. 2005b. Close correlation between Sr/Ca ratio and SPECMAP record in bulk sediments from the Southern Cape Basin. Geo-Marine Letters, 25: 265-271.

Ziebis, W. and Forster, S., 1996. Impact of biogenic sediment topography on oxygen fluxes in permeable seabeds. Mar. Ecol. Prog. Ser., 140: 227-237.